Geometry & Topology

Volume 29 (2025)

Mutations and faces of the Thurston norm ball dynamically represented by multiple distinct flows

Anna Parlak

msp

msp

Geometry & Topology **29**:4 (2025) 2105–2173
DOI: 10.2140/gt.2025.29.2105
Published: 27 June 2025

Mutations and faces of the Thurston norm ball dynamically represented by multiple distinct flows

ANNA PARLAK

A pseudo-Anosov flow on a hyperbolic 3-manifold dynamically represents a top-dimensional face F of the Thurston norm ball if the cone on F is dual to the cone spanned by the homology classes of closed orbits of the flow. Fried showed that for every fibered face of the Thurston norm ball there is a unique, up to isotopy and reparametrization, flow which dynamically represents the face. Using veering triangulations we have found that there are nonfibered faces of the Thurston norm ball which are dynamically represented by multiple topologically inequivalent flows. This raises the question of how distinct flows representing the same face are related.

We define combinatorial mutations of veering triangulations along surfaces that they carry. We give sufficient and necessary conditions for the mutant triangulation to be veering. After appropriate Dehn filling, these veering mutations correspond to transforming one 3-manifold M with a pseudo-Anosov flow transverse to an embedded surface S into another 3-manifold admitting a pseudo-Anosov flow transverse to a surface homeomorphic to S. We show that a nonfibered face of the Thurston norm ball can be dynamically represented by two distinct flows that differ by a veering mutation. Furthermore, one of the discussed pairs of homeomorphic veering mutants can be used to construct counterexamples to the classification theorem of Anosov flows on Bonatti–Langevin manifolds published in the 90s.

57K30, 57Q15; 37D20, 57K32

1 Introduction

Let M be a compact oriented 3-manifold M whose interior admits a complete hyperbolic structure. The *Thurston norm* on $H_2(M, \partial M; \mathbb{R})$ measures the minimal topological complexity of surfaces that represent

a homology class; see Thurston [50]. It has been intensively studied in various different contexts. It is related to finite depth foliations (see Gabai [18]), the Alexander polynomial (see Dunfield [9] and McMullen [35]), the L^2-torsion function (see Friedl and Lück [16]), Floer homology (see Ozsváth and Szabó [43]) and many other aspects of 3-dimensional topology. Here we focus on the connection between the Thurston norm on $H_2(M, \partial M; \mathbb{R})$ and nonsingular flows on M. Originally this connection was drawn by Fried [13; 14] and Mosher [41; 42]. The topic has reemerged recently in work of Landry [28; 29; 30] and Landry, Minsky and Taylor [31; 32], where they relate the Thurston norm with veering triangulations.

Since the unit norm ball $\mathbb{B}_{\mathrm{Th}}$ of the Thurston norm is a compact polytope [50, Theorem 2], we can speak about its *faces*. Thurston proved that all ways in which M fibers over the circle are encoded by finitely many, potentially zero, top-dimensional faces of $\mathbb{B}_{\mathrm{Th}}$, called *fibered faces* [50, Theorem 3]. The first known connection between pseudo-Anosov flows and the Thurston norm concerned only these faces. Assuming that M is closed, Fried proved that associated to a fibered face $\mathtt{F}$ there is a unique, up to isotopy and reparametrization, pseudo-Anosov flow Ψ on M with the property that a class $\eta \in H_2(M; \mathbb{Z})$ can be represented by a cross-section to Ψ if and only if η is in the interior of the cone $\mathbb{R}_+ \cdot \mathtt{F}$ [14, Theorem 7]. Mosher extended Fried's result by showing that $\eta \in H_2(M; \mathbb{Z})$ can be represented by a surface that is *almost transverse* to Ψ if and only if η is in $\mathbb{R}_+ \cdot \mathtt{F}$ [40, Theorem 1.4]. Results of Fried and Mosher are stated for closed manifolds, but they can be generalized to the case of flows on 3-manifolds with toroidal boundary whose interior admits a complete hyperbolic structure; see [30, Theorem 3.5]. In this case, the relevant flows are obtained from pseudo-Anosov flows by *blowing-up* finitely many closed orbits into toroidal boundary components; see Mosher [42, Section 3.2] and Bonatti and Iakovoglou [4, Section 3.6].

The relationship between pseudo-Anosov flows and the Thurston norm extends beyond the fibered case. In this more general setup, we consider flows which do not admit cross-sections. Such flows are called *noncircular*. Given a potentially noncircular flow Ψ on M denote, by $\mathcal{C}(\Psi)$ the cone in $H_2(M, \partial M; \mathbb{R})$ spanned by the homology classes whose algebraic intersection with the homology classes of closed orbits of Ψ is nonnegative. Following Mosher [41], we say that Ψ *dynamically represents* a (not necessarily fibered, not necessarily top-dimensional) face $\mathtt{F}$ of the Thurston norm ball in $H_2(M, \partial M; \mathbb{R})$ if $\mathcal{C}(\Psi) = \mathbb{R}_+ \cdot \mathtt{F}$ and $\mathbb{R}_+ \cdot \mathtt{F}$ is the maximal cone in $H_2(M, \partial M; \mathbb{R})$ in which the Thurston norm agrees with the minus Euler class of the normal plane bundle to Ψ. From the results of Fried and Mosher mentioned in the last paragraph, it follows that every fibered face is dynamically represented by a flow which is unique up to isotopy and reparametrization. In the nonfibered case, Mosher found sufficient conditions on a noncircular flow to dynamically represent a face of the Thurston norm ball [41, Theorem 2.7] and showed that there are noncircular flows representing nonfibered faces [41, Section 4]. However, the question of whether, for every nonfibered face $\mathtt{F}$ of the Thurston norm ball in $H_2(M, \partial M; \mathbb{R})$, there is a (blown-up) pseudo-Anosov flow Ψ which dynamically represents $\mathtt{F}$ remains open.

We answer two closely related questions. First, if there is a flow which dynamically represents a nonfibered face, is this flow necessarily unique, up to isotopy and reparametrization? In Section 5 we give explicit examples of flows which represent the same nonfibered face of the Thurston norm ball but are not even

topologically equivalent, thus showing that the answer to this question is negative; see Theorem 5.2. These examples have been found using *veering triangulations*, a combinatorial tool to study pseudo-Anosov flows. We refer the reader to Section 2.3 for an outline of the connection between veering triangulations and pseudo-Anosov flows.

Once we know that a nonfibered face can be dynamically represented by two topologically inequivalent flows we may ask how the two distinct flows which dynamically represent the same face are related. Veering triangulations can be helpful in solving this problem as well. The veering census (see Giannopolous, Schleimer and Segerman [20]) and other computational tools to study triangulations [7; 8; 47] can be used to find many examples of veering triangulations that *combinatorially represent* the same face of the Thurston norm ball. At the beginning of Section 4 and in Section 4.2 we briefly outline what the search for appropriate examples boils down to. Since veering triangulations are finite objects that satisfy very restrictive conditions, comparing two veering triangulations is easier than comparing their underlying flows. An analysis of certain examples of veering triangulations which combinatorially represent the same face of the Thurston norm ball led us to define *combinatorial mutations of veering triangulations* along surfaces that they carry. Our main goal is to carefully study these operations and demonstrate that in special cases they can yield distinct flows representing the same face of the Thurston norm ball.

1.1 Combinatorial mutations of veering triangulations

A veering triangulation $\mathcal{V}$ of a 3-manifold M is determined by three pieces of combinatorial data: an ideal triangulation $\mathcal{T}$, a taut structure α on $\mathcal{T}$ and a smoothing of the dual spine of $\mathcal{T}$ into a branched surface $\mathcal{B}$ with certain properties; see Definitions 2.1 and 2.5. Associated to $(\mathcal{T},\alpha)$ there is a finite system of *branch equations* such that if w is a nonzero nonnegative integral solution to this system then w determines a surface S_w which is *carried* by $(\mathcal{T},\alpha)$; see Section 2.1.3. We also say that S_w is carried by $\mathcal{V}$. We will restrict our attention to those carried surfaces whose boundary components lying in the same boundary component of M have the same orientation. We say that such surfaces are *properly carried*. We characterize surfaces properly carried by a veering triangulation in Corollary 2.14. If S_w is properly carried then the result of cutting M along a surface S_w^ϵ properly embedded in M and homotopic to S_w is a *sutured manifold*; see Section 3.3. We denote it by $M|S_w^\epsilon$.

The surface S_w^ϵ is naturally equipped with an ideal triangulation $\mathcal{Q}_{\mathcal{V},w}$ induced from $\mathcal{V}$. Let $\mathrm{Aut}^+(\mathcal{Q}_{\mathcal{V},w})$ be the group of orientation-preserving combinatorial automorphisms of $\mathcal{Q}_{\mathcal{V},w}$. Associated to $\varphi\in\mathrm{Aut}^+(\mathcal{Q}_{\mathcal{V},w})$ there always is a *mutant manifold* M^φ, obtained from the sutured manifold $M|S_w^\epsilon$ by identifying the two copies of S_w^ϵ in its boundary via φ. Our goal is to mimic this construction in the combinatorial setup of triangulations. Unfortunately, it is not as straightforward as it may sound. The main difficulty is the fact that S_w is often not embedded. Thus we may view cutting $\mathcal{T}$ along S_w as equivalent to cutting it along a certain branched surface F_w which fully carries S_w; see Section 3.4. This in turn causes the problem of not being able to use φ directly to reglue the top boundary F_w^+ of $\mathcal{T}|F_w$ to its bottom boundary F_w^-. In Section 3.5 we define a *regluing map* $r(\varphi)\colon F_w^+\to F_w^-$ determined by φ and use it to define a *mutant*

triangulation $\mathcal{T}^\varphi$. Without further assumptions on φ, not only can this triangulation fail to be veering, but it also might not be a triangulation of M^φ. We deal with these issues in Sections 3.6 and 3.7.

Studying mutations has a long history, particularly in knot theory; see for instance Dunfield, Garoufalidis, Shumakovitch and Thistlethwaite [10], Kirk and Livingston [26], Millichap [37] and Morton and Traczyk [39]. Mutant knots share many properties, and much work on mutations concentrates on establishing which knot invariants distinguish mutants. Another thread in the theory is finding sufficient conditions on a surface S and its homeomorphism φ so that M and M^φ share some property. For instance, in [48, Theorem 4.4] Ruberman considered mutations of hyperbolic 3-manifolds and found sufficient conditions for the mutant manifold M^φ to be hyperbolic and have the same hyperbolic volume as M. Our goal to find conditions under which $\mathcal{T}^\varphi$ is a veering triangulation of M^φ fits into this second framework.

1.2 Properties of the mutant triangulation

To analyze the homeomorphism type of the manifold underlying $\mathcal{T}^\varphi$, we introduce the notion of *edge product disks*, a special type of product disks in the sutured manifold $M|S^\epsilon_w$; see Section 3.4. Then we define what it means for $\varphi \in \mathrm{Aut}^+(\mathcal{Q}_{\mathcal{V},w})$ to *misalign edge product disks*; see Definition 3.8. Using this we prove:

Theorem 3.10 *The mutant triangulation $\mathcal{T}^\varphi$ is an ideal triangulation of M^φ if and only if φ misaligns edge product disks.*

To find sufficient conditions for the mutant triangulation to be veering, we first need to ensure that it admits a taut structure. It turns out that for this it also suffices to assume that φ misaligns edge product disks. However, we prove a slightly stronger result:

Proposition 3.16 *The mutant triangulation $\mathcal{T}^\varphi$ admits a taut structure if and only if every vertical annulus or Möbius band in M^φ lies in a prismatic region of M^φ.*

The backward direction of Proposition 3.16 is proved by explicitly constructing a taut structure α^φ on $\mathcal{T}^\varphi$ from the taut structure α on $\mathcal{T}$. We say that $(\mathcal{T},\alpha)$ and $(\mathcal{T}^\varphi,\alpha^\varphi)$ are *taut mutants*.

Intuitively, the condition that appears in the above proposition means that φ might align edge product disks, but it does so in a way which is not visible from the perspective of $\mathcal{T}^\varphi$; see Lemma 3.15. Nonetheless, in light of Theorem 3.10 it is convenient to assume that φ misalign edge product disks, so that we deal only with triangulations of M^φ. This assumption is further justified by the fact that in Proposition 3.17 we prove that when φ aligns edge product disks M^φ cannot admit a veering triangulation.

To obtain sufficient conditions on the taut triangulation $(\mathcal{T}^\varphi,\alpha^\varphi)$ to admit a veering structure, we make use of the branched surface $\mathcal{B}$ defining the veering structure on $\mathcal{V}=(\mathcal{T},\alpha,\mathcal{B})$. This branched surface intersects the 2-skeleton of $\mathcal{T}$ in a train track; see Figure 6. Therefore any surface S_w carried by $\mathcal{V}$ inherits

a train track $\tau_{\mathcal{V},w}$ which is dual to its ideal triangulation $\mathcal{Q}_{\mathcal{V},w}$. By $\mathrm{Aut}^+(\mathcal{Q}_{\mathcal{V},w} \mid \tau_{\mathcal{V},w})$ we denote the subgroup of $\mathrm{Aut}^+(\mathcal{Q}_{\mathcal{V},w})$ consisting of orientation-preserving combinatorial automorphisms of $\mathcal{Q}_{\mathcal{V},w}$ which preserve $\tau_{\mathcal{V},w}$.

Theorem 3.19 *Let S_w be a surface properly carried by a veering triangulation $\mathcal{V} = (\mathcal{T}, \alpha, \mathcal{B})$ of M. Suppose that $\varphi \in \mathrm{Aut}^+(\mathcal{Q}_{\mathcal{V},w})$ misaligns edge product disks. If additionally $\varphi \in \mathrm{Aut}^+(\mathcal{Q}_{\mathcal{V},w} \mid \tau_{\mathcal{V},w})$ then $(\mathcal{T}^\varphi, \alpha^\varphi)$ admits a veering structure.*

Under the assumptions of this theorem, the branched surface $\mathcal{B}$ dual to $\mathcal{T}$ mutates into a branched surface $\mathcal{B}^\varphi$ that is dual to $\mathcal{T}^\varphi$ and satisfies Definition 2.5. We say that $\mathcal{V}^\varphi = (\mathcal{T}^\varphi, \alpha^\varphi, \mathcal{B}^\varphi)$ is obtained from $\mathcal{V} = (\mathcal{T}, \alpha, \mathcal{B})$ by a *veering mutation* or that $\mathcal{V}^\varphi$ and $\mathcal{V}$ are *veering mutants*.

Observe that Theorem 3.19 gives a sufficient condition for a taut mutant $(\mathcal{T}^\varphi, \alpha^\varphi)$ to be veering. It is, however, possible that $(\mathcal{T}^\varphi, \alpha^\varphi)$ admits a veering structure even when $\varphi \notin \mathrm{Aut}^+(\mathcal{Q}_{\mathcal{V},w} \mid \tau_{\mathcal{V},w})$. This can happen whenever, after cutting $\mathcal{T}$ along F_w, the cut triangulation $\mathcal{T}|F_w$ admits a veering structure $\mathcal{B}^*|F_w$ which mutates into a branched surface that is dual to $\mathcal{T}^\varphi$ and satisfies Definition 2.5. If $\mathcal{B}^*|F_w \neq \mathcal{B}|F_w$ we do not consider such triangulations to be veering mutants. This construction can be used to prove a generalization of Theorem 3.19 giving a sufficient and necessary conditions on a taut mutant of a veering triangulation to be veering.

Theorem 3.21 *Let S_w be a surface properly carried by a veering triangulation $\mathcal{V} = (\mathcal{T}, \alpha, \mathcal{B})$ of M. Suppose that $\varphi \in \mathrm{Aut}^+(\mathcal{Q}_{\mathcal{V},w})$ misaligns edge product disks. The taut triangulation $(\mathcal{T}^\varphi, \alpha^\varphi)$ admits a veering structure if and only if there is a veering structure $\mathcal{B}^*|F_w$ on $(\mathcal{T}|F_w, \alpha|F_w)$ such that the isomorphism $\varphi\colon \mathcal{Q}^+_{\mathcal{V},w} \to \mathcal{Q}^-_{\mathcal{V},w}$ sends $\tau^{*\,+}_{\mathcal{V},w}$ to $\tau^{*\,-}_{\mathcal{V},w}$.*

In Section 3.8 we give an example of a pair of veering triangulations which are taut mutants but not veering mutants. This proves that the generalization appearing in Theorem 3.21 is not just theoretical, but actually arises in practice. In the same subsection we also define a *veering mutation with insertion*, a certain generalization of a veering mutation where the related triangulations have different numbers of tetrahedra.

1.3 Homeomorphic veering mutants

In Section 4 we analyze a few examples of homeomorphic veering mutants. Apart from illustrating our constructions, we use these examples to establish the following facts connecting veering mutations and faces of the Thurston norm ball:

Fact 4.2 (Veering mutations and faces of the Thurston norm ball) (1) *There are nonfibered faces of the Thurston norm ball that can be represented by two combinatorially nonisomorphic veering mutants.*

(2) *A veering mutation along a surface representing a class lying at the boundary of the cone on a fibered face may yield a veering triangulation representing a nonfibered face of the Thurston norm ball of the mutant manifold.*

Analyzing two veering mutants of the complement of the 10^3_{12} link leads to the following discovery:

Fact 4.7 *The complement of the 10^3_{12} link admits two fibrations over the circle such that:*

- *The fiber is a genus-two surface with four punctures.*
- *The monodromy of one fibration is obtained from the monodromy of the other fibration by post-composing it with an involution. In particular, the stretch factors of the monodromies are equal.*
- *The monodromies are not conjugate in the mapping class group of a genus-two surface with four punctures.*

The last part of Fact 4.7 follows from the observation that the Euler classes of the two fibrations lie in different orbits under the action of $\mathrm{Homeo}(M)$ on $H^2(M, \partial M; \mathbb{R})$. Examples of such fibrations of the same manifold were known previously; see for instance McMullen and Taubes [36, Theorem 1.2]. What is new here is that we get fiber bundles which are not isomorphic, even though both their total spaces and fibers are homeomorphic, and the stretch factors of their monodromies are the same.

1.4 Multiple distinct flows dynamically representing the same face of the Thurston norm ball

Given a veering triangulation $\mathcal{V}$ of M, it is possible to construct a transitive pseudo-Anosov flow Ψ on a closed Dehn filling N of M, provided that a certain natural condition on the Dehn filling slopes is satisfied; see Agol and Tsang [1, Theorem 5.1], stated here as Theorem 2.20. Let Ψ° be the blown-up flow on M. If $\mathcal{V}$ combinatorially represents a face $\mathtt{F}$ of the Thurston norm ball in $H_2(M, \partial M; \mathbb{R})$ then Ψ° dynamically represents $\mathtt{F}$; see Landry, Minsky and Taylor [31, Theorem 6.1], stated here as Theorem 2.29. Under additional assumptions on the Dehn filling slopes, there is also a face $\mathtt{F}_N$ of the Thurston norm ball in $H_2(N; \mathbb{R})$ such that $\mathbb{R}_+ \cdot \mathtt{F}_N = \mathcal{C}(\Psi)$; see Landry [29, Theorem A], stated here as Theorem 2.30. These results are the main ingredients to prove the following theorem:

Theorem 5.2 *There are nonfibered faces of the Thurston norm ball that can be dynamically represented by two topologically inequivalent flows.*

In the case of manifolds with nonempty boundary, we show that a nonfibered face can be dynamically represented by two topologically inequivalent blown-up Anosov flows constructed from a pair of homeomorphic veering mutants. Unfortunately, the corresponding Anosov flows on the Dehn-filled manifold cannot be used to prove the theorem in the closed case because the manifold is toroidal. For this reason, we refer to a different pair of veering triangulations which represent the same face of the Thurston norm ball and, after appropriate Dehn filling, yield transitive pseudo-Anosov flows on a hyperbolic 3-manifold. These veering triangulations are not related by a veering mutation; see Fact 4.6. In particular, it is worth emphasizing that not all pairs of veering triangulations combinatorially representing the same face of the Thurston norm ball are related by a veering mutation or even a veering mutation with insertion.

Remark Although Anosov flows underlying homeomorphic veering mutants $\mathcal{V}$ and $\mathcal{V}^{\varrho\sigma}$ discussed in Section 4.1 cannot be used to prove Theorem 5.2 in the closed case, they have another interesting feature. The closed manifold N obtained by Dehn filling $M \cong M^{\varrho\sigma}$ along the boundary of the mutating surface is a graph manifold constructed from the orientable circle bundle over a 2-holed $\mathbb{R}P^2$ by identifying its two toroidal boundary components. In [2] Barbot calls such manifolds *BL-manifolds*. The Anosov flows Ψ and $\Psi^{\varrho\sigma}$ on N built from $\mathcal{V}$ and $\mathcal{V}^{\varrho\sigma}$, respectively, are counterexamples to the claim, which appears as [2, Theorem B(2)], that all non-$\mathbb{R}$-covered Anosov flows on a fixed BL-manifold are topologically equivalent; see Remark 5.3.

1.5 Polynomial invariants of veering triangulations representing the same face of the Thurston norm ball

In [32] Landry, Minsky, and Taylor introduced two polynomial invariants of veering triangulations: the *taut polynomial* and the *veering polynomial*. They proved that the taut polynomial generalizes the *Teichmüller polynomial*, an invariant of a fibered face of the Thurston norm ball defined by McMullen in [34], to faces of the Thurston norm ball that are combinatorially represented by veering triangulations [32, Theorem 7.1]. In Table 3 we list the taut and veering polynomials of veering triangulations representing the same face of the Thurston norm ball that we discussed in Section 4. We deduce that in the nonfibered case the taut and veering polynomials are not invariants of faces of the Thurston norm ball combinatorially represented by veering triangulations.

Fact 6.1 *There are nonfibered faces of the Thurston norm ball that can be combinatorially represented by two distinct veering triangulations with different taut polynomials, and different veering polynomials.*

1.6 Further questions

In Section 7 we speculate about what happens on the level of flows when we perform a veering mutation. We also ask a few questions concerning veering mutations, faces of the Thurston norm ball dynamically represented by multiple distinct flows, connections between this work and a recent result of Barthelmé, Frankel and Mann [3] characterizing topologically inequivalent pseudo-Anosov flows on a fixed manifold, and hyperbolic volumes of veering mutants.

Acknowledgements

I am grateful to Michael Landry and Chi Cheuk Tsang for answering my questions about their work connecting veering triangulations and pseudo-Anosov flows. I thank Saul Schleimer for discussions on veering triangulations analyzed in Section 4.1. I thank Thomas Barthelmé and Chi Cheuk Tsang for discussions that led to Remark 5.3. Finally, I thank the referee for their valuable comments and suggestions.

This project was partially supported by the Simons Investigator Award 409745 of Vladimir Marković.

2 Veering triangulations and pseudo-Anosov flows

Let M be a compact oriented 3-manifold. By an *ideal triangulation* of M we mean an expression of $M - \partial M$ as a collection of finitely many ideal tetrahedra with triangular faces identified in pairs by homeomorphisms which send vertices to vertices. Links of ideal vertices of the triangulation correspond to boundary components of M.

Let $\mathcal{T}$ be a finite ideal triangulation of M. Every triangular face of $\mathcal{T}$ has two *embeddings* into two, not necessarily distinct, tetrahedra. Every edge of $\mathcal{T}$ has finitely many embeddings into tetrahedra of $\mathcal{T}$ and the same number of embeddings into faces of $\mathcal{T}$. By *edges of a triangle/tetrahedron* or *triangles of a tetrahedron* we mean embeddings of these ideal simplices into the boundary of a higher-dimensional ideal simplex. Similarly, by *triangles/tetrahedra attached to an edge* we mean triangles/tetrahedra in which the edge is embedded, together with this embedding. Observe that triangles/tetrahedra attached to an edge can be circularly ordered, and hence we can speak about consecutive triangles/tetrahedra attached to an edge.

Every ideal triangulation $\mathcal{T}$ determines a 2-dimensional complex $\mathcal{D}$ dual to $\mathcal{T}$, called the *dual spine* of $\mathcal{T}$. For every tetrahedron t of $\mathcal{T}$ there is a vertex $v = v(t)$ of $\mathcal{D}$. If tetrahedra t_1 and t_2 of $\mathcal{T}$ admit faces f_1 and f_2, respectively, which are identified in $\mathcal{T}$, then in $\mathcal{D}$ there is an edge joining their dual vertices v_1 and v_2. Finally, each edge e of $\mathcal{T}$ gives a 2-cell of $\mathcal{D}$ which is glued along the edges of $\mathcal{D}$ that are dual to the consecutive triangles attached to e. Since there are no higher-dimensional cells in $\mathcal{D}$, and 0- and 1-cells have special names, we will often refer to the 2-cells of $\mathcal{D}$ as just "cells".

Translating between properties of an ideal triangulation and properties of its dual spine is straightforward. Throughout the paper we freely alternate between these two perspectives depending on which one is more useful in a given context.

2.1 Taut triangulations

In [27, Introduction] Lackenby introduced *taut ideal triangulations* of 3-manifolds. Using the duality between an ideal triangulation and its dual spine we define tautness of an ideal triangulation in terms of properties of its dual spine.

Definition 2.1 A *taut structure* α on an ideal triangulation $\mathcal{T}$ is a choice of orientations on the edges of its dual spine $\mathcal{D}$ such that

(1) every vertex v of $\mathcal{D}$ has two incoming edges and two outgoing edges,

(2) every cell s of $\mathcal{D}$ has exactly one vertex b_s such that the two edges of s adjacent to v both point out of b_s,

(3) every cell s of $\mathcal{D}$ has exactly one vertex t_s such that the two edges of s adjacent to v both point into t_s.

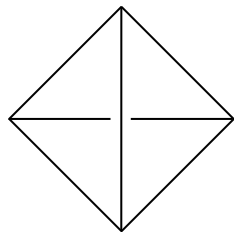

Figure 1: The taut tetrahedron.

A *taut triangulation* is a pair $(\mathcal{T},\alpha)$, where $\mathcal{T}$ is an ideal triangulation, and α is a taut structure on $\mathcal{T}$. If $(\mathcal{T},\alpha)$ is taut then for every cell s of the dual spine of $\mathcal{T}$ the vertex from Definition 2.1(2) is called the *bottom vertex* of s, and the vertex from Definition 2.1(3) is called the *top vertex* of s.

Remark 2.2 Taut triangulations are often called *transverse taut triangulations*; see eg [12; 45; 46].

Intuitively, tautness of an ideal triangulation gives an upwards direction which is consistent throughout the whole triangulation. Under the duality, orientations on the edges of $\mathcal{D}$ translate into coorientations on the faces of $\mathcal{T}$. If $(\mathcal{T},\alpha)$ is taut then, by Definition 2.1(1), every tetrahedron t of $\mathcal{T}$ has two faces whose coorientations point into t, and two faces whose coorientations point out of t. We call the pair of faces whose coorientations point out of t the *top faces* of t and the pair of faces whose coorientations point into t the *bottom faces* of t. We also define the *top diagonal* of t to be the common edge of the two top faces of t and the *bottom diagonal* of t to be the common edge of the two bottom faces of t. By Definition 2.1(2), every edge of $\mathcal{T}$ is embedded as the top diagonal in precisely one tetrahedron of $\mathcal{T}$. Similarly, Definition 2.1(3) implies that every edge of $\mathcal{T}$ is embedded as the bottom diagonal in precisely one tetrahedron of $\mathcal{T}$. We encode a taut structure on a tetrahedron by drawing it as a quadrilateral with two diagonals — one on top of the other; see Figure 1. Then the convention is that coorientations on all faces point towards the reader. In other words, we view the tetrahedron *from above*.

2.1.1 The horizontal branched surface Let e be an edge of a taut triangulation $(\mathcal{T},\alpha)$. To every embedding $\epsilon(e)$ of e into a tetrahedron t of $\mathcal{T}$ we assign a dihedral angle 0 or π in the following way. If $\epsilon(e)$ is either the top or the bottom diagonal of t we assign to $\epsilon(e)$ the angle π. Otherwise we assign to $\epsilon(e)$ the angle 0. This equips the 2-skeleton of $\mathcal{T}$ with a structure of a branched surface with branch locus equal to the 1-skeleton of $\mathcal{T}$; see Figure 2. We call it the *horizontal branched surface* associated to $\mathcal{T}$, and denote it by $\mathcal{H}$.

Let $-\alpha$ denote the taut structure on $\mathcal{T}$ obtained by reversing orientations of all edges of the dual spine $\mathcal{D}$ of $\mathcal{T}$. Taut triangulations $(\mathcal{T},\alpha)$ and $(\mathcal{T},-\alpha)$ determine the same dihedral angles between consecutive faces attached to edges of $\mathcal{T}$ and thus the same horizontal branched surface. We call $(\mathcal{T},\pm\alpha)$ a *taut angle structure* on $\mathcal{T}$. This term will appear in Section 2.2.3.

2.1.2 The boundary track Recall that boundary components of M correspond to links of vertices of $\mathcal{T}$. An ideal vertex of tetrahedron t of $\mathcal{T}$ meets three faces of t. Thus an ideal triangulation $\mathcal{T}$ of M

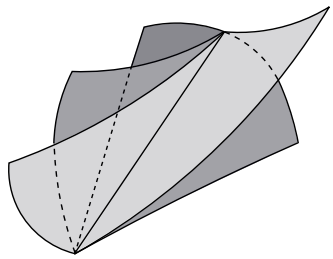

Figure 2: The horizontal branched surface associated to a taut triangulation.

determines a triangulation $\partial\mathcal{T}$ of ∂M. If $\mathcal{T}$ is additionally taut, the smoothing of the 2-skeleton $\mathcal{T}^{(2)}$ into the horizontal branched surface determines a smoothing of $\partial\mathcal{T}$ into a train track. We call this train track the *boundary track* of $\mathcal{T}$ and denote it by β. If an ideal vertex of t meets faces f_1, f_2 and f_3 of t then exactly one pair (f_i, f_j), for $i \neq j$, is adjacent either along the top or along the bottom diagonal of t. In the construction of the horizontal branched surface of $\mathcal{T}$ we assign to such a pair the dihedral angle π, and to the remaining pairs we assign the dihedral angle 0. Thus every complementary region of β is a bigon. This has important implications for the topology of ∂M. If τ is a train track in a surface S without boundary then the Euler characteristic of S is equal to half the sum of indices of all complementary regions of τ in S, where the index of a complementary region C is the quantity

$$\operatorname{index}(C) = 2\chi(C) - \#\text{cusps in } \partial C.$$

It follows that any surface admitting a bigon train track has zero Euler characteristic. Among closed orientable surfaces only the torus satisfies this condition. Below we state this observation as a lemma. We will refer to it in the proof of Proposition 3.16 to show that in some situations the mutant triangulation does not admit a taut structure.

Lemma 2.3 *Suppose that an oriented 3-manifold M admits a taut ideal triangulation. Then the boundary of M is nonempty and consists of tori.* □

2.1.3 Surfaces carried by a taut triangulation Let $(\mathcal{T}, \alpha)$ be a taut triangulation of an oriented 3-manifold M, with the set T of tetrahedra, the set F of faces and the set E of edges. Recall from Section 2.1.1 that α determines a branched surface structure on $\mathcal{T}^{(2)}$, which we call the horizontal branched surface and denote by $\mathcal{H}$; see Figure 2. The 1-skeleton of $\mathcal{T}$ is the branch locus of $\mathcal{H}$. Thus each (oriented) edge e of $(\mathcal{T}, \alpha)$ determines a *branch equation* defined as follows. Let $f_1, f_2, \dots, f_k$ be triangles attached to e on the left side, ordered from the bottom to the top. Let $f_1', f_2', \dots, f_l'$ be triangles attached to e on the right side, also ordered from the bottom to the top. Then the branch equation determined by e is given by

$$f_1 + f_2 + \cdots + f_k = f_1' + f_2' + \cdots + f_l'. \tag{2.4}$$

Let $w = (w_f)_{f \in F}$ be a nonzero nonnegative integral solution to the system of branch equations of $(\mathcal{T}, \alpha)$. We call the number w_f the *weight* of f and w a *weight system* on $(\mathcal{T}, \alpha)$. Using weights of triangles

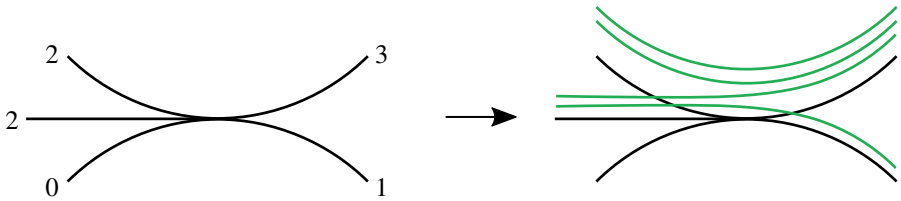

Figure 3: From a solution to branch equations to an embedded surface.

we can define the weight w_e of an edge $e \in E$ as the sum of weights of faces attached to e on one of its sides. For an edge satisfying the branch equation (2.4) we have

$$w_e = \sum_{i=1}^{k} w_{f_i} = \sum_{j=1}^{l} w_{f'_j}.$$

Equip the triangles of $\mathcal{T}$ with an orientation determined by their coorientation via the right-hand rule. Then the (relative) 2-chain

$$S_w = \sum_{f \in F} w_f f$$

is a 2-cycle giving an oriented surface properly immersed in M. It is embedded if and only if $w_e \leq 1$ for every $e \in E$. Let $x \in E \cup F$. If $w_x > 1$ then multiple copies of x are pinched together. Pulling these overlapping regions of S_w slightly apart yields an oriented surface S_w^ϵ which is properly embedded in M; see Figure 3. We say that S_w^ϵ is *carried* by $(\mathcal{T}, \alpha)$. If additionally for every boundary component T of M all connected components of $S_w^\epsilon \cap T$ have the same orientation, we say that S_w^ϵ (or S_w) is *properly carried* by $(\mathcal{T}, \alpha)$.

More generally, we say that a surface S properly embedded in M is *carried* by $(\mathcal{T}, \alpha)$ if there exists a nonzero nonnegative integral solution $w = (w_f)_{f \in F}$ to the system of branch equations of $(\mathcal{T}, \alpha)$ such that S is homotopic to the relative 2-cycle S_w. If S_w is properly carried then we say that S is properly carried. Note that the same properly embedded surface S can be carried by $(\mathcal{T}, \alpha)$ in multiple different ways. When we write S_w or S_w^ϵ we always mean a surface in a fixed carried position corresponding to the weight system w.

If there exists a strictly positive integral solution w to the system of branch equations of $(\mathcal{T}, \alpha)$, we say that $(\mathcal{T}, \alpha)$ is *layered*. If there exists a nonnegative nonzero integral solution, but no strictly positive integral solution, then we say that $(\mathcal{T}, \alpha)$ is *measurable*. If there is no nonnegative nonzero solution to the system of branch equations of $(\mathcal{T}, \alpha)$ then we say that $(\mathcal{T}, \alpha)$ is *nonmeasurable*.

2.1.4 The Euler class of a taut triangulation A taut triangulation $(\mathcal{T}, \alpha)$ of M determines the *Euler class* $\chi_{(\mathcal{T},\alpha)}$, an element of $H^2(M, \partial M; \mathbb{R})$ which satisfies $\chi_{(\mathcal{T},\alpha)}([S]) = \chi(S)$ for every surface S carried by $(\mathcal{T}, \alpha)$; see [27, page 390; 32, Section 5.2]. It can be defined as follows. Let Γ be the 1-skeleton of the dual spine of $(\mathcal{T}, \alpha)$. By Definition 2.1(1), every vertex v of Γ has two incoming edges and two outgoing

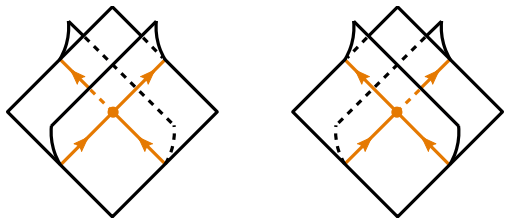

Figure 4: The dual spine of a veering triangulation can be smoothed into a branched surface which around every vertex looks like one of the above configurations. Orientation on the edges of the branch locus is relevant.

edges. Therefore Γ forms a 1-cycle. Let $[\Gamma]$ be the associated homology class in $H_1(M;\mathbb{R})$. The *Euler class* $\chi_{(\mathcal{T},\alpha)}$ is defined by the equality

$$\chi_{(\mathcal{T},\alpha)}(\cdot) = -\tfrac{1}{2}\langle[\Gamma],\cdot\rangle,$$

where $\langle\cdot,\cdot\rangle$ denotes the algebraic intersection pairing.

2.2 Veering triangulations

Taut triangulations are abundant in 3-manifolds [27, Theorem 1]. In contrast, veering triangulations, a subclass of taut triangulations defined below, are very rare. It is conjectured that any hyperbolic 3-manifold with toroidal boundary admits only finitely many, potentially zero.

Definition 2.5 A *veering structure* on a taut ideal triangulation is a smoothing of its dual spine into a branched surface $\mathcal{B}$ which locally around every vertex looks as in either of the pictures in Figure 4.

A *veering triangulation* is a taut ideal triangulation with a veering structure. We call the branched surface $\mathcal{B}$ from Definition 2.5 the *stable branched surface* of a veering triangulation. We emphasize that its branch locus is oriented by the taut structure on the triangulation.

The stable branched surface $\mathcal{B}$ of a veering triangulation can be transversely orientable or not. If $\mathcal{B}$ is transversely orientable, we say that $\mathcal{V}$ is *edge-orientable*. Otherwise we say that $\mathcal{V}$ is not edge-orientable. We refer the reader to [45] for more information about edge-orientability and how it affects certain polynomial invariants of veering triangulations.

Remark 2.6 In [51] a branched surface which locally around every vertex looks like in Figure 4, and has only solid tori or torus shells as complementary regions, is called a *veering branched surface*. However, the author of [51] orients the branch locus of this branched surface in the opposite direction.

Definition 2.5 implies that a veering triangulation is determined by three pieces of combinatorial data:

(1) an ideal triangulation $\mathcal{T}$,

(2) a taut structure α; see Definition 2.1,

(3) a veering structure $\mathcal{B}$; see Definition 2.5.

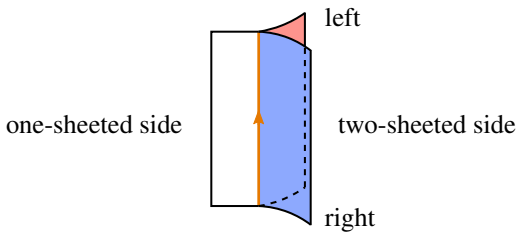

Figure 5: One of the sectors on the two-sheeted side veers to the right, the other veers to the left.

For brevity, we typically denote a veering triangulation by a calligraphic letter $\mathcal{V}$, potentially with some sub- or superscript, by which we mean $\mathcal{V} = (\mathcal{T}, \alpha, \mathcal{B})$.

Definition 2.5 is "dual" to the now-standard definition of a veering triangulation that requires the existence of a certain coloring on the edges of triangulation; see [12, Definition 5.1]. Below we explain how to translate between the two definitions. When viewing the dual spine of a veering triangulation as a branched surface, we call its 2-cells *sectors*. Every edge d of $\mathcal{B}$ is adjacent to three sectors of $\mathcal{B}$. The structure of a branched surface on $\mathcal{B}$ determines the *one-sheeted side* of d and the *two-sheeted side* of d; see Figure 5. We say that a sector s adjacent to d is *large* relative to d if it is on the one-sheeted side of d. Otherwise we say that s is *small* relative to d. Thus two out of three sectors adjacent to d are small relative to d. Since d is oriented, and the manifold underlying $\mathcal{V}$ is oriented, we can detect in which direction (right/left) each of these small sectors veers. One of them veers to the right of d, and the other to the left of d. These directions are marked in Figure 5.

Lemma 2.7 *Let s be a sector of the stable branched surface of a veering triangulation. Let d_1 and d_2 be two consecutive edges of s. Let v be the common vertex of d_1 and d_2.*

(1) *If the orientations of d_1 and d_2 both point into v, then s is large relative to both d_1 and d_2.*

(2) *If the orientations of d_1 and d_2 both point out of v, then s is small relative to both d_1 and d_2, and if it veers right (respectively, left) of d_1, then it veers right (respectively, left) of d_2.*

(3) *If the orientation of d_1 points into v and the orientation of d_2 points out of v, then either s is small relative to d_1 and large relative to d_2, or s is small relative to both d_1 and d_2, in which case if it veers right (respectively, left) of d_1, then it veers right (respectively, left) of d_2.*

In particular, s has at least four edges.

Proof The statement of this lemma is a verbalization of the local picture of $\mathcal{B}$ presented in Figure 4. □

Lemma 2.7 says that if s veers to the right (respectively, left) of d then for every other edge d' of s such that s is small relative to d', s veers to the right (respectively, left) of d'. Since, by Lemma 2.7(2), s is small relative to at least two of its edges, the *veering direction* of s is well defined. We can therefore assign colors, red and blue, to the sectors of $\mathcal{B}$ so that right-veering sectors are colored blue and left-veering sectors are colored red; see Figure 5. We call them the *veering colors* on $\mathcal{B}$. Dually, we obtain a coloring on the edges of $\mathcal{V}$.

Corollary 2.8 *Let $\mathcal{V}$ be a veering triangulation. The veering colors on sectors of the stable branched surface of $\mathcal{V}$ determine colors on edges of $\mathcal{V}$ such that for every tetrahedron t of $\mathcal{V}$ the following two conditions hold*:

- *Let e_0, e_1 and e_2 be edges of a top face of t, ordered counterclockwise as viewed from above and so that e_0 is the top diagonal of t. Then e_1 is red and e_2 is blue.*
- *Let e_0, e_1 and e_2 be edges of a bottom face of t, ordered counterclockwise as viewed from above and so that e_0 is the bottom diagonal of t. Then e_1 is blue and e_2 is red.* □

The conditions from Corollary 2.8 are exactly the veeringness conditions that appear in [12, Definition 5.1]. Therefore if a triangulation is veering in the sense of Definition 2.5 then it is veering in the sense of [12, Definition 5.1]. The converse also holds. This can be seen by observing that colors on edges of a veering tetrahedron t that satisfy the conditions listed in Corollary 2.8 determine how to smooth the dual spine of t into a branched surface which locally around its vertices looks like the one presented in Figure 4: blue edges are dual to right veering sectors, and red edges are dual to left veering sectors; see Figure 5.

Remark 2.9 The dual spine of a veering triangulation $\mathcal{V}$ can be smoothed into another branched surface, called the *unstable branched surface* of $\mathcal{V}$. We denote it by $\mathcal{B}^u$; see [12, Section 6.1]. It is also encoded by the colors on edges of $\mathcal{V}$. If t is a tetrahedron of $\mathcal{V}$ whose bottom diagonal is blue (respectively, red) then $\mathcal{B}^u_t = \mathcal{B}^u \cap t$ is obtained from Figure 4, left (respectively, Figure 4, right), by rotating it by π in the plane of the page and then reversing orientations of all edges in the branch locus.

Remark 2.10 If M admits a veering triangulation $\mathcal{V} = (\mathcal{T}, \alpha, \mathcal{B})$ then it also admits a veering triangulation $-\mathcal{V} = (\mathcal{T}, -\alpha, -\mathcal{B}^u)$, where $-\alpha$ is obtained from α by reversing orientations of all edges of the dual spine of $\mathcal{T}$, and $-\mathcal{B}^u$ is the unstable branched surface of $\mathcal{V}$ with orientation on the branch locus given by $-\alpha$.

In Proposition 3.17 we will use the following crucial fact about veering triangulations:

Theorem 2.11 (Hodgson, Rubinstein, Segerman and Tillmann [23, Theorem 1.5]) *Suppose that M is a compact oriented 3-manifold that admits a veering triangulation. Then the interior of M admits a complete hyperbolic metric.* □

2.2.1 The stable train track of a veering triangulation Let $\mathcal{B}$ be the stable branched surface of a veering triangulation $\mathcal{V}$. For every face f of $\mathcal{V}$ the intersection of $\mathcal{B}$ with f is a train track with one switch v_f in the interior of f and three branches, each joining v_f with the midpoint of an edge of f. The union of all these train tracks in faces of $\mathcal{V}$ gives a train track in the horizontal branched surface of $\mathcal{V}$. We call it the *stable train track* of $\mathcal{V}$, and denote it by τ. A picture of τ restricted to the faces of one veering tetrahedron is presented in Figure 6.

Let $\tau_f = \tau \cap f$. It is a trivalent train track with one large branch and two small branches. We say that an edge e of f is the *large edge* of f if it is dual to the large branch of τ_f. Otherwise we say that e is a small edge of f. The key property of the stable train track is stated in the following lemma:

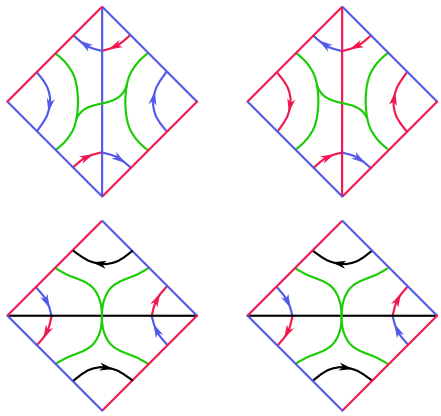

Figure 6: Left column: a veering tetrahedron with blue top diagonal. Right column: a veering tetrahedron with red top diagonal. Top faces are presented in the top row, bottom faces in the bottom row. The stable train track is in green. Oriented arcs around vertices correspond to branches of the boundary track.

Lemma 2.12 *Let f be a top face of a tetrahedron t of a veering triangulation $\mathcal{V}$. Then the large edge of f is identified with the bottom diagonal of the tetrahedron immediately above f.*

Proof Let t' be the tetrahedron immediately above f. There is a bottom face f' of t' such that the large edge of f is identified with an edge e' of f'. The picture of the stable train track in the bottom faces of a veering tetrahedron (Figure 6) indicates that e' must be the bottom diagonal of t'. □

The stable branched surface and the stable train track carry the same combinatorial information. However, it is beneficial to have both these perspectives on the same object, as they have different applications in this paper. In Section 3.7 we use the stable train track to define a certain subgroup of the group of orientation-preserving combinatorial automorphisms of a surface carried by a veering triangulation. The whole branched surface is more natural to use in the proof of Theorem 3.19, which says that under certain conditions a mutant of a veering triangulation is veering.

2.2.2 The boundary track of a veering triangulation Let $\mathcal{V} = (\mathcal{T}, \alpha, \mathcal{B})$ be a veering triangulation of a 3-manifold M. In Section 2.1.2 we defined the boundary track β of $(\mathcal{T}, \alpha)$. A (bigon) complementary region r of β has three switches, corresponding to three edges of some tetrahedron t meeting at a vertex of that tetrahedron. A switch in the boundary of r is smooth if and only if it is an endpoint of either the top or the bottom diagonal of t. We say that r is *ascending* if its smooth switch is an endpoint of the top diagonal of t. Otherwise we say that r is *descending*.

Now that we have a veering structure on the triangulation as well, we can color the switches and branches of the boundary track using the colors of edges determined by Corollary 2.8 and the following rules. If a switch s of β is an endpoint of an edge e we color s by the color of e. If a branch b of β corresponds to an arc around a vertex v of a triangle f we color b by the color of the edge of f opposite to v; see Figure 6.

This coloring on the boundary track of a veering triangulation was first introduced by Futer and Guéritaud in [17, Section 2]. We orient b using the coorientation on f and the right-hand rule. With this orientation, if S_w is a surface carried by $\mathcal{V}$, as defined in Section 2.1.3, then ∂S_w is an oriented smooth 1-cycle in β.

If b connects two switches of the same color (necessarily of a different color than b; see Corollary 2.8), we say that b is a *ladderpole branch*. In Figure 6 ladderpole branches are shown as arcs connecting a diagonal edge to a nondiagonal edge of the same color, or vice versa. Since every edge of $\mathcal{V}$ is the top diagonal of exactly one tetrahedron and the bottom diagonal of exactly one tetrahedron, every switch of β is adjacent to exactly two ladderpole branches. It follows that the union of all ladderpole branches is a disjoint union of simple closed curves on ∂M. We call these curves the *ladderpole curves* of $\mathcal{V}$. We say that a ladderpole curve l is red (respectively, blue) if it consists of red (respectively, blue) ladderpole branches. Each boundary component of M contains an even number of ladderpole curves which alternate in color.

Let S_w^ϵ be a surface properly embedded in M obtained by slightly pulling apart the overlapping regions of S_w. Recall from Section 2.1.3 that S_w is not properly carried if there is a boundary component T of M such that two connected components $S_w^\epsilon \cap T$ have opposite orientations. In the following lemma we characterize the boundary slopes of such surfaces.

Lemma 2.13 *A surface S_w carried by a veering triangulation of M is not properly carried if and only if there is a boundary component T of M such that ∂S_w runs both along a blue ladderpole curve of T and along a red ladderpole curve of T.*

Proof Using Figure 6 we can make the following observations:

(1) Let l_b be a blue ladderpole branch. Let r_b^a and r_b^d be the ascending and the descending complementary region of β adjacent to l_b, respectively. Then l_b is oriented from the smooth switch of r_b^a to the smooth switch of r_b^d. The remaining branches of r_b^a are oriented towards l_b, while the remaining branches of r_b^d are oriented away from l_b.

(2) Let l_r be a red ladderpole branch. Let r_r^a and r_r^d be the ascending and the descending complementary region of β adjacent to l_r, respectively. Then l_r is oriented from the smooth switch of r_r^d to the smooth switch of r_r^a. The remaining branches of r_r^a are oriented away from l_r, while the remaining branches of r_r^d are oriented towards l_b.

It follows that two smooth parallel cycles in β contained in the same boundary component of M have opposite orientations if and only if one of them runs along a red ladderpole curve and the other runs along a blue ladderpole curve. □

Observe that a surface S_w carried by $\mathcal{V}$ inherits from $\mathcal{V}$ both an ideal triangulation and the stable train track. We denote these structures in S_w by $\mathcal{Q}_{\mathcal{V},w}$ and $\tau_{\mathcal{V},w}$, respectively. It turns out that one can recognize whether S_w is properly carried by analyzing the complementary regions of $\tau_{\mathcal{V},w}$. If a boundary component of S_w runs along a blue ladderpole slope then the corresponding vertex of $\mathcal{Q}_{\mathcal{V},w}$ is contained in a cusp-free complementary region r of $\tau_{\mathcal{V},w}$; see Figure 6. Moreover, the boundary of r crosses only red edges. We will

say that r is red. Analogously, if a boundary component of S_w runs along a red ladderpole slope then the corresponding vertex of $\mathcal{Q}_{\mathcal{V},w}$ is contained in a cusp-free complementary region of $\tau_{\mathcal{V},w}$ whose boundary crosses only blue edges. We will say that such complementary regions are blue. Using this terminology, Lemma 2.13 implies the following characterization of carried surfaces which are not properly carried:

Corollary 2.14 *Let S_w be a surface carried by a veering triangulation $\mathcal{V}$ of M. The surface S_w is properly carried by $\mathcal{V}$ if and only if any two cusp-free complementary regions of $\tau_{\mathcal{V},w}$ that have different color intersect different boundary components of M.* □

2.2.3 The veering census Data on veering triangulations of orientable 3-manifolds consisting of up to 16 tetrahedra is available in the veering census [20]. A veering triangulation in the census is described by a string of the form

(2.15) `[isoSig]_[taut angle structure].`

The first part of this string is the isomorphism signature of the triangulation. It identifies a triangulation uniquely up to combinatorial isomorphism [6, Section 3]. The second part of the string records a taut angle structure, that is a taut structure up to reversing the orientation of all dual edges. A string of the form (2.15) is called a *taut signature* and we use it whenever we refer to any particular veering triangulation from the veering census.

The following lemma has been well known since the development of the veering census. It explains why there is at most one veering triangulation with a fixed underlying taut ideal triangulation. We include its proof here because we will use it in Section 3.8.

Lemma 2.16 *Suppose that $(\mathcal{T},\alpha)$ is a taut triangulation. If $(\mathcal{T},\alpha)$ admits a veering structure then this structure is unique.*

Proof Suppose that there are two veering triangulations $\mathcal{V}=(\mathcal{T},\alpha,\mathcal{B})$ and $\mathcal{V}'=(\mathcal{T},\alpha,\mathcal{B}')$. If they are distinct then there is a tetrahedron t of $\mathcal{T}$ such that $\mathcal{B}_t=\mathcal{B}\cap t$ and $\mathcal{B}'_t=\mathcal{B}'\cap t$ are different. Let f be a top face of t. Let τ_f and τ'_f be the stable train tracks in f determined by $\mathcal{B}$ and $\mathcal{B}'$, respectively. Definition 2.5 and the assumption that $\mathcal{B}_t\neq\mathcal{B}'_t$ imply that $\tau_f\neq\tau'_f$. In particular, there is an edge e_1 of f which is dual to the large branch of τ_f and a distinct edge e_2 of f, of a different color than e_1, which is dual to the large branch of τ'_f. Applying Lemma 2.12 to $\mathcal{V}$ yields that e_1 is identified with the bottom diagonal of the tetrahedron immediately above f, and applying it to $\mathcal{V}'$ yields that e_2 is identified with the bottom diagonal of the tetrahedron immediately above f. Since e_1 and e_2 cannot be identified in $\mathcal{T}$, this is a contradiction to the assumption that the taut ideal triangulations underlying $\mathcal{V}$ and $\mathcal{V}'$ are the same. □

2.3 The connection with pseudo-Anosov flows

Recall from the introduction that veering triangulations are combinatorial tools to study pseudo-Anosov flows. In this subsection we will make this statement more precise.

Definition 2.17 A continuous flow $\Psi\colon N\times\mathbb{R}\to N$ on a closed 3-manifold N is *pseudo-Anosov* if there are 2-dimensional singular foliations $\mathcal{F}^s$ and $\mathcal{F}^u$ on N with the following properties:

- $\mathcal{F}^s$ and $\mathcal{F}^u$ intersect along the flow lines of Ψ.
- Ψ admits finitely many (potentially zero) isolated closed orbits $\ell_1,\dots,\ell_k$ such that for $i=1,2,\dots,k$ in a sufficiently small tubular neighborhood of ℓ_i the foliation $\mathcal{F}^{s/u}$ is isotopic to the mapping torus of the $(2\pi m_i/p_i)$-rotation of the p_i-pronged foliation of a disk (with the prong singularity in the center), for some $p_i\geq 3$ and $m_i\in\mathbb{Z}$. These orbits are called the *singular orbits* of Ψ.
- Away from the singular orbits of Ψ, foliations $\mathcal{F}^s$ and $\mathcal{F}^u$ are nonsingular and transverse to each other.
- Two flow lines contained in the same leaf of $\mathcal{F}^s$ are forward asymptotic, and two flow lines contained in the same leaf of $\mathcal{F}^u$ are backward asymptotic.

If Ψ has a dense orbit then we say that Ψ is *transitive*. If Ψ does not have any singular orbits then it is called an *Anosov flow*. We will not pay much attention to the parametrization of a flow. In fact, we will consider two flows which are topologically equivalent to be the same; see definition below.

Definition 2.18 Two flows Ψ and Ψ' on N are *topologically equivalent* (or *orbit equivalent*) if there is a homeomorphism $h\colon N\to N$ which takes oriented orbits of Ψ to oriented orbits of Ψ'.

In the literature there is also a notion of a smooth pseudo-Anosov flow; see [1, Definition 5.8]. Recently Shannon proved that any continuous transitive Anosov flow is topologically equivalent to a smooth Anosov flow [49, Section 5]; see Definition 2.18. His methods generalize to transitive continuous pseudo-Anosov flows [1, Theorem 5.10]. Thus up to topological equivalence we may assume that our flows are smooth. The reason we prefer the above definition is that it focuses on topological properties of pseudo-Anosov flows which are crucial for our purposes — namely, the existence of foliations $\mathcal{F}^s$ and $\mathcal{F}^u$ with prescribed behavior. These foliations are called the *stable* and *unstable foliations* of the flow, respectively. If ℓ is a p-pronged orbit of Ψ, where $p\geq 2$ and $p=2$ corresponds to a nonsingular orbit, the compact core of $N-\ell$ has a boundary torus T_ℓ which meets the singular leaves of $\mathcal{F}^s$ along p parallel simple closed curves, and similarly for the singular leaves of $\mathcal{F}^u$. We call all these $2p$ parallel curves the *prong curves* of Ψ in T_ℓ. Splitting $\mathcal{F}^s$ and $\mathcal{F}^u$ open along their singular leaves yields a pair of laminations $\mathcal{L}^s$ and $\mathcal{L}^u$ in N, called the *stable* and *unstable laminations* of Ψ. Leaves of $\mathcal{L}^{s/u}$ are open annuli, open Möbius bands or planes. Möbius bands appear if and only if $\mathcal{L}^{s/u}$ is not transversely orientable.

The simplest examples of pseudo-Anosov flows are the suspension flows of pseudo-Anosov homeomorphisms of closed surfaces on their mapping tori. Their stable/unstable foliations are formed by the mapping tori of the stable/unstable foliations of the monodromy of the fibration. Suspension flows have an additional property: an embedded surface which intersects every flow line with positive sign. Such a surface is called a *cross-section* to the flow. Any flow which admits a cross-section is called *circular*. From the suspension flow of a pseudo-Anosov homeomorphism one can construct infinitely many other

pseudo-Anosov flows via the Goodman–Fried surgery [15; 21]. In particular, Goodman–Fried surgery can be used to construct noncircular pseudo-Anosov flows, including pseudo-Anosov flows on nonfibered 3-manifolds.

Let Ψ be a pseudo-Anosov flow on a closed 3-manifold N. Fix a finite nonempty collection Λ of closed orbits of Ψ which includes all singular orbits of Ψ. To be able to construct a veering triangulation of $N-\Lambda$ encoding Ψ a technical condition, called *no perfect fits relative to* Λ, has to be satisfied. We refer the reader to [1, Definition 5.12] for a precise definition of this term. Here we will work combinatorially with veering triangulations, and deduce appropriate statements concerning flows using the following two theorems.

Theorem 2.19 (Agol and Guéritaud, unpublished) *Let Ψ be a pseudo-Anosov flow on a closed 3-manifold N. Suppose that Λ is a finite nonempty collection of closed orbits of Ψ which includes all singular orbits of Ψ and such that Ψ has no perfect fits relative to Λ. Then $N-\Lambda$ admits a veering triangulation $\mathcal{V}$ such that the stable (respectively, unstable) branched surface of $\mathcal{V}$, when embedded in N via the inclusion $(N-\Lambda)\hookrightarrow N$, fully carries the stable (respectively, unstable) lamination of Ψ. The ladderpole curves of $\mathcal{V}$ are homotopic to the prong curves of Ψ in $\partial(N-\Lambda)$.* □

If $\mathcal{V}$ arises from Ψ via the Agol–Guéritaud construction we will say that $\mathcal{V}$ *encodes* Ψ. Tsang proved that every pseudo-Anosov flow Ψ is without perfect fits relative to some collection Λ of closed orbits of Ψ which contains all singular orbits and one additional orbit [53, Proposition 2.7]. Thus every pseudo-Anosov flow can be encoded by some veering triangulation. The situation is the cleanest when Ψ is not an Anosov flow and does not have perfect fits relative to its collection $\mathrm{Sing}(\Psi)$ of singular orbits. Then the veering triangulation of $N-\mathrm{Sing}(\Psi)$ obtained via the Agol–Guéritaud construction can be considered to be canonical for Ψ. In the remaining cases, there might be many choices for an additional orbit to be added to the set Λ, and thus no canonical veering triangulations encoding the flow. The proof of Theorem 2.19 appears in [31, Section 4]. The theorem is stated there only for the case when Ψ does not have perfect fits relative to $\mathrm{Sing}(\Psi)$, but the proof applies equally well to the case when the set Λ only properly contains $\mathrm{Sing}(\Psi)$.

Another theorem connecting veering triangulations and pseudo-Anosov flows says that one can go also in the other direction: use veering triangulations to construct pseudo-Anosov flows.

Theorem 2.20 (Agol and Tsang [1, Theorem 5.1]) *Let $\mathcal{V}$ be a veering triangulation of a 3-manifold M. Suppose that M has k boundary components $T_1,\dots,T_k$. Let l_i be the collection of blue ladderpole curves of $\mathcal{V}$ on T_i, and let s_i be a connected simple closed curve on T_i. If $p_i=|\langle \ell_i, s_i\rangle|$ is greater than one for every $i=1,2,\dots,k$, then the Dehn filled manifold $M(s_1,\dots,s_k)$ admits a transitive pseudo-Anosov flow Ψ with the following properties:*

- *Ψ is without perfect fits relative to a collection $\Lambda=\{\ell_1,\dots,\ell_k\}$ of closed orbits isotopic to the cores of the filling solid tori.*

- *The orbit ℓ_i is p_i-pronged for $i = 1, 2, \dots, k$.*
- *The stable (respectively, unstable) lamination of Ψ is fully carried by the stable (respectively, unstable) branched surface of $\mathcal{V}$.* □

The fact that the stable lamination of Ψ is fully carried by the stable branched surface of the veering triangulation is not explicitly stated in [1, Theorem 5.1] but it follows from [1, Proposition 5.13]. (Note that the authors call the stable branched surface from Definition 2.5 the unstable branched surface, and orient the edges of its branch locus in the opposite direction.) If $\mathcal{V}$ is a veering triangulation of M and Ψ is a pseudo-Anosov flow on some closed Dehn filling N of M constructed by the Agol–Tsang construction we will say that Ψ is *built from* $\mathcal{V}$. The fact that Agol and Guéritaud's construction and Agol and Tsang's construction are each other's inverses appears in [52, Theorem 2.1]; see also the program of Schleimer and Segerman outlined in [12, Section 1.2].

Let $\mathcal{V}$ be a veering triangulation of M encoding a pseudo-Anosov flow Ψ on some closed Dehn filling N of M. If we view M as a cusped 3-manifold $N - \Lambda$, then it is naturally equipped with a flow $\Psi_{N-\Lambda}$, the restriction of Ψ to the complement of Λ. The flow $\Psi_{N-\Lambda}$ is not pseudo-Anosov: orbits of Ψ that are asymptotic to an element of Λ become orbits of $\Psi_{N-\Lambda}$ that escape to infinity. Alternatively, we can view M as a manifold obtained from N by *blowing up* elements of Λ into toroidal boundary components. There is a notion of the *blown-up flow* Ψ° on M [42, Section 3.2]. See also [4, Section 3.6] for the construction of Ψ° in the context of smooth flows. The orbits of Ψ that are asymptotic to an element of Λ become orbits of Ψ° that are asymptotic to a prong curve on some boundary component of M (which is an orbit of Ψ°). By splitting the stable/unstable foliations of Ψ open along the leaves through each orbit of Λ we obtain a pair of laminations in M. We will call these laminations the stable/unstable laminations of Ψ°, respectively. Theorem 2.20 immediately implies the following statement:

Corollary 2.21 *Suppose that a pseudo-Anosov flow Ψ is built from a veering triangulation $\mathcal{V}$ of M. The following statements are equivalent.*

- *$\mathcal{V}$ is edge-orientable.*
- *The stable lamination of Ψ is transversely orientable.*
- *The stable lamination of Ψ° is transversely orientable.* □

Given a flow Ψ on an oriented 3-manifold N and an oriented surface S properly embedded in N, we will say that S is *transverse* to Ψ if S is transverse to the orbits of Ψ and the orientation on $TS \oplus T\Psi$ agrees with the orientation of M. Another useful connection between veering triangulations and pseudo-Anosov flows says that if a veering triangulation $\mathcal{V}$ is built from a pseudo-Anosov flow Ψ then all surfaces carried by $\mathcal{V}$ are transverse to the blown-up flow Ψ°.

Theorem 2.22 (Landry, Minsky and Taylor [31, Theorem 5.1]) *Suppose that $\mathcal{V}$ is a veering triangulation of M encoding a pseudo-Anosov flow Ψ on some closed Dehn filling N of M. Then any surface carried by $\mathcal{V}$ is transverse to the blown-up flow Ψ° on M.* □

2.4 Veering triangulations and the Thurston norm

Given a compact oriented 3-manifold M, Thurston defined a seminorm $\|\cdot\|_{\mathrm{Th}}$ on $H_2(M,\partial M;\mathbb{R})$ as follows. Every integral class $\eta \in H_2(M,\partial M;\mathbb{Z})$ can be represented by a properly embedded surface $S \subset M$ [50, Lemma 1]. If S is connected, we set

$$\chi_-(S) = \max\{0, -\chi(S)\},$$

where $\chi(S)$ denotes the Euler characteristic of S. Otherwise, denote by $S_1, S_2, \dots, S_k$ connected components of S and set

$$\chi_-(S) = \sum_{i=1}^{k} \chi_-(S_i).$$

We define a quantity $\|\eta\|_{\mathrm{Th}}$ as the infimum of $\chi_-(S)$ over all surfaces S which are properly embedded in M and represent η. The function $\|\cdot\|_{\mathrm{Th}}$ can be extended to $H_2(M,\partial M;\mathbb{Q})$ by requiring linearity on each ray through the origin in $H_2(M,\partial M;\mathbb{R})$, and then to $H_2(M,\partial M;\mathbb{R})$ by requiring continuity [50, Section 1]. If every surface representing a nonzero class in $H_2(M,\partial M;\mathbb{Z})$ has negative Euler characteristic then $\|\cdot\|_{\mathrm{Th}}$ is a norm [50, Theorem 1], called the *Thurston norm*. If a properly embedded surface S does not have any homologically trivial components and satisfies $\chi_-(S) = -\|\eta\|_{\mathrm{Th}}$ then it is called a *taut representative* of η or a *Thurston norm minimizing representative* of η. The unit norm ball $\mathbb{B}_{\mathrm{Th}}$ of $\|\cdot\|_{\mathrm{Th}}$ is a polytope with rational vertices [50, Theorem 2]. Thus we can speak about *faces* of the Thurston norm ball.

A connection between the Thurston norm and pseudo-Anosov flows on closed hyperbolic 3-manifolds was established by Fried and Mosher in the 80s and 90s. The first result in that direction concerned only fibered faces:

Theorem 2.23 (Fried [13, Theorem 7]) *Let N be a closed hyperbolic 3-manifold. Let $\mathtt{F}$ be a fibered face of the Thurston norm ball in $H_2(N;\mathbb{R})$. There is a unique, up to isotopy and reparametrization, circular pseudo-Anosov flow Ψ such that a class $\eta \in H_2(N;\mathbb{Z})$ can be represented by a cross-section to Ψ if and only if η is in the interior of $\mathbb{R}_+ \cdot \mathtt{F}$.* □

The importance of this result lies in the fact that when $b_1(N) > 1$ there are infinitely many fibrations lying over $\mathtt{F}$, and thus one can construct infinitely many suspension flows on N: one for each fibration. Theorem 2.23 implies that all these flows are the same up to isotopy and reparametrization. We will say that the unique flow Ψ associated to a fibered face $\mathtt{F}$ *dynamically represents* $\mathtt{F}$.

Mosher extended Fried's result by showing that if a circular flow Ψ dynamically represents a fibered face $\mathtt{F}$ then $\eta \in H_2(N;\mathbb{Z})$ can be represented by a surface that is *almost transverse* to Ψ if and only if η is in $\mathbb{R}_+ \cdot \mathtt{F}$ [40, Theorem 1.4]. Almost transversality means that the surface is transverse to a slightly modified flow $\Psi^{\#}$ obtained by *dynamically blowing up* finitely many closed orbits of Ψ into a collection of annuli; see [41, Section 1.3] for details. If S is almost transverse to Ψ then the algebraic intersection of $[S]$

with the homology class $[\gamma]$ of every closed orbit γ of Ψ is nonnegative. Conversely, if $\eta \in H_2(M;\mathbb{Z})$ is such that $\langle \eta, [\gamma] \rangle \geq 0$ for every closed orbit γ of Ψ then η can be represented by a taut surface which is almost transverse to Ψ [41, Theorem 1.3.2]. Using these facts, Mosher extended the notion of dynamical representation of faces of the Thurston norm ball to nonfibered faces [41]. Given a pseudo-Anosov flow Ψ on a closed 3-manifold N let $\mathcal{C}(\Psi) \subset H_2(N;\mathbb{R})$ be the nonnegative span of the second homology classes whose algebraic intersection with the homology class of every closed orbit of Ψ is nonnegative. By the aforementioned result [41, Theorem 1.3.2], we can think of $\mathcal{C}(\Psi)$ as the cone of homology classes of surfaces that are almost transverse to Ψ. Associated to Ψ there is also a second cohomology class, the *Euler class* of the normal plane bundle to Ψ, denoted by χ_Ψ; see [41, Section 2.4] for a formula for the computation of χ_Ψ. Its main feature is that it correctly computes the Thurston norm of surfaces that are almost transverse to Ψ in the sense that if $\eta \in \mathcal{C}(\Psi)$ then $\|\eta\|_{\mathrm{Th}} = -\chi_\Psi(\eta)$ [41, page 262].

Definition 2.24 We say that a pseudo-Anosov flow Ψ on a closed hyperbolic 3-manifold N *dynamically represents* a face $\mathtt{F}$ of the Thurston norm ball $\mathbb{B}_{\mathrm{Th}}$ in $H_2(N;\mathbb{R})$ if $\mathcal{C}(\Psi) = \mathbb{R}_+ \cdot \mathtt{F}$ and $\mathtt{F}$ is the maximal face of $\mathbb{B}_{\mathrm{Th}}$ over which the Thurston norm agrees with $-\chi_\Psi$.

By our earlier discussion and the fact that fibered faces are always top dimensional, the circular flow Ψ associated to a fibered face $\mathtt{F}$ as in Theorem 2.23 dynamically represents $\mathtt{F}$. Furthermore, Mosher found sufficient conditions on a noncircular pseudo-Anosov flow to dynamically represent a nonfibered face of the Thurston norm ball in [41, Theorem 2.7]. In [41, Section 4] he presented an example of a noncircular pseudo-Anosov flow which dynamically represents a top-dimensional nonfibered face of the Thurston norm ball, as well as an example of a pseudo-Anosov flow which does not dynamically represent any face of the Thurston norm ball. In the latter case $\mathcal{C}(\Psi)$ is properly contained in the cone on some face of the Thurston norm ball [40, Theorem 2.8]. The results of Mosher raise the following two questions:

Question 1 Let N be a closed 3-manifold. Given a nonfibered face $\mathtt{F}$ of the Thurston norm ball in $H_2(N;\mathbb{R})$, is there a pseudo-Anosov flow Ψ on N which dynamically represents $\mathtt{F}$?

Question 2 Suppose that a nonfibered face $\mathtt{F}$ of the Thurston norm ball is dynamically represented by Ψ. Is the flow Ψ unique, up to isotopy and reparametrization?

Question 1 is still open. In Section 5 we will use veering triangulations to show that for some nonfibered faces the answer to Question 2 is negative. Once we know that a face of the Thurston norm ball can be represented by multiple distinct flows, we may ask another question:

Question 3 Suppose that a face $\mathtt{F}$ of the Thurston norm ball is dynamically represented by two topologically inequivalent flows Ψ and Ψ'. How are Ψ and Ψ' related?

This problem also can be approached by employing veering triangulations. We partially answer this question in the case of nonfibered faces of manifolds with nonempty boundary in Section 5.

Both Fried and Mosher worked in the setup of closed 3-manifolds. However, the Thurston norm can be defined for any compact oriented atoroidal 3-manifold M. Thus we can ask Questions 1–3 also in the context of faces of the Thurston norm ball in $H_2(M, \partial M; \mathbb{R})$ when $\partial M \neq \varnothing$. Since we will work with veering triangulations, considering 3-manifolds with $\partial M \neq \varnothing$ is in fact more natural, and is a necessary intermediate step when trying to answer the questions in the closed case. Instead of pseudo-Anosov flows we then consider blown-up pseudo-Anosov flows. Definition 2.24 can be generalized to these flows in a natural way. The fact that suspension flows of pseudo-Anosov homeomorphisms of surfaces with boundary dynamically represent fibered faces of the Thurston norm ball of their mapping tori (ie an analogue of Fried's Theorem 2.23) was proved by Landry in [30, Theorem 3.5].

We will rely on results of Landry, Minsky and Taylor, stated below, connecting the Thurston norm directly with veering triangulations. Recall from Section 2.1.3 that a veering triangulation $\mathcal{V}$ of M may carry surfaces properly embedded in M. Each such surface is a Thurston norm minimizing representative of its homology class [27, Theorem 3], and is transverse to the blown-up flow encoded by $\mathcal{V}$ [31, Theorem 5.1] (stated here as Theorem 2.22). In analogy to the cone $\mathcal{C}(\Psi)$ of homology classes of surfaces almost transverse to a flow Ψ, let $\mathcal{C}(\mathcal{V})$ be the cone of homology classes of surfaces carried by $\mathcal{V}$.

Definition 2.25 A veering triangulation $\mathcal{V}$ of M *combinatorially represents* a face $\mathtt{F}$ of the Thurston norm ball in $H_2(M, \partial M; \mathbb{R})$ if $\mathcal{C}(\mathcal{V}) = \mathbb{R}_+ \cdot \mathtt{F}$.

When defining dynamical representation (Definition 2.24) we require not only equality of appropriate cones, but also that $\mathtt{F}$ is the maximal face over which the Thurston norm agrees with minus the Euler class of the normal plane bundle to the flow. In the setup of veering triangulations, maximality is always satisfied: $\mathcal{C}(\mathcal{V})$ is equal to the cone where the Thurston norm agrees with minus the Euler class of $\mathcal{V}$ [32, Theorem 5.12].

Theorem 2.26 (Landry, Minsky and Taylor [32, Theorems 5.12 and 5.15]) *If $\mathcal{V}$ is a layered or measurable veering triangulation of M, then there is a (not necessarily top-dimensional) face $\mathtt{F}$ of the Thurston norm ball in $H_2(M, \partial M; \mathbb{R})$ with $\mathcal{C}(\mathcal{V}) = \mathbb{R}_+ \cdot (\mathtt{F})$. Furthermore, $\mathtt{F}$ is fibered if and only if $\mathcal{V}$ is layered.*

The above theorem says that layered and measurable veering triangulations always combinatorially represent some face of the Thurston norm ball. This is in contrast with pseudo-Anosov flows, for which it is possible that $\mathcal{C}(\Psi)$ is nonempty, but is a proper subset of the cone on some face of the Thurston norm ball [41, Section 4]. It is also known that if a fibered face is combinatorially represented by a veering triangulation, then this veering triangulation is unique [38, Proposition 2.7]. Note that not every fibered face is combinatorially represented by some veering triangulation, because the circular flow associated to the face might have singular orbits.

Remark 2.27 In the proof of [32, Theorem 5.12] the authors show that if $\mathbb{R}_+ \cdot \mathtt{F} = \mathcal{C}(\mathcal{V})$ then $\mathcal{V}$ not only carries *some* taut representative of every $\eta \in \mathbb{R}_+ \cdot \mathtt{F}$, but it carries *every* taut representative of η. Thus in

particular if $\mathcal{C}(\mathcal{V}) = \mathcal{C}(\mathcal{V}')$ for some veering triangulations $\mathcal{V}$ and $\mathcal{V}'$ of a fixed manifold, then $\mathcal{V}$ carries S if and only if $\mathcal{V}'$ carries S.

Remark 2.28 For a taut triangulation $(\mathcal{T}, \alpha)$ let $\mathrm{Aut}^+(\mathcal{T} \mid \alpha)$ denote the group of orientation-preserving combinatorial automorphisms of $\mathcal{T}$ which preserve α. Recall from Section 2.2.3 that if $\mathcal{V} = (\mathcal{T}, \alpha, \mathcal{B})$ is veering and $\phi \in \mathrm{Aut}^+(\mathcal{T} \mid \alpha)$ then $\mathcal{V}$ and $\phi(\mathcal{V}) = (\phi(\mathcal{T}), \phi(\alpha), \phi(\mathcal{B}))$ have the same taut signature in the veering census. Thus the same entry in the veering census may encode multiple veering triangulations representing different faces of the Thurston norm ball which lie in the same orbit of the action of $\mathrm{Homeo}^+(M)$ on $H_2(M, \partial M; \mathbb{R})$. Furthermore, veering triangulations $\mathcal{V}$ and $-\mathcal{V}$ also have the same taut signature. They satisfy $\mathcal{C}(\mathcal{V}) = -\mathcal{C}(\mathcal{V})$ and represent a pair of opposite faces of the Thurston norm ball.

Landry, Minsky and Taylor defined the *flow graph* of a veering triangulation $\mathcal{V}$ whose oriented cycles correspond to orbits of the flow encoded by $\mathcal{V}$. We refer the reader to [32, Section 4] for the definition of the flow graph, and to [31, Section 6] for an explanation of the relationship between the flow graph of $\mathcal{V}$ and orbits of the flow encoded by $\mathcal{V}$. From their results it follows that the blown-up pseudo-Anosov flow on the 3-manifold underlying a layered or measurable veering triangulation dynamically encodes a face of the Thurston norm ball.

Theorem 2.29 (Landry, Minsky and Taylor [31, Theorem 6.1; 32, Theorem 5.1]) *Let $\mathcal{V}$ be a veering triangulation of M. Suppose that $\mathcal{V}$ encodes a pseudo-Anosov flow Ψ on some closed Dehn filling N of M. Let Ψ° be the associated blown-up flow on M. Then*

$$\mathcal{C}(\Psi^\circ) = \mathcal{C}(\mathcal{V}).$$

Under additional assumptions, we also have an analogous theorem concerning the pseudo-Anosov flow Ψ on N. There is a (potentially empty) subcone $\mathcal{C}(\mathcal{V}|N) \subset \mathcal{C}(\mathcal{V}) \subset H_2(M, \partial M; \mathbb{R})$ of homology classes of surfaces carried by $\mathcal{V}$ whose boundary components have slopes consistent with the Dehn filling slopes yielding N out of M. These surfaces cap off to embedded surfaces in N. We denote by $\mathcal{C}_N(\mathcal{V}) \subset H_2(N; \mathbb{R})$ the nonnegative span of homology classes of these capped-off surfaces.

Theorem 2.30 (Landry [29, Theorem A] and Landry, Minsky and Taylor [31, Theorem 6.1]) *Let $\mathcal{V}$ be a veering triangulation of M. Suppose that $\mathcal{V}$ encodes a pseudo-Anosov flow Ψ on some closed Dehn filling N of M such that the core curves of the filling solid tori are singular orbits of Ψ with at least three prongs. Then N is hyperbolic. Furthermore, if $\mathcal{C}_N(\mathcal{V}) \neq \varnothing$, there is a face $\mathtt{F}$ of the Thurston norm ball in $H_2(N; \mathbb{R})$ such that $\mathbb{R}_+ \cdot \mathtt{F} = \mathcal{C}_N(\mathcal{V}) = \mathcal{C}(\Psi)$.*

The face $\mathtt{F}$ is determined by the Euler class χ_Ψ of the normal plane bundle to Ψ in the sense that $\chi_\Psi(\eta) = -\|\eta\|_{\mathrm{Th}}$ for every $\eta \in \mathbb{R}_+ \cdot \mathtt{F}$. Mosher's example of a pseudo-Anosov flow Ψ on a closed hyperbolic 3-manifold N which does not dynamically represent a whole face of the Thurston norm ball

in $H_2(N;\mathbb{R})$ is such that there is a class $\eta \in H_2(N;\mathbb{R})$ for which $\chi_\Psi(\eta) = -\|\eta\|_{\mathrm{Th}}$, but which pairs negatively with the homology class of some nonsingular closed orbit of Ψ [41, Section 4]. In this case $\mathcal{C}(\Psi)$ is a proper subset of the cone on some face of the Thurston norm ball in $H_2(N;\mathbb{R})$. This "pathology" does not happen under the assumptions of Theorem 2.30 because of Theorem 2.29 and the fact that if $\langle \eta, [\gamma] \rangle < 0$ for a singular orbit γ with at least three prongs then $\chi_\Psi(\eta) < \|\eta\|_{\mathrm{Th}}$; see [41, pages 259–261].

3 Mutations of veering triangulations

For the remainder of this paper by $X|Y$ we denote the metric completion of $X - Y$ with respect to the path metric on $X - Y$ induced from X.

Let S be an oriented surface properly embedded in an oriented compact 3-manifold M so that any two boundary components of S contained in the same boundary component of M have the same orientation. We say that $M|S$ is the *cut manifold* obtained from M by *decomposing* it along S. The orientation on S determines a transverse orientation on S via the right-hand rule. By S^+ we denote the boundary copy of S in $M|S$ which is cooriented out of $M|S$, and by S^- we denote the boundary copy of S in $M|S$ which is cooriented into $M|S$. Any homeomorphism $\varphi\colon S^+ \to S^-$ gives rise to a *mutant manifold* M^φ obtained from $M|S$ by gluing S^+ to S^- via φ. This manifold admits an embedded surface S^φ homeomorphic to S. We say that M^φ is obtained from M by *mutating* it *along* S via φ. We also say that S is a *mutating surface*.

In this section we approach the following problem: assuming that M admits a veering triangulation $\mathcal{V} = (\mathcal{T}, \alpha, \mathcal{B})$, when does the mutant manifold M^φ admit a veering triangulation? We restrict our considerations to the case when the mutating surface is carried by $\mathcal{V}$ with weights $w = (w_f)_{f\in F}$ and the homeomorphism φ comes from an orientation-preserving combinatorial automorphism φ of the ideal triangulation $\mathcal{Q}_{\mathcal{V},w}$ of S_w; we discuss this triangulation in detail in Section 3.2. In Sections 3.1 and 3.3 we recall the notions of combinatorial isomorphisms of triangulations and sutured manifolds, respectively. Section 3.4 is devoted to analyzing a certain *cut triangulation* $\mathcal{T}|F_w$ and its relation to the cut manifold $M|S_w^\epsilon$. In Section 3.5, given a pair (S_w, φ), we define a *mutant triangulation* $\mathcal{T}^\varphi$ of $\mathcal{T}$. In Section 3.6 we find a sufficient and necessary condition on φ that guarantees $\mathcal{T}^\varphi$ is an ideal triangulation of M^φ. In Section 3.7 we find a sufficient and necessary condition for the existence of a taut structure α^φ on $\mathcal{T}^\varphi$, and furthermore conditions which ensure that $(\mathcal{T}^\varphi, \alpha^\varphi)$ admits a veering structure $\mathcal{B}^\varphi$. In Section 3.8 we generalize this result to give sufficient and necessary conditions on $(\mathcal{T}^\varphi, \alpha^\varphi)$ to admit a veering structure. We also generalize a *veering mutation* $(\mathcal{T}, \alpha, \mathcal{B}) \rightsquigarrow (\mathcal{T}^\varphi, \alpha^\varphi, B^\varphi)$ to a *veering mutation with insertion*.

3.1 Triangulations: face identifications and combinatorial automorphisms

We will use a taut ideal triangulation $(\mathcal{T}, \alpha)$ of a 3-manifold to construct another ideal triangulation of a, typically different, 3-manifold using a combinatorial automorphism of a surface carried by $(\mathcal{T}, \alpha)$. In this subsection we explain the standard conventions used to encode triangulations and their combinatorial automorphisms.

Recall from Section 2 that by an ideal triangulation of a compact 3-manifold M we mean an expression of $M - \partial M$ as a collection of finitely many ideal tetrahedra with triangular faces identified in pairs by homeomorphisms which send vertices to vertices. An identification between a face f of tetrahedron t and a face f' of tetrahedron t' can be encoded by a bijection between their vertices. In our construction we will "forget" identifications between a subset of faces of the triangulation, and replace them with different ones. The whole procedure will be governed by a combinatorial automorphism of a carried surface.

Suppose that S_w is a surface carried by $(\mathcal{T}, \alpha)$ as in Section 2.1.3. Since S_w is built out of triangles and edges of $\mathcal{T}$, it inherits an ideal triangulation from $\mathcal{T}$. We discuss this triangulation in detail in Section 3.2. For now, we will denote this triangulation of S_w by $\mathcal{Q}$. Similarly as in the case of a 3-dimensional triangulation, $\mathcal{Q}$ is an expression of $S_w - \partial S_w$ as a collection of finitely many ideal triangles with edges identified in pairs by homeomorphisms which send vertices to vertices.

We recall the definition of a combinatorial isomorphism between a pair of 2-dimensional triangulations:

Definition 3.1 Let $\mathcal{Q}_1$ and $\mathcal{Q}_2$ be finite (ideal) 2-dimensional triangulations. For $i = 1, 2$ let F_i and E_i denote the sets of triangles and edges of $\mathcal{Q}_i$, respectively. A *combinatorial isomorphism* from $\mathcal{Q}_1$ to $\mathcal{Q}_2$ consists of

- a bijection $\varphi\colon F_1 \to F_2$,
- for each $f \in F_1$ a bijection φ_f between the edges of f and edges of $\varphi(f)$ such that if edges e of f and e' of f' are identified in $\mathcal{Q}_1$ then edges $\varphi_f(e)$ of $\varphi(f)$ and $\varphi_{f'}(e')$ of $\varphi(f')$ are identified in $\mathcal{Q}_2$.

If for every triangle of $\mathcal{Q}_1$ and $\mathcal{Q}_2$ we fix a bijection between its edges and vertices, we can view φ_f as a bijection between vertices of f and vertices of f'. It is standard to fix this bijection so that a vertex v of f is associated to the edge of f opposite to v.

Different combinatorial isomorphisms from $\mathcal{Q}_1$ to $\mathcal{Q}_2$ may have the same bijection $\varphi\colon F_1 \to F_2$. Nonetheless, for simplicity we often abuse the notation and denote a combinatorial isomorphism by $\varphi\colon \mathcal{Q}_1 \to \mathcal{Q}_2$, understanding that it carries information about both a bijection $\varphi\colon F_1 \to F_2$ and bijections $\{\varphi_f \mid f \in F_1\}$.

If $\mathcal{Q}$ is an ideal triangulation then a combinatorial isomorphism $\varphi\colon \mathcal{Q} \to \mathcal{Q}$ is called a *combinatorial automorphism* of $\mathcal{Q}$. We denote the group of orientation-preserving combinatorial automorphism of $\mathcal{Q}$ by $\mathrm{Aut}^+(\mathcal{Q})$. It follows directly from Definition 3.1 that $\mathrm{Aut}^+(\mathcal{Q})$ is finite.

We sometimes refer to two 3-dimensional ideal triangulations as either combinatorially isomorphic or not. A combinatorial isomorphism between a pair of 3-dimensional ideal triangulations $\mathcal{T}_1$ and $\mathcal{T}_2$ is determined by a bijection φ from the set of tetrahedra of $\mathcal{T}_1$ to the set of tetrahedra of $\mathcal{T}_2$ and a collection of permutations φ_t, one for each tetrahedron t of $\mathcal{T}_1$, between the faces of tetrahedron t of $\mathcal{T}_1$ and faces of tetrahedron $\varphi(t)$ such that if faces f of t and f' of t' are identified in $\mathcal{T}_1$ then faces $\varphi_t(f)$ of $\varphi(t)$ and $\varphi_{t'}(f')$ of $\varphi(t')$ are identified in $\mathcal{T}_2$. In other words, it suffices to replace in Definition 3.1 triangles by

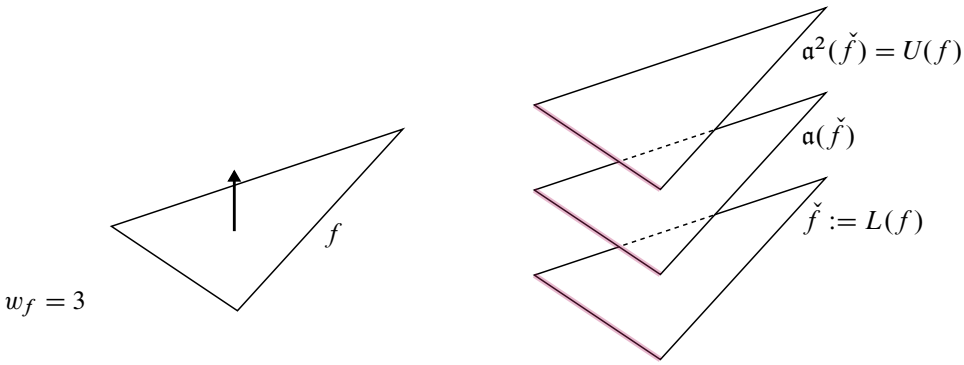

Figure 7: A face f with weight 3. Coorientation on f determines an order on the copies of f in $\mathcal{Q}_{\mathcal{V},w}$. Shaded edges are $\mathfrak{a}^k(\check{e})$, $\mathfrak{a}^{k+1}(\check{e})$ and $\mathfrak{a}^{k+2}(\check{e})$, from bottom to top, for an edge e of f and some $0 \le k \le w_e - 3$.

tetrahedra and edges by triangular faces. The pair $(\varphi, \{\varphi_t\})$ determines images of edges of $\mathcal{T}_1$ because, under the bijection which sends face f of t to a vertex of t opposite to f, permutations φ_t contain information about where the vertices are sent, and thus where the pairs of vertices are sent.

3.2 Triangulation of a surface carried by a veering triangulation

Let $\mathcal{V} = (\mathcal{T}, \alpha, \mathcal{B})$ be a finite veering triangulation of M with the set T of tetrahedra, the set F of 2-dimensional faces and the set E of edges. Let $w = (w_f)_{f \in F}$ be a weight system on $(\mathcal{T}, \alpha)$. We denote the triangulation of S_w inherited from $\mathcal{T}$ by $\mathcal{Q}_{\mathcal{V},w}$. A properly embedded surface S_w^ϵ obtained by slightly pulling apart overlapping regions of S_w also can be seen as triangulated by $\mathcal{Q}_{\mathcal{V},w}$. Recall that each triangle of $\mathcal{V}$ is equipped with a trivalent train track; see Figure 6. Therefore the surfaces S_w and S_w^ϵ come equipped with a train track dual to their triangulation $\mathcal{Q}_{\mathcal{V},w}$. We will denote this train track by $\tau_{\mathcal{V},w}$ and call it the *stable train track* of S_w or S_w^ϵ.

Let $F_w = \{f \in F \mid w_f > 0\}$ and $E_w = \{e \in E \mid w_e > 0\}$. Given $f \in F_w$ there are w_f copies of f in the triangulation $\mathcal{Q}_{\mathcal{V},w}$, and given $e \in E_w$ there are w_e copies of e in $\mathcal{Q}_{\mathcal{V},w}$. Coorientation on the faces of $\mathcal{V}$ and a fixed embedding of S_w^ϵ in M determine a linear order on the copies of a given simplex of $\mathcal{V}$ in $\mathcal{Q}_{\mathcal{V},w}$: from the lowermost to the uppermost; see Figure 7. Denote by $F_{\mathcal{V},w}$ and $E_{\mathcal{V},w}$ the sets of triangles and edges of $\mathcal{Q}_{\mathcal{V},w}$, respectively. We define maps

$$L\colon F_w \cup E_w \to F_{\mathcal{V},w} \cup E_{\mathcal{V},w} \quad \text{and} \quad U\colon F_w \cup E_w \to F_{\mathcal{V},w} \cup E_{\mathcal{V},w}$$

such that, given a simplex $x \in F_w \cup E_w$, the simplex $L(x)$ denotes the *lowermost copy* of x in $\mathcal{Q}_{\mathcal{V},w}$ and $U(x)$ denotes the *uppermost copy* of x in $\mathcal{Q}_{\mathcal{V},w}$. Observe that both L and U are injective. To simplify notation we will sometimes denote $L(x)$ by $\check{x}$. Given $f \in F_w$ we will denote by σ_f^L and σ_f^U the bijections between the edges of f and the corresponding edges of $L(f)$ and $U(f)$, respectively. Furthermore we define

$$\mathfrak{a}\colon (F_{\mathcal{V},w} \cup E_{\mathcal{V},w}) - U(F_w \cup E_w) \to (F_{\mathcal{V},w} \cup E_{\mathcal{V},w}) - L(F_w \cup E_w)$$

such that if $y \notin U(F_w \cup E_w)$ then $\mathfrak{a}(y)$ is the simplex of $\mathcal{Q}_{\mathcal{V},w}$ which is a copy of the same simplex of $\mathcal{V}$ as y and lies *immediately above* y in M; see Figure 7. Simplex $\mathfrak{a}(y)$ exists by the assumption that $y \notin U(F_w \cup E_w)$ (is not uppermost), and is never in $L(F_w \cup E_w)$, because lowermost copies do not have copies of the same simplex below them. If $w_x = k \geq 0$ then $\mathfrak{a}^0(\check{x})$, $\mathfrak{a}(\check{x}), \dots, \mathfrak{a}^{k-1}(\check{x})$ are defined, where by $\mathfrak{a}^0(\check{x})$ we mean $\check{x}$.

3.3 Sutured manifolds

Let S be an oriented surface properly embedded in an oriented 3-manifold M with empty or toroidal boundary. Assume additionally that any two boundary components of S contained in the same boundary component of M have the same orientation. Then the cut manifold $M|S$ is an example of a *sutured manifold*, defined below.

Definition 3.2 [19, Definition 3.1] A *sutured manifold* (N, γ) is a compact oriented 3-manifold N together with a set $\gamma \subset \partial N$ of pairwise-disjoint annuli $A(\gamma)$, called *sutured annuli*, and tori $T(\gamma)$, called *sutured tori*, such that

- the interior of each component of $A(\gamma)$ contains a homologically nontrivial oriented simple closed curve called a *suture*,
- every connected component of $R(\gamma) = \partial N - \operatorname{int}(\gamma)$ is oriented so that every connected component of $\partial R(\gamma)$ when equipped with the boundary orientation represents the same homology class in $H_1(\gamma)$ as some suture.

A fixed orientation of (N, γ) endows $R(\gamma)$ with coorientation. This determines a decomposition of $R(\gamma)$ into $R^+(\gamma)$, where the coorientation points out of N, and $R^-(\gamma)$ where the coorientation points into N. We call $R^+(\gamma)$ the *top boundary* of the sutured manifold N, and $R^-(\gamma)$ its *bottom boundary*. We also denote them by $\partial^+ N$ and $\partial^- N$, respectively. A boundary component of a sutured annulus A of (N, γ) that is contained in $\partial^+ N$ (respectively, $\partial^- N$) is called its *top* (respectively, *bottom*) *boundary* and denoted by $\partial^+ A$ (respectively, $\partial^- A$).

The pair $(M|S, \partial M|\partial S)$ is an example of a sutured manifold. Its sutured tori correspond to the boundary tori of M that are disjoint from S. A boundary torus of M containing k boundary components of S gives rise to k sutured annuli in $(M|S, \partial M|\partial S)$. For brevity, we often say that $M|S$ is a sutured manifold, without explicitly indicating its sutured tori and annuli.

3.4 Cutting veering triangulations along carried surfaces

Let $\mathcal{V}$ be a finite veering triangulation of a 3-manifold M with the set T of tetrahedra, the set F of triangular faces and the set E of edges. Let S_w be a surface properly carried by $\mathcal{V}$ with weights $(w_f)_{f \in F}$. As in Section 3.2, we denote by F_w the set of $f \in F$ for which $w_f > 0$.

Recall from Section 2.2 that the calligraphic letter $\mathcal{V}$ implicitly denotes three pieces of combinatorial data: an ideal triangulation $\mathcal{T}$, a taut structure α and a veering structure $\mathcal{B}$. We denote the result of

decomposing $\mathcal{T}$ along F_w by $\mathcal{T}|F_w$. All faces of $\mathcal{T}|F_w$ inherit coorientations from $\mathcal{V}=(\mathcal{T},\alpha,\mathcal{B})$. We denote this choice of coorientations on the faces of $\mathcal{T}|F_w$ by $\alpha|F_w$. By F_w^+ we denote the boundary triangles of $\mathcal{T}|F_w$ which are cooriented out of $\mathcal{T}|F_w$ and by F_w^- the boundary triangles of $\mathcal{T}|F_w$ which are cooriented into $\mathcal{T}|F_w$. Finally, after cutting the stable branched surface $\mathcal{B}$ along $\mathcal{B}\cap F_w$, we obtain a branched surface $\mathcal{B}|F_w$. For simplicity, we denote the triple $(\mathcal{T}|F_w,\alpha|F_w,\mathcal{B}|F_w)$ by $\mathcal{V}|F_w$. In Sections 3.4–3.6 we do not make use of this (partial) veering structure, and consider only the pair $(\mathcal{T}|F_w,\alpha|F_w)$.

The set F_w can be seen as a branched surface embedded in M which fully carries S_w^ϵ. We denote the (sutured) manifold underlying $\mathcal{T}|F_w$ by $M|F_w$. Note that $\mathcal{T}|F_w$ is not an ideal triangulation of $M|F_w$ in the sense introduced at the beginning of Section 2. The manifold $M|F_w$ is expressed as a union of ideal tetrahedra of $\mathcal{T}|F_w$, but only some of their faces are identified in pairs by homeomorphisms sending vertices to vertices. The remaining faces make up the triangulations of the top and bottom boundaries of $M|F_w$. To avoid any confusion we call $\mathcal{T}|F_w$ a *cut triangulation*. In this section we will establish a relationship between $M|F_w$ and $M|S_w^\epsilon$.

Recall from Section 3.2 that S_w^ϵ is triangulated by $\mathcal{Q}_{\mathcal{V},w}$. We denote the corresponding triangulations of $S_w^{\epsilon+}$ and $S_w^{\epsilon-}$ in $M|S_w^\epsilon$ by $\mathcal{Q}^+_{\mathcal{V},w}$ and $\mathcal{Q}^-_{\mathcal{V},w}$, respectively. Given a simplex x of $\mathcal{Q}_{\mathcal{V},w}$ we denote by x^+ and x^- the corresponding simplices of $\mathcal{Q}^+_{\mathcal{V},w}$ and $\mathcal{Q}^-_{\mathcal{V},w}$, respectively. Notation that we use below was introduced in Section 3.2.

Let $e\in E_w=\{e\in E\mid w_e>0\}$. Recall that $\check{e}$ is a shorthand for $L(e)$, the lowermost copy of e in $\mathcal{Q}_{\mathcal{V},w}$. Suppose that $w_e=k\geq 2$. Then for $i=1,2,\dots,k-1$ there is a disk D_i^e properly embedded in $M|S_w^\epsilon$ whose boundary decomposes into four arcs: one arc corresponding to the edge $\mathfrak{a}^{i-1}(\check{e})^-$ of $\mathcal{Q}^-_{\mathcal{V},w}$, one arc corresponding to the edge $\mathfrak{a}^i(\check{e})^+$ of $\mathcal{Q}^+_{\mathcal{V},w}$ and two arcs each of which joins $\mathfrak{a}^{i-1}(\check{e})^-$ to $\mathfrak{a}^i(\check{e})^+$ and intersects a suture of $(M|S_w^\epsilon,\partial M|\partial S_w^\epsilon)$ exactly once; see Figure 8. We call $\mathfrak{a}^{i-1}(\check{e})^-$ the *bottom base* of the disk D_i^e and $\mathfrak{a}^i(\check{e})^+$ its *top base*. We denote them by $\partial^- D_i^e$ and $\partial^+ D_i^e$, respectively. The set $\partial_v D_i^e=\partial D_i^e-\operatorname{int}(\partial^+ D_i^e)-\operatorname{int}(\partial^- D_i^e)$ is called the *vertical boundary* of D_i^e.

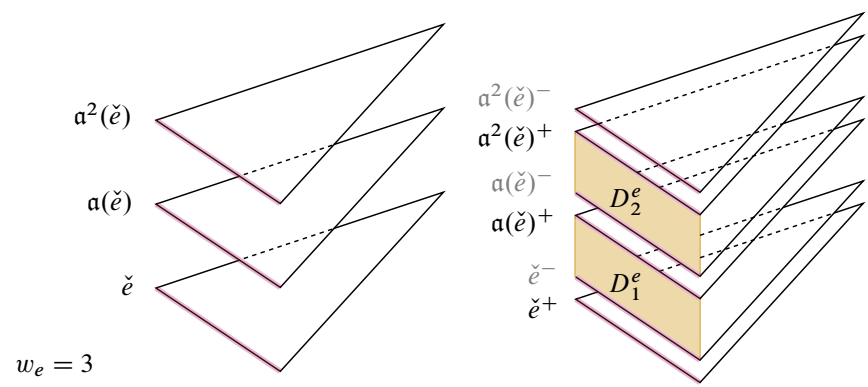

Figure 8: Two edge product disks D_1^e and D_2^e associated to an edge $e\in E$ of weight 3. For each copy of e in $\mathcal{Q}_{\mathcal{V},w}$ we draw only one triangle attached to it so that the disks D_1^e and D_2^e are clearly visible. To simplify notation we denote $L(e)$ by $\check{e}$.

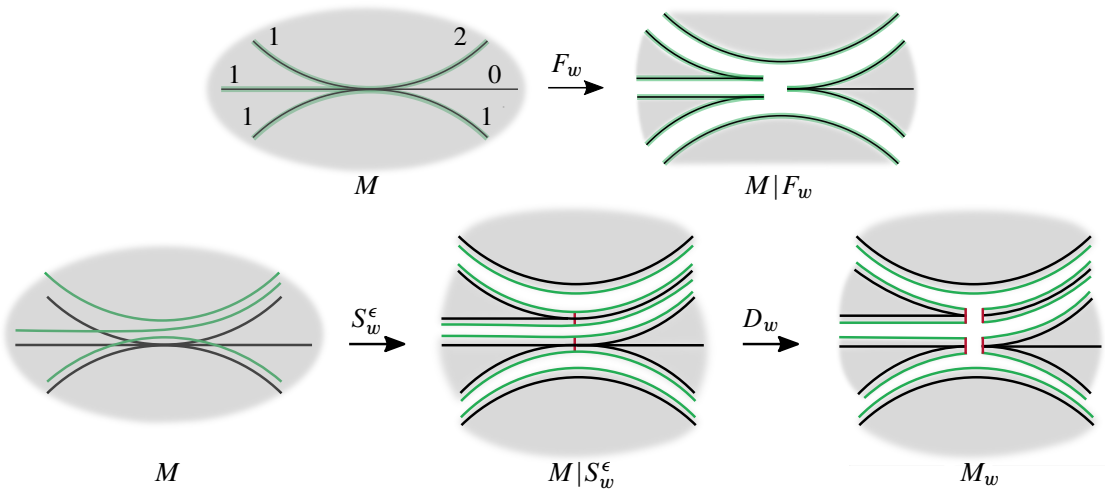

Figure 9: Top: Cutting along F_w. A weight on a face is indicated by the number immediately above the face. Bottom: First arrow: cutting along an embedded surface S^ϵ_w. Second arrow: cutting along edge product disks.

Disk D^e_i intersects the sutures of $(M|S^\epsilon_w, \partial M|\partial S^\epsilon_w)$ exactly twice. In the theory of sutured manifolds, properly embedded disks with this property are called *product disks*.

Let D_w denote the set of product disks in $M|S^\epsilon_w$ associated to the edges of $\mathcal{V}$ with $w_e > 1$. We say that an element of D_w is an *edge product disk*. Note that $M|S^\epsilon_w$ can admit more product disks, which are not elements of D_w. Let $M_w = (M|S^\epsilon_w)|D_w$. Since M_w arises as a result of decomposing a sutured manifold along finitely many product disks, it is also a sutured manifold; see [19, Definition 3.8]. Figure 9 illustrates the relationship between $M|F_w$ and M_w that we formalize in Lemma 3.4, after introducing necessary notation below.

Triangulations $\mathcal{Q}^+_{\mathcal{V},w}, \mathcal{Q}^-_{\mathcal{V},w} \subset M|S^\epsilon_w$ determine a pair of triangulations $\overline{\mathcal{Q}^+_{\mathcal{V},w}}$ and $\overline{\mathcal{Q}^-_{\mathcal{V},w}}$ in the top and the bottom boundary of M_w, respectively. For any triangle $g^\pm$ of $\mathcal{Q}^\pm_{\mathcal{V},w}$ there is an associated triangle $\overline{g^\pm}$ of $\overline{\mathcal{Q}^\pm_{\mathcal{V},w}}$. We will always assume that the indexing of edges/vertices of $\overline{g^\pm}$ is the same as in $g^\pm$. The only difference between $\mathcal{Q}^\pm_{\mathcal{V},w}$ and $\overline{\mathcal{Q}^\pm_{\mathcal{V},w}}$ is that there might be triangles $g^\pm_1$ and $g^\pm_2$ of $\mathcal{Q}^\pm_{\mathcal{V},w}$ which are identified along an edge e_1 of $g^\pm_1$ and an edge e_2 of $g^\pm_2$ such that the corresponding edges $\bar{e}_1$ of $\overline{g^\pm_1}$ and $\bar{e}_2$ of $\overline{g^\pm_2}$ are not identified in $\overline{\mathcal{Q}^\pm_{\mathcal{V},w}}$. This happens if and only if the common edge of $g^\pm_1$ and $g^\pm_2$ is the top or bottom base of an edge product disk from D_w.

For any $f \in F$ with $w_f > 1$, the sutured manifold M_w admits $(w_f - 1)$ connected components of the form $f \times [0,1]$. We call them *triangular prisms*, and denote the set of such triangular prisms in M_w by P_w. Each $P \in P_w$ is a sutured 3-ball, so we can speak about its top and bottom boundaries $\partial^+ P$ and $\partial^- P$, respectively. Observe that if $\partial^- P = \overline{g^-} \in \overline{F^-_{\mathcal{V},w}}$ then $\partial^+ P = \overline{\mathfrak{a}(g)^+} \in \overline{F^+_{\mathcal{V},w}}$. We call $\partial_v P = \partial P - \operatorname{int}(\partial^+ P) - \operatorname{int}(\partial^- P)$ the *vertical boundary* of P.

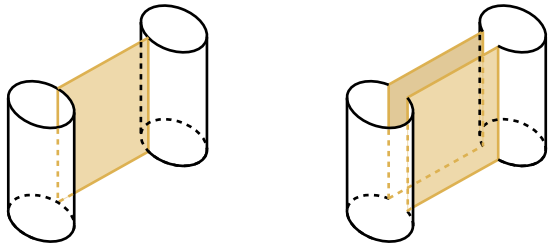

Figure 10: Left: the product D disk in $M|S^\epsilon_w$. Right: two disks contained in a sutured annulus of M_w arising from cutting $M|S^\epsilon_w$ along D.

Each edge product disk $D \in D_w$ gives rise to two disks D' and D'' contained in the sutured annuli of M_w; see Figure 10. We denote the set of such disks contained in the sutured annuli of M_w by $D(M_w)$. Let

$$\text{coll}\colon M_w \to \text{coll}(M_w) \tag{3.3}$$

be the map which vertically collapses every $D \in D(M_w)$ to $\partial^- D$ and every $P \in P_w$ to $\partial^- P$.

Lemma 3.4 *The image of $M_w - P_w$ under* coll *is homeomorphic to $M|F_w$. Furthermore, for any $f \in F_w$,*

- *if $\overline{g^+}$ is a triangle of $\partial^+(M_w - P_w)$ with $\text{coll}(\overline{g^+}) = f^+$ then $\overline{g^+} = \overline{L(f)^+}$,*
- *if $\overline{g^-}$ is a triangle of $\partial^-(M_w - P_w)$ with $\text{coll}(\overline{g^-}) = f^-$ then $\overline{g^-} = \overline{U(f)^-}$.*

Proof The manifold M_w can be seen as a sutured manifold $M|(S^\epsilon_w \cup D_w)$. Observe that $S^\epsilon_w \cup D_w$ can be obtained from F_w in the following three steps:

(1) Replace every edge e in the branch locus of F_w by $e \times [0,1]$, keeping the triangles that were on the two sides of e attached to $e \times \{0\} \subset e \times [0,1]$.

(2) For every $f \in F_w$ with $w_f > 1$ add an additional $(w_f - 1)$ copies of f and for every edge e of f attach them along $e \times \{0\}$ immediately above f.

(3) For every $e \times [0,1]$ that occurs as a result of (1), spread the triangles that are on the two sides of $e \times \{0\}$ evenly along $e \times [0,1]$.

The last step is possible because edges in the branch locus of F_w correspond to the edges of $\mathcal{V}$ with weight greater than one, and thus there are at least two triangles attached to either side of $e \times [0,1]$.

It follows that collapsing every $D \in D(M_w)$ vertically to $\partial^- D$ collapses $S^\epsilon_w \cup D_w$ into a branched surface whose branch locus can be identified with that of F_w, but which has multiple parallel copies of $f \in F_w$ whenever $w_f > 1$. Each region between two parallel copies of f corresponds a triangular prism P with its vertical boundary collapsed and such that $\partial^- P = \overline{\mathfrak{a}^k(\check{f})^-}$ and $\partial^+ P = \overline{\mathfrak{a}^{k+1}(\check{f})^+}$ for some $0 \le k \le w_f - 2$ (recall that $\check{f} = L(f)$). Therefore collapsing each such P into $\partial^- P$ results in collapsing them all to the lowermost copy of f. Performing this for all $f \in F_w$ yields F_w. It follows that $\text{coll}(M_w - P_w)$ can be identified with $M|F_w$.

The "furthermore" part follows from the observation that $\overline{L(f)^+}$ is the only copy of f in $\overline{\mathcal{Q}^+_{\mathcal{V},w}}$ which does not have a triangular prism below it, and $\overline{U(f)^-}$ is the only copy of f in $\overline{\mathcal{Q}^-_{\mathcal{V},w}}$ which does not have a triangular prism above it. □

3.5 The mutant triangulation

In this subsection we explain how to construct the *mutant triangulation* $\mathcal{T}^\varphi$ out of the cut triangulation $(\mathcal{T}|F_w, \alpha|F_w)$, defined in Section 3.4, and a combinatorial automorphism $\varphi \in \mathrm{Aut}^+(\mathcal{Q}_{\mathcal{V},w})$. This mutant triangulation is not guaranteed to be veering even when we do have a partial veering structure $\mathcal{B}|F_w$ on $(\mathcal{T}|F_w, \alpha|F_w)$. In Section 3.6 we give sufficient and necessary conditions on φ that guarantee $\mathcal{T}^\varphi$ is an ideal triangulation of M^φ. In Section 3.7 we put additional restrictions on φ which allow us to define taut and veering structures on $\mathcal{T}^\varphi$, thus resulting in a veering triangulation $\mathcal{V}^\varphi = (\mathcal{T}^\varphi, \alpha^\varphi, \mathcal{B}^\varphi)$.

Recall from Section 3.2 that $F_{\mathcal{V},w}$ denotes the set of triangles of $\mathcal{Q}_{\mathcal{V},w}$. A combinatorial automorphism $\varphi \in \mathrm{Aut}^+(\mathcal{Q}_{\mathcal{V},w})$ gives a bijection $\varphi\colon F_{\mathcal{V},w} \to F_{\mathcal{V},w}$ and a set of bijections $\{\varphi_g\}_{g\in F_{\mathcal{V},w}}$ between the edges of $g \in F_{\mathcal{V},w}$ and the edges of $\varphi(g) \in F_{\mathcal{V},w}$. Using the natural correspondence between the triangulations $\mathcal{Q}^+_{\mathcal{V},w}$ and $\mathcal{Q}^-_{\mathcal{V},w}$ in the top and bottom boundaries of $M|S^\epsilon_w$, respectively, we can view $\varphi \in \mathrm{Aut}^+(\mathcal{Q}_{\mathcal{V},w})$ as a combinatorial isomorphism $\varphi\colon \mathcal{Q}^+_{\mathcal{V},w} \to \mathcal{Q}^-_{\mathcal{V},w}$. Thus we can use φ to construct a mutant manifold M^φ out of $M|S^\epsilon_w$.

However, as explained in Section 3.4, when we work with the triangulation $(\mathcal{T}, \alpha)$ of M, we generally do not cut along S^ϵ_w, but along F_w. Thus to construct the mutant triangulation $\mathcal{T}^\varphi$ we need to specify a *regluing map* $r(\varphi) = (r^\varphi\colon F^+_w \to F^-_w, (r^\varphi_{f^+})_{f^+\in F^+_w})$ determined by φ, consisting of a bijection $r^\varphi\colon F^+_w \to F^-_w$ and a family of bijections $(r^\varphi_{f^+})_{f^+\in F^+_w}$ between edges of $f^+ \in F^+_w$ and edges of $r^\varphi(f^+) \in F^-_w$. The map $r(\varphi)$ has to be such that $\mathcal{T}^\varphi$ obtained from $(\mathcal{T}|F_w, \alpha|F_w)$ by identifying F^+_w with F^-_w via $r(\varphi)$ is, at least under certain conditions, a triangulation of M^φ. In this section we will define $r(\varphi)$. A sufficient and necessary condition on φ for the mutant triangulation to be a triangulation of M^φ appears in Theorem 3.10.

Below we use notation introduced in Section 3.2. In particular, recall that given $f \in F_w$, by $U(f)$ and $L(f)$ we denote the uppermost and the lowermost copies of f in $\mathcal{Q}_{\mathcal{V},w}$, respectively. Furthermore, let $\iota\colon M_w \to M|S^\epsilon_w$ be the surjective immersion, induced by cutting $M|S^\epsilon_w$ along D_w, which sends $\overline{g^+}$ to g^+ and $\overline{g^-}$ to g^- for every $g \in F_{\mathcal{V},w}$. Given $P \in P_w$ we will say that $\iota(P)$ is a triangular prism in $M|S^\epsilon_w$. To simplify notation, we set $P^\iota = \iota(P)$ and $\partial^\pm P^\iota = \iota(\partial^\pm P)$.

Before we formally define $r(\varphi)$ let us briefly explain the idea behind its definition. A triangle g^+ of $\mathcal{Q}^+_{\mathcal{V},w}$ does not have a triangular prism below it if and only if it is in $L(F_w)^+$; see Figure 7. Thus there is a natural identification between $L(F_w)^+$ and F^+_w. In particular, $r^\varphi(f^+)$ will depend on $\varphi(L(f)^+)$. Similarly, a triangle g^- of $\mathcal{Q}^-_{\mathcal{V},w}$ does not have a triangular prism above it if and only if it is in $U(F_w)^-$. Therefore we can identify $U(F_w)^-$ with F^-_w. If $\varphi(L(f)^+)$ is the bottom base of a triangular prism P^ι

then it is not immediately clear to which triangle of F_w^- the map r^φ should send f^+. In this case we flow upwards through the prism P^ι and look at $\varphi(\partial^+ P^\iota)$. If it is in $U(F_w)^-$ then the image of f^+ under r^φ will be the triangle f'^- with $U(f')^- = \varphi(\partial^+ P^\iota)$. Otherwise, we continue flowing upwards through triangular prisms. Below we describe this procedure more formally and prove that it always terminates.

Given $f \in F_w$ we define a sequence $g^\varphi(f) = (g_i)_{i\geq 1}$ of triangles of $\mathcal{Q}_{\mathcal{V},w}$ as follows. The first element g_1 is equal to $\varphi(L(f))$. For $i \geq 1$ if $g_i \in U(F_w)$ we are done. Otherwise, there is another triangle $\mathfrak{a}(g_i)$ of $\mathcal{Q}_{\mathcal{V},w}$ which is a copy of the same triangle of $(\mathcal{T}, \alpha)$ as g_i and lies immediately above g_i. Then we set $g_{i+1} = \varphi(\mathfrak{a}(g_i))$.

Lemma 3.5 *For every $f \in F_w$ the sequence $g^\varphi(f)$ is finite. Furthermore, if $f, f' \in F_w$ are distinct then the last elements of $g^\varphi(f)$ and $g^\varphi(f')$ are distinct.*

Proof Since the triangulation $\mathcal{Q}_{\mathcal{V},w}$ consists of finitely many triangles and g_i completely determines g_{i+1}, if the sequence $g^\varphi(f)$ is infinite then it is eventually periodic. That is, there are integers $m \geq 0$ and $N \geq 1$ such that $g_{m+j} = g_{m+kN+j}$ for any $j \in \{1, 2, \dots, N\}$ and $k \geq 0$. Pick minimal such m and N. We can write $g^\varphi(f)$ as

$$g^\varphi(f) = g_1, g_2, \dots, g_m, (h_1, \dots, h_N), (h_1, h_2, \dots, h_N), \dots.$$

First observe that we can assume that $m < N$. Otherwise, using the definition of $g^\varphi(f)$ and the fact that φ is a bijection on the set of triangles of $\mathcal{Q}_{\mathcal{V},w}$, we get that $g_{m-k} = h_{N-k}$ for any $k \in \{0, 1, \dots, N-1\}$. This means that the period $(h_1, \dots, h_N)$ starts immediately after g_{m-N} if $m > N$, or there is no preperiodic sequence at all if $m = N$. This is a contradiction with the minimality of m. On the other hand, if $m < N$ we obtain the equality $L(f) = \mathfrak{a}(h_{N-m})$. This is a contradiction, because the lowermost copy of f in $\mathcal{Q}_{\mathcal{V},w}$ does not have any copies of f below it, so in particular it cannot lie immediately above h_{N-m}. Thus $g^\varphi(f)$ is finite.

Now suppose that for some $1 \leq k \leq l$ we have

$$g^\varphi(f) = (g_1, g_2, \dots, g_k) \quad \text{and} \quad g^\varphi(f) = (g'_1, g'_2, \dots, g'_l).$$

If $g_k = g'_l$ then $g_1 = g'_{l-k+1}$. If $l < k$ we get $L(f) = \mathfrak{a}(g'_{l-k})$, which is a contradiction, because $L(f)$ is the lowermost copy of f in $\mathcal{Q}_{\mathcal{V},w}$ while $\mathfrak{a}(g'_{l-k})$ lies above g'_{l-k}. If $k = l$ we get $L(f) = L(f')$ and thus $f = f'$ by the injectivity of L. □

Let $f \in F_w$. Denote by $k \geq 1$ the length of the sequence $g^\varphi(f)$. By definition, $g_i \notin U(F_w)$ for all $i \in \{1, 2, \dots, k-1\}$ and $g_k \in U(F_w)$. Since U is injective, there is a unique $f' \in F_w$ such that $g_k = U(f')$. Let f^+ and f'^- be the triangles corresponding to f and f' in F_w^+ and F_w^-, respectively, and set

$$r^\varphi(f^+) = f'^- \in F_w^-.$$

Lemma 3.5 and injectivity of U imply that r^φ is a bijection. Thus it determines a pairing between faces of the top boundary F_w^+ of the cut triangulation $(\mathcal{T}|F_w, \alpha|F_w)$ and faces of the bottom boundary F_w^- of $(\mathcal{T}|F_w, \alpha|F_w)$. To define a mutant triangulation built out of $(\mathcal{T}|F_w, \alpha|F_w)$ it therefore remains to

specify, for every $f \in F_w$, a bijection r^{φ}_{f+} between the edges of f^+ and that of f'^-. As in Section 3.2, to simplify notation we will denote $L(f)$ by $\check{f}$. Recall from Definition 3.1 that φ associates to $\check{f}$ a bijection $\varphi_{\check{f}}$ between the edges of $\check{f}$ and edges of $g_1 = \varphi(\check{f})$. Analogously, for $i = 1, 2, \dots, k-1$ there is a bijection φ_i between the edges of $\mathfrak{a}(g_i)$ and edges of $g_{i+1} = \varphi(\mathfrak{a}(g_i))$. Let δ_i be the bijection between the edges of g_i and edges of $\mathfrak{a}(g_i)$ such that $\delta_i(e) = \mathfrak{a}(e)$ for any edge e of g_i. Recall from Section 3.2 that σ^L_f and σ^U_f denote the bijections between the edges of f and edges of $L(f)$ and $U(f)$, respectively. Using this we set

$$r^{\varphi}_{f+} = (\sigma^U_{f'})^{-1} \circ \varphi_{k-1} \circ \delta_{k-1} \circ \varphi_{k-2} \circ \delta_{k-2} \circ \cdots \circ \varphi_1 \circ \delta_1 \circ \varphi_{\check{f}} \circ \sigma^L_f.$$

We will also write $r^{\varphi}_{f+} = (\sigma^U_{f'})^{-1} \circ (\varphi_i \circ \delta_i)_{i=1}^{k-1} \circ \varphi_{\check{f}} \circ \sigma^L_f$ for brevity. We define the *mutant triangulation* $\mathcal{T}^{\varphi}$ as the triangulation obtained from $(\mathcal{T}|F_w, \alpha|F_w)$ by identifying a triangle $f^+ \in F^+_w$ with the triangle $r^{\varphi}(f^+) \in F^-_w$ in such a way that an edge e of f^+ is identified with the edge $r^{\varphi}_{f+}(e)$ of $r^{\varphi}(f^+)$.

Observe that $\mathcal{T}^{\varphi}$ is an ideal triangulation of $M^{r(\varphi)}$ which is not necessarily homeomorphic to M^{φ}. We explore this problem in the next subsection. For now, we state the relationship between $r(\varphi) = (r^{\varphi}\colon F^+_w \to F^-_w, (r^{\varphi}_{f+})_{f^+ \in F^+_w})$ and $\varphi = (\varphi\colon \mathcal{Q}^+_{\mathcal{V},w} \to \mathcal{Q}^-_{\mathcal{V},w}, (\varphi_g)_{g^+ \in F^+_{\mathcal{V},w}})$.

Lemma 3.6 *Let $f \in F_w$. Suppose that*

$$r^{\varphi}(f^+) = f'^- \quad \text{and} \quad r^{\varphi}_{f+} = (\sigma^U_{f'})^{-1} \circ (\varphi_i \circ \delta_i)_{i=1}^{k-1} \circ \varphi_{\check{f}} \circ \sigma^L_f.$$

Then:

(1) *$k = 1$ if and only if $\varphi(L(f)^+) = U(f')^-$ and their vertices are identified by $\varphi_{\check{f}}$.*

(2) *$k \geq 2$ if and only if there is a sequence $(P^{\iota}_1, \dots, P^{\iota}_{k-1})$ of triangular prisms in $M|S^{\epsilon}_w$ with the following properties*:
   - *$\varphi(L(f)^+) = \partial^- P^{\iota}_1$ and their vertices are identified by $\varphi_{\check{f}}$,*
   - *the vertex v of $\partial^- P^{\iota}_i$ is below the vertex $\delta_i(v)$ of $\partial^+ P^{\iota}_i$ for $i = 1, 2, \dots, k-1$,*
   - *$\varphi(\partial^+ P^{\iota}_i) = \partial^- P^{\iota}_{i+1}$ and their vertices are identified by φ_i for $i = 1, 2, \dots, k-2$,*
   - *$\varphi(\partial^+ P^{\iota}_{k-1}) = U(f')^-$ and their vertices are identified by φ_{k-1}.*

   Denote by $P(f)$ the quotient space of $L(f)^+ \cup \big(\bigcup_{i=1}^{k-1} P^{\iota}_i\big) \cup U(f')^-$ by the identifications listed above. Vertically collapsing $P(f)$ results in an identification of $L(f)^+$ with $U(f')^-$ with vertex correspondence given by $(\varphi_i \circ \delta_i)_{i=1}^{k-1} \circ \varphi_{\check{f}}$.

Proof We view φ as a combinatorial automorphism $\varphi\colon \mathcal{Q}^+_{\mathcal{V},w} \to \mathcal{Q}^-_{\mathcal{V},w}$. The assumption on r^{φ}_{f+} implies that $g^{\varphi}(f)$ has length k. Let $g^{\varphi}(f) = (g_1, \dots, g_k)$. By the definition of $g^{\varphi}(f)$ we get that $\varphi(L(f)^+) \in U(F_w)^-$ if and only if $k = 1$. In this case indeed $\varphi(L(f)^+) = g_1^- = U(f')^-$ and the vertex correspondence between these triangles is given by $\varphi_{\check{f}}$.

For the case $k \geq 2$ the existence of $P^{\iota}_1, P^{\iota}_2, \dots, P^{\iota}_{k-1}$ follows from the definition of $g^{\varphi}(f)$. Namely, since $g_i^- \notin U(F_w)^-$ and $g^-_{i+1} = \varphi(\mathfrak{a}(g_i)^+)$ for $1 \leq i \leq k-1$, there are prisms $P^{\iota}_1, \dots, P^{\iota}_{k-1}$ in $M|S^{\epsilon}_w$ satisfying $\partial^- P^{\iota}_i = g_i^-$ and $\partial^+ P^{\iota}_i = \mathfrak{a}(g_i)^+$, and such that identifications on $\partial^{\pm} P^{\iota}_i$ are as required. □

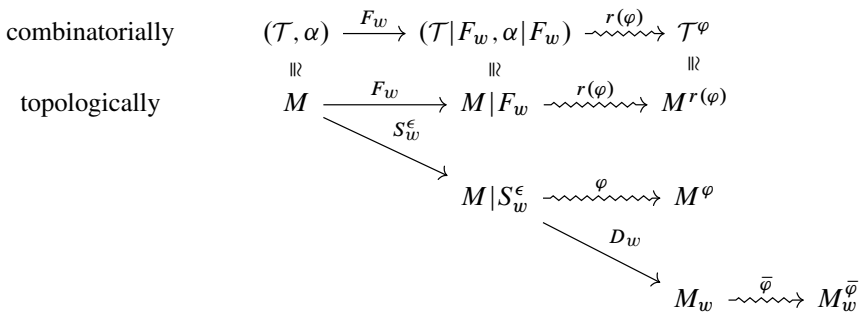

Figure 11: Each straight arrow corresponds to cutting the 3-manifold on the left of the arrow open along the set specified above the arrow. Each squiggly arrow corresponds to gluing the top boundary of the sutured manifold on the left of the arrow to its bottom boundary via the map specified above the arrow.

3.6 The manifold underlying the mutant triangulation

The mutant triangulation $\mathcal{T}^\varphi$ defined in Section 3.5 is an ideal triangulation of $M^{r(\varphi)}$. In this section we study the relationship between $M^{r(\varphi)}$ and M^φ, and derive sufficient and necessary condition for them to be homeomorphic.

Recall from Lemma 3.4 that $M|F_w$ is more closely related to $M_w=(M|S^\epsilon_w)|D_w$ than it is to $M|S^\epsilon_w$. As in Section 3.4, we will denote the triangulations in the top and bottom boundary of M_w by $\overline{\mathcal{Q}^+_{\mathcal{V},w}}$ and $\overline{\mathcal{Q}^-_{\mathcal{V},w}}$, respectively. A combinatorial isomorphism $\varphi\colon \mathcal{Q}^+_{\mathcal{V},w}\to\mathcal{Q}^-_{\mathcal{V},w}$ determines a map $\overline{\varphi}\colon \overline{\mathcal{Q}^+_{\mathcal{V},w}}\to\overline{\mathcal{Q}^-_{\mathcal{V},w}}$ via $\overline{\varphi}(\bar f)=\overline{\varphi(f)}$ and $\overline{\varphi}_{\bar f}=\varphi_f$. Note that $\overline{\varphi}$ is not a combinatorial automorphism in the sense of Definition 3.1, as it can map a pair nonadjacent triangles to a pair of adjacent triangles, and vice versa. Nonetheless, we can use $\overline{\varphi}$ to construct a mutant manifold $M^{\overline{\varphi}}_w$ out of M_w. Figure 11 summarizes relationships between M^φ, $M^{r(\varphi)}$ and $M^{\overline{\varphi}}_w$.

The relationship between M^φ and $M^{\overline{\varphi}}_w$ is the easiest to state:

Lemma 3.7 *$M^{\overline{\varphi}}_w$ is obtained from M^φ by cutting it along finitely many (potentially zero) disks, annuli and Möbius bands.*

Proof Recall that $M_w=(M|S^\epsilon_w)|D_w$ is obtained from $M|S^\epsilon_w$ by cutting it along finitely many product disks. These cuts persists in the mutant manifold $M^{\overline{\varphi}}_w$. Since $\overline{\varphi}$ maps $\bar f$ to $\overline{\varphi(f)}$ with vertex correspondence φ_f, these cuts are the only difference between M^φ and $M^{\overline{\varphi}}_w$.

Observe that under φ the top boundary of an edge product disk $D\in D_w$ can be mapped to the bottom boundary of an edge product disk $D'\in D_w$. Thus edge product disks can match up into annuli or Möbius bands in M^φ which are cut in $M^{\overline{\varphi}}_w$. □

We will say that the disks, annuli and Möbius bands in M^φ coming from edge product disks are *vertical*. Below we define a property of φ which ensures the existence of vertical annuli or Möbius bands:

Definition 3.8 Let S_w be a surface properly carried by a veering triangulation $\mathcal{V}$. We say $\varphi \in \mathrm{Aut}^+(\mathcal{Q}_{\mathcal{V},w})$ *aligns edge product disks* if there is a sequence of edge product disks $(D_i)_{i\in I} \subset D_w$ in $M|S_w^\epsilon$ which glue up to an annulus or a Möbius band in M^φ. Otherwise we say that φ *misaligns edge product disks*.

In Theorem 3.10 we will prove that the mutant triangulation $\mathcal{T}^\varphi$ is an ideal triangulation of M^φ if and only if φ misaligns edge product disks. The forward direction will rely on an observation that when φ aligns edge product disks, M^φ and $M^{r(\varphi)}$ either have different numbers of connected components or have nonhomeomorphic boundaries. The boundary of M^φ is composed of sutured annuli and tori of $M|S_w^\epsilon$. Since S_w^ϵ is an oriented surface in an oriented 3-manifold M, it induces orientations on the boundaries of sutured annuli of $M|S_w^\epsilon$. Furthermore, since φ is orientation preserving, it sends a top boundary of a sutured annulus of $M|S_w^\epsilon$ to a bottom boundary of a sutured annulus of $M|S_w^\epsilon$ in an orientation-preserving way. It follows that all boundary components of M^φ are tori.

Lemma 3.4 implies that by identifying, for every $f \in F_w$, f^+ with $\overline{L(f)^+}$ and f^- with $\overline{U(f)^-}$, we can view $M^{r(\varphi)}$ as a quotient space of $\mathrm{coll}(M_w - P_w)$. Therefore boundary components of $M^{r(\varphi)}$ are composed of the images of sutured annuli and tori of $M_w - P_w$ under the collapsing map (3.3). Given a sutured annulus A of $M|S_w^\epsilon$ the image $\mathrm{coll}(\iota^{-1}(A))$ is either an annulus or a disjoint union of bigon disks and intervals. The latter option happens if and only if $A \cap D_w \neq \varnothing$. In this case D_w separates A into finitely many rectangles that we call D_w*-rectangles*.

Definition 3.9 Let A be a sutured annulus of $M|S_w^\epsilon$. We say that a subset $R \subset A$ is a D_w*-rectangle* if there are edge product disks $D, D' \in D_w$ such that the boundary of R decomposes into four arcs: one arc $\partial^+ R$ contained in $\partial^+ A$, one arc $\partial^- R$ contained in $\partial^- A$, one arc contained in $\partial_v D$ and one arc contained in $\partial_v D'$. We call the last two arcs in the boundary of R the *vertical sides* of R.

We say that a D_w-rectangle R is *prismatic* if there is a triangular prism $P \in P_w$ such that $P \cap \iota^{-1}(R) = \iota^{-1}(R)$. Otherwise we say that R is *nonprismatic*. If R is nonprismatic then $\mathrm{coll}(\iota^{-1}(R))$ is a bigon disk. In this case the boundary of $\mathrm{coll}(\iota^{-1}(R))$ decomposes into the *positive boundary* $\partial^+ \mathrm{coll}(\iota^{-1}(R)) = \mathrm{coll}(\iota^{-1}(\partial^+ R))$, and the *negative boundary* $\partial^- \mathrm{coll}(\iota^{-1}(R)) = \mathrm{coll}(\iota^{-1}(\partial^- R))$; see Figure 22. When R is prismatic, $\mathrm{coll}(\iota^{-1}(R))$ is an interval.

Theorem 3.10 *The mutant triangulation $\mathcal{T}^\varphi$ is an ideal triangulation of M^φ if and only if φ misaligns edge product disks.*

Proof By Lemma 3.4, we can view $M^{r(\varphi)}$ as a quotient space of $\mathrm{coll}(M_w - P_w)$. The map

$$\partial^+(\mathrm{coll}(M_w - P_w)) \to \partial^-(\mathrm{coll}(M_w - P_w))$$

by which we quotient $\mathrm{coll}(M_w - P_w)$ to get $M^{r(\varphi)}$ is obtained from

$$r(\varphi) = (r^\varphi \colon F_w^+ \to F_w^-, (r^\varphi_{f^+})_{f^+\in F_w^+})$$

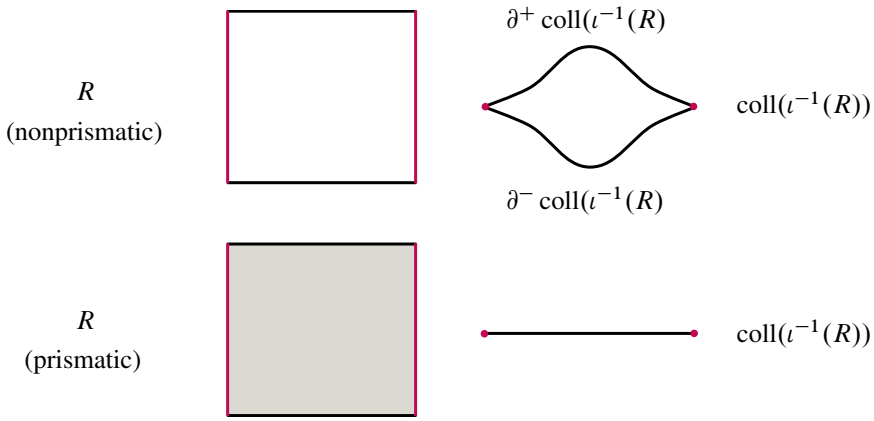

Figure 12: Top: a nonprismatic D_w-rectangle and its image under coll. Bottom: a prismatic D_w-rectangle and its image under coll. Red vertical intervals correspond to the intersection of R with D_w.

by modifying the bijections r^{φ}_{f+} to make up for the identifications $f^+ \sim \overline{L(f)^+}$ and $f^- \sim \overline{U(f)^-}$. For simplicity, we abuse the notation and denote this map by $r(\varphi)$. Let V^{φ}_w denote the set of vertical annuli and Möbius bands in M^{φ}. This set is nonempty if and only if φ aligns edge product disks.

First suppose that φ aligns edge product disks.

Case 1 There is a boundary torus T of M^{φ} such that $T \cap V^{\varphi}_w \neq \varnothing$ and T is not composed entirely of prismatic D_w-rectangles.

Observe that $T \cap V^{\varphi}_w$ consists of finitely many parallel simple closed curves in T. We denote the connected components of $T \cap V^{\varphi}_w$ by $d_1, \dots, d_r$ for $r \geq 1$, and we assume that they are circularly ordered so that d_i and d_{i+1} cobound an annulus $X_i \subset T$ whose interior is disjoint from V^{φ}_w (the subscript r is taken modulo r). Let $A_1, \dots, A_N$ be sutured annuli of $M|S^{\epsilon}_w$ such that $\varphi(\partial^+ A_j) = \partial^- A_{j+1}$ for every $j = 1, 2, \dots, N$ (the subscript j is taken modulo N) and T is the quotient of $A_1 \sqcup A_2 \sqcup \cdots \sqcup A_N$ by φ. Each $A_j \cap X_i$ consists of finitely many D_w-rectangles; see Figure 13, left. Let $\mathcal{R}^j_i$ be the collection of D_w-rectangles making up $A_j \cap X_i$ (in Figure 13, left, that would be all rectangles in one row) and let $\mathcal{R}_i$ be the union of all $\mathcal{R}^j_i$. By the assumption that T is not composed entirely of prismatic D_w-rectangles, there must be $i \in \{1, 2, \dots, r\}$ such that $\mathcal{R}_i$ contains a nonprismatic D_w-rectangle.

If every nonprismatic D_w-rectangle $R \in \mathcal{R}_i$ has both vertical sides contained in $d_i \cup d_{i+1}$ then each $\mathcal{R}^j_i$ either contains only prismatic D_w-rectangles or contains exactly one nonprismatic D_w-rectangle. Furthermore, since there is at least one nonprismatic D_w-rectangle in $\mathcal{R}_i$, there is at least one $\mathcal{R}^j_i$ of the latter type. Thus, by the definition of $r(\varphi)$, there are nonprismatic D_w-rectangles $R_1, \dots, R_n \in \mathcal{R}_i$ for $1 \leq n \leq N$ such that $r(\varphi)(\partial^+ \operatorname{coll}(\iota^{-1}(R_j))) = \partial^- \operatorname{coll}(\iota^{-1}(R_{j+1}))$, where the subscript j is taken modulo n. Since the image of a nonprismatic D_w-rectangle under coll is a bigon disk (see Figure 12), this gives us a sequence of bigon disks glued to each other top to bottom. The bigons $\operatorname{coll}(\iota^{-1}(R_j))$

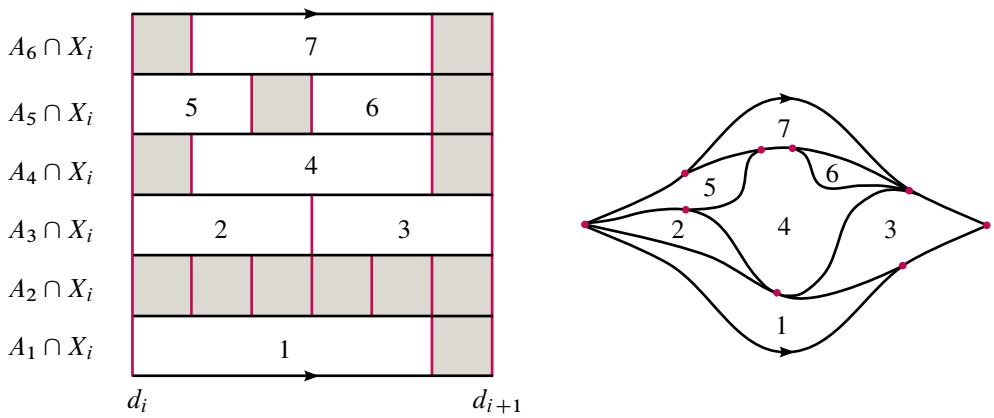

Figure 13: Left: An annular subset X_i of a boundary torus T of M^φ cobounded by a pair of vertical annuli or Möbius bands. Red intervals correspond to the intersection of X_i with edge product disks. Prismatic D_w-rectangles are shaded gray. Nonprismatic D_w-rectangles are numbered. Right: Spherical boundary component of $M^{r(\varphi)}$ corresponding to X_i. A bigon arising as a result of collapsing a nonprismatic D_w-rectangle labeled with i on the left is labeled with i.

inherit orientation on their boundary from R_j. Thus the assumption that φ is orientation preserving together with Lemma 3.6 imply that the quotient space of $\operatorname{coll}(\iota^{-1}(\mathcal{R}_i))$ by $r(\varphi)$ is a sphere. This means that $M^{r(\varphi)}$ admits a spherical boundary component. Since M^φ has only toroidal boundary components, these manifolds cannot be homeomorphic.

Now suppose that $R \in \mathcal{R}_i$ is a nonprismatic D_w-rectangle which has a vertical side d that is disjoint from $d_i \cup d_{i+1}$. An example of such a situation is presented in Figure 13. The assumption that $\operatorname{int}(X_i) \cap V_w^\varphi = \varnothing$ implies that there is a nonprismatic D_w-rectangle $R' \in \mathcal{R}_i$ such that $r(\varphi)$ identifies $\operatorname{coll}(\iota^{-1}(d))$ with an interior point of $\partial^- \operatorname{coll}(\iota^{-1}(R'))$. Therefore the quotient space of $\operatorname{coll}(\iota^{-1}(\mathcal{R}_i))$ by $r(\varphi)$ is again a sphere, and thus $M^{r(\varphi)}$ is not homeomorphic to M^φ.

Case 2 For every boundary torus T of M^φ either $T \cap V_w^\varphi = \varnothing$ or T is composed entirely of prismatic D_w-rectangles.

Since $V_w^\varphi \neq \varnothing$, the assumption of this case implies that there is a connected component of M^φ consisting entirely of the images of triangular prisms under ι. In particular, M^φ has strictly more connected components than $M^{r(\varphi)}$, so these manifolds are not homeomorphic. (Note, however, that $M^{r(\varphi)}$ may be homeomorphic to the union of other connected components of M^φ.)

Now suppose that φ misaligns edge product disks. Then there are no vertical annuli or Möbius bands in M^φ, and hence, by Lemma 3.7, $M_w^{\overline{\varphi}}$ can be obtained from M^φ by cutting it along finitely many vertical disks. Equivalently, M^φ is the quotient space of $\operatorname{coll}(M_w)$ by $\overline{\varphi}$.

Lemma 3.6 explains how the definition of the regluing map simulates the process of collapsing triangular prisms into their bottom triangles. Thus $r(\varphi)$ on F_w^+ respects not only the identification between $L(f)^+$

and $\varphi(L(f)^+)$, for all $f \in F_w$, but also the identification between g^+ and $\varphi(g^+)$ for all $g \in F_{\mathcal{V},w}$ such that either g or $\mathfrak{a}^{-1}(g)$ appears in the sequence $g^\varphi(f)$ for some $f \in F_w$. If there is $g \in F_{\mathcal{V},w} - L(F_w)$ such that for every $f \in F_w$ neither g nor $\mathfrak{a}^{-1}(g)$ appears in $g^\varphi(f)$, then there are triangular prisms of $M_w = (M|S^\epsilon_w)|D_w$ through which we have not passed when defining $r(\varphi)$. These triangular prisms would arrange into solid tori components of $M^{\overline{\varphi}}_w$ consisting entirely of triangular prisms. However, the assumption that φ misaligns edge product disks implies that $M^{\overline{\varphi}}_w$ does not admit such solid tori components. Therefore when φ misaligns edge product disks Lemma 3.6 implies that the quotient space of $\mathrm{coll}(M_w)$ by $\overline{\varphi}$ is homeomorphic to the quotient space of $\mathrm{coll}(M_w - P_w)$ by $r(\varphi)$. The latter is $M^{r(\varphi)}$, while the former — as explained in the previous paragraph — is M^φ. Thus $M^{r(\varphi)}$ is homeomorphic to M^φ. □

Remark 3.11 In the proof of Theorem 3.10 we constructed a sphere out of bigon disks. This may look like a contradiction to the fact, mentioned in Section 2.1, that only surfaces with zero Euler characteristic can admit a bigon train track. However, the obtained decomposition of S^2 into bigons is not a bigon track in the usual sense. If τ is a train track on S then for every switch v of τ which is not contained in ∂S there must be two complementary regions of τ which meet v along a smooth point in their boundary. In the construction we get two points in the sphere which meet only cusps of bigons.

3.7 Veeringness of the mutant triangulation

In Section 3.6 we found a sufficient and necessary condition on φ for the mutant triangulation $\mathcal{T}^\varphi$ to be a triangulation of M^φ. In this subsection we are interested in endowing $\mathcal{T}^\varphi$ with a veering structure.

By tautness, edges of the dual spine $\mathcal{D}$ of $(\mathcal{T}, \alpha)$ admit orientations such that every vertex v of $\mathcal{D}$ has exactly two incoming edges and two outgoing edges; this is Definition 2.1(1). When we construct $\mathcal{T}^\varphi$ out of $(\mathcal{T}|F_w, \alpha|F_w)$ we always identify a face $f^+ \in F^+_w$ with a face $r^\varphi(f^+) \in F^-_w$. Therefore there is a natural orientation on the edges of the dual spine $\mathcal{D}^\varphi$ of $\mathcal{T}^\varphi$ that is induced from the orientation on the edges of the dual spine of $\mathcal{T}$. With this orientation $\mathcal{D}^\varphi$ satisfies Definition 2.1(1). To obtain a taut structure on $\mathcal{T}^\varphi$ it suffices to find a sufficient condition on $r(\varphi)$ that guarantees every 2-cell of $\mathcal{D}^\varphi$ has exactly one top vertex and exactly one bottom vertex. To derive such a condition it is helpful to analyze the structure of $\mathcal{D}|F_w$ and its relationship to $(\mathcal{T}|F_w, \alpha|F_w)$. First, observe that edges of $(\mathcal{T}|F_w, \alpha|F_w)$ can be classified into four types. We say that an edge e of $(\mathcal{T}|F_w, \alpha|F_w)$, or $\mathcal{V}|F_w$, is

- *internal* if e is neither an edge of a triangle from F^+_w nor an edge of a triangle from F^-_w,
- *positive* if e is an edge of a triangle from F^+_w and is not edge of a triangle from F^-_w,
- *negative* if e is an edge of a triangle from F^-_w and is not an edge of a triangle from F^+_w,
- *mixed* if e is an edge of a triangle from F^+_w and also an edge of a triangle from F^-_w.

Assume that $\mathcal{T}$ and $\mathcal{D}$ are embedded in M so that they are dual to one another. For every 2-cell p of $\mathcal{D}|F_w$ there is a 2-cell s of $\mathcal{D}$ such that p is a connected component of $s|F_w$. If $s \cap F_w = \varnothing$ then we say that p is an *internal cell* of $\mathcal{D}|F_w$. Now suppose that $s \cap F_w \neq \varnothing$. If p contains the top vertex of s we say

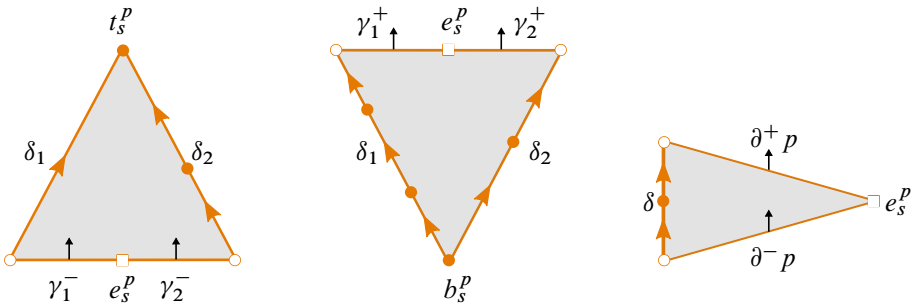

Figure 14: Left: negative cell of $\mathcal{D}|F_w$. Center: positive cell of $\mathcal{D}|F_w$. Right: mixed cell of $\mathcal{D}|F_w$. The number of vertices in the interiors of δ_1, δ_2 and δ may vary.

that p is a *negative cell* of $\mathcal{D}|F_w$; see Figure 14, left. If p contains the bottom vertex of s we say that p is a *positive cell* of $\mathcal{D}|F_w$; see Figure 14, center. If p contains neither the top nor the bottom vertex of s we say that p is a *mixed cell* of $\mathcal{D}|F_w$; see Figure 14, right. Naturally, an internal/positive/negative/mixed cell of $\mathcal{D}|F_w$ is dual to an internal/positive/negative/mixed edge of $(\mathcal{T}|F_w, \alpha|F_w)$.

For every cell s of $\mathcal{D}$ such that $s \cap F_w \neq \varnothing$, we denote by e_s the intersection of s with its dual edge in $(\mathcal{T}, \alpha)$. Then every connected component p of $s|F_w$ has a point in its boundary corresponding to e_s that we will denote by e_s^p. If p is negative then there is a point t_s^p in the boundary of p corresponding to the top vertex t_s of s. If p is positive then there is a point b_s^p in the boundary of p corresponding to the bottom vertex b_s of s.

If p is a negative cell of $\mathcal{D}|F_w$ then its boundary decomposes into

- two arcs γ_1^- and γ_2^- meeting at e_s^p, both cooriented into p,
- two arcs δ_1 and δ_2 meeting at t_s^p, both oriented so that they point into t_s^p.

See Figure 14, left. We say that γ_1^- and γ_2^- are *maximal negative arcs* in the boundary of p.

If p is a positive cell of $\mathcal{D}|F_w$ then its boundary decomposes into

- two arcs γ_1^+ and γ_2^+ meeting at e_s^p, both cooriented out of p,
- two arcs δ_1 and δ_2 meeting at b_s^p, both oriented so that they point out of b_s^p.

See Figure 14, center. We say that γ_1^+ and γ_2^+ are *maximal positive arcs* in the boundary of p.

If p is a mixed cell of $\mathcal{D}|F_w$ then its boundary decomposes into

- two arcs $\partial^+ p$ and $\partial^- p$ meeting at e_s^p, such that $\partial^+ p$ is cooriented out of p and $\partial^- p$ is cooriented into p,
- one arc δ oriented from $\partial^- p$ to $\partial^+ p$.

See Figure 14, right. We say that $\partial^+ p$ is the *maximal positive arc* in the boundary of p, and that $\partial^- p$ is the *maximal negative arc* in the boundary of p.

If $\gamma^{\pm}$ is a maximal positive/negative arc in the boundary of a cell p of $\mathcal{D}|F_w$ we say that e_s^p is the *internal endpoint* of $\gamma^{\pm}$.

Via duality between internal/positive/negative/mixed cells of $\mathcal{D}|F_w$ and internal/positive/negative/mixed edges of $(\mathcal{T}|F_w, \alpha|F_w)$, respectively, we get a combinatorial sufficient condition on $r(\varphi)$ that guarantees $\mathcal{T}^{\varphi}$ admits a taut structure in Lemma 3.12. In Lemma 3.15 we explain how this condition relates to the matching of edge product disks of $M|S_w^{\epsilon}$ under φ.

Lemma 3.12 *If for every mixed edge e of $(\mathcal{T}|F_w, \alpha|F_w)$ there is a positive edge e^+ of $(\mathcal{T}|F_w, \alpha|F_w)$ and a negative edge e^- of $(\mathcal{T}|F_w, \alpha|F_w)$ such that e, e^+ and e^- are identified in $\mathcal{T}^{\varphi}$ then the triangulation $\mathcal{T}^{\varphi}$ admits a taut structure.*

Proof We assume that the 1-skeleton of D^{φ} is equipped with the orientation induced by $\alpha|F_w$. It suffices to show that under the assumption of the lemma, every 2-cell of D^{φ} has exactly one top vertex and exactly one bottom vertex; see Definition 2.1.

Denote by Γ^+ (respectively, Γ^-) the set of maximal positive (respectively, negative) arcs in the boundaries of cells of $\mathcal{D}|F_w$. Recall that $\mathcal{T}^{\varphi}$ is the quotient space of $(\mathcal{T}|F_w, \alpha|F_w)$ under the regluing map $r(\varphi)$. Dually we get a regluing map $\Gamma(\varphi) = \{\Gamma^{\varphi}\colon \Gamma^+ \to \Gamma^-, (\Gamma^{\varphi}_{\gamma^+})_{\gamma^+\in\Gamma^+}\}$, where Γ^{φ} is a bijection between Γ^+ and Γ^- and $\Gamma^{\varphi}_{\gamma^+}$ is a bijection between the endpoints of γ^+ and the endpoints of $\Gamma^{\varphi}(\gamma^+)$, such that the quotient of $\mathcal{D}|F_w$ by $\Gamma(\varphi)$ gives $\mathcal{D}^{\varphi}$. Since the 1-skeleton of $\mathcal{D}^{\varphi}$ arises from recombining the 1-skeleton of $\mathcal{D}$, we get that $\Gamma^{\varphi}_{\gamma^+}$ must send the internal endpoint of γ^+ to the internal endpoint of $\Gamma^{\varphi}(\gamma^+)$.

Let p be a positive cell of $\mathcal{D}|F_w$. Denote by γ_1^+ and γ_2^+ the two distinct maximal positive arcs in the boundary of p. For $i = 1, 2$ the bijection Γ^{φ} can send γ_i^+ only to a maximal negative arc in the boundary of a mixed cell or to a maximal negative arc in the boundary of a negative cell. Let $q_1, \dots, q_m$ be the maximal collection of mixed cells of $\mathcal{D}|F_w$ such that $\Gamma^{\varphi}(\gamma_1^+) = \partial^- q_1$ and $\Gamma^{\varphi}(\partial^+ q_i) = \partial^- q_{i+1}$ for $i = 1, 2, \dots, m-1$. Let $q_1', \dots, q_n'$ be the maximal collection of mixed cells of $\mathcal{D}|F_w$ such that $\Gamma^{\varphi}(\gamma_2^+) = \partial^- q_1'$ and $\Gamma^{\varphi}(\partial^+ q_j') = \partial^- q_{j+1}'$ for $j = 1, 2, \dots, n-1$. First assume that these collections of mixed cells are nonempty, that is $m, n \geq 1$. By maximality and the fact that positive cells do not have arcs in Γ^-, there are negative cells p' and p'' of $\mathcal{D}|F_w$ such that $\Gamma^{\varphi}(\partial^+ q_m)$ is a maximal negative arc in the boundary of p' and $\Gamma^{\varphi}(\partial^+ q_n')$ is a maximal negative arc in the boundary of p''. The cells $q_1, \dots, q_m, q_1', \dots, q_n'$ must all be distinct, and hence $\Gamma^{\varphi}(\partial^+ q_m)$ and $\Gamma^{\varphi}(\partial^+ q_n')$ are distinct. Since $\Gamma(\varphi)$ sends internal endpoints of arcs to internal endpoints of arcs, we must have $p' = p''$. Thus we obtain a cell of $\mathcal{D}^{\varphi}$ composed of $p, q_1, \dots, q_m, q_1', \dots, q_n', p' = p''$. Such a cell has exactly one top vertex (coming from $p' = p''$) and exactly one bottom vertex (coming from p). If $m = 0$ it suffices to replace $\Gamma^{\varphi}(\partial^+ q_m)$ with $\Gamma^{\varphi}(\gamma_1^+)$, and if $n = 0$ it suffices to replace $\Gamma^{\varphi}(\partial^+ q_n')$ with $\Gamma^{\varphi}(\gamma_2^+)$, to still get a cell of $\mathcal{D}^{\varphi}$ with precisely one top vertex and precisely one bottom vertex.

It follows that every 2-cell of $\mathcal{D}^{\varphi}$ is either

- composed of one internal cell of $\mathcal{D}|F_w$, or

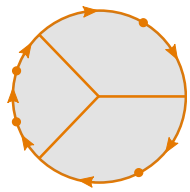

Figure 15: Gluing mixed cells of $\mathcal{D}|F_w$ cyclically yields a cell of $\mathcal{D}^\varphi$ whose edges are cyclically oriented.

- composed of one positive cell of $\mathcal{D}|F_w$, one negative cell of $\mathcal{D}|F_w$ and finitely many (potentially zero) mixed cells of $\mathcal{D}|F_w$, or
- composed of finitely many mixed cells of $\mathcal{D}|F_w$.

The last type of cells of $\mathcal{D}^\varphi$ have cyclically oriented edges in their boundary; see Figure 15. These are the only cells of $\mathcal{D}^\varphi$ that do not satisfy Definition 2.1. Using the duality between positive/negative/mixed cells of $\mathcal{D}|F_w$ and positive/negative/mixed edges of $(\mathcal{T}|F_w, \alpha|F_w)$ it is easy to see that if for every mixed edge e of $(T|F_w, \alpha|F_w)$ there is a positive edge e^+ of $(T|F_w, \alpha|F_w)$ and a negative edge e^- of $(T|F_w, \alpha|F_w)$ such that e, e^+ and e^- are identified in $\mathcal{T}^\varphi$ then $\mathcal{D}^\varphi$ does not admit such cells. Thus under this assumption, $\alpha|F_w$ induces a taut structure on $\mathcal{T}^\varphi$. □

We will devote the rest of this subsection to restate the condition of Lemma 3.12 in terms of φ and then prove that it is not only sufficient but also necessary for the existence of a taut structure on $\mathcal{T}^\varphi$. Recall that by $D(M_w)$ we denote the set of disks contained in the sutured annuli of M_w arising from cutting $M|S^\epsilon_w$ along D_w. Let $D(M_w - P_w)$ be the subset of $D(M_w)$ consisting only of those disks which are not contained in the sutured annuli of triangular prisms of M_w. Lemma 3.4 implies the following relationship between mixed edges of $(\mathcal{T}|F_w, \alpha|F_w)$ and disks $D(M_w - P_w)$ contained in the sutured annuli of $M_w - P_w$:

Corollary 3.13 *For every one sided-edge e of $(\mathcal{T}|F_w, \alpha|F_w)$ there is precisely one $D' \in D(M_w - P_w)$ such that $e = \mathrm{coll}(D')$.* □

However, we are mainly interested in the relationship between mixed edges of $(\mathcal{T}|F_w, \alpha|F_w)$ and edge product disks in $M|S^\epsilon_w$.

Definition 3.14 Let $D', D'' \in D(M_w)$ be such that $\iota(D') = \iota(D'') = D \in D_w$. We say that the edge product disk D

- *has prisms on both sides* if there are triangular prisms $P', P'' \in P_w$ such that D' is contained in the sutured annulus of P' and D'' is contained in the sutured annulus of P'',
- *has a prism on one side* if exactly one disk out of D' and D'' is contained in the sutured annulus of some triangular prism of M_w,
- *does not have a prism on either side* if $D, D' \in D(M_w - P_w)$.

Using this definition, we can restate Corollary 3.13 and say that an edge product disk $D \in D_w$ corresponds to two, one or zero mixed edges of $(\mathcal{T}|F_w, \alpha|F_w)$ if and only if D does not have a prism on either side, has a prism on one side or has prisms on both sides, respectively.

Let V be a vertical annulus or a vertical Möbius band in M^φ. Let $D_1, \dots, D_N$ be edge product disks of $M|S^\epsilon_w$ such that V is the quotient space of $D_1 \sqcup \cdots \sqcup D_N$ by φ. We say that V *lies in a prismatic region of* M^φ if D_i has prisms on both sides for every $1 \le i \le N$. Using this terminology we can now restate the assumption of Lemma 3.12 in terms of topological properties of M^φ:

Lemma 3.15 *The following statements are equivalent*:

(1) *For every mixed edge e of $(\mathcal{T}|F_w, \alpha|F_w)$ there is a positive edge e^+ of $(\mathcal{T}|F_w, \alpha|F_w)$ and a negative edge e^- of $(\mathcal{T}|F_w, \alpha|F_w)$ such that e, e^+ and e^- are identified in $\mathcal{T}^\varphi$.*

(2) *Every vertical annulus or Möbius band in M^φ lies in a prismatic region of M^φ.*

Proof We show both directions by contraposition. First we show that (2) implies (1). Observe that if e is an edge of triangle from F^+_w then the edge $r(\varphi)(e)$ might not be well defined, because a positive edge can be mapped to two different mixed edges. However, if e is a mixed edge then $r(\varphi)(e)$ is well defined, because e is an edge of only one $f^+ \in F^+_w$.

In what follows the subscript i is taken modulo n. Suppose that there is a collection $e_1, \dots, e_n$ of mixed edges of $(\mathcal{T}|F_w, \alpha|F_w)$ such that $r(\varphi)(e_i) = e_{i+1}$ for every $1 \le i \le n$. By Corollary 3.13, there is a collection $D'_1, \dots, D'_n \in D(M_w - P_w)$ of disks contained in the sutured annuli of $M_w - P_w$ such that $\operatorname{coll}(D'_i) = e_i$. Let $D_i = \iota(D'_i) \in D_w$. By the definition of $r(\varphi)$, for every $1 \le i \le n$ either $\varphi(\partial^+ D_i) = \partial^- D_{i+1}$ or there is $k_i \ge 1$ and a collection of edge product disks $D^{(1)}_i, \dots, D^{(k_i)}_i \in D_w$ (which all have prisms on at least one side) such that $\varphi(\partial^+ D_i) = \partial^- D^{(1)}_i$ and $\varphi(\partial^+ D^{(j)}_i) = \partial^- D^{(j+1)}_i$ for every $1 \le j \le k_i - 1$ and $\varphi(\partial^+ D^{(k_i)}_i) = \partial^- D_{i+1}$. Therefore the quotient of $\bigsqcup_{i=1}^n D_i \sqcup \bigsqcup_{j=1}^{k_i} D^{(j)}_i$ by φ is a vertical annulus or Möbius band V in M^φ. Since $D'_i \in D(M_w - P_w)$, D_i does not have prisms on both sides. It follows that V does not lie in a prismatic region of M^φ.

Now let $D_1, \dots, D_n \in D_w$ be a collection of edge product disks in $M|S^\epsilon_w$ such that $\varphi(\partial^+ D_i) = \partial^- D_{i+1}$ for every $1 \le i \le n$. Denote by V the quotient space of $D_1 \sqcup \cdots \sqcup D_n$ by φ. If V does not lie in a prismatic region of M^φ there is $1 \le k \le n$ and a sequence $1 \le i_1 < i_2 < \cdots < i_k \le n$ such that D_{i_j} does not have prisms on both sides for every $1 \le j \le k$, and for every $l \notin \{i_1, i_2, \dots, i_k\}$ the edge product disk D_l has prisms on both sides. For $1 \le j \le k$ if D_{i_j} does not have a prism on either side there are disks $D'_{i_j}, D''_{i_j} \in D(M_w - P_w)$ such that $\iota(D'_{i_j}) = \iota(D''_{i_j}) = D_{i_j}$. If D_{i_j} has a prism on one side, there is $D'_{i_j} \in D(M_w - P_w)$ such that $\iota(D'_{i_j}) = D_{i_j}$. By Corollary 3.13 there are mixed edges $e_{i_j} = \operatorname{coll}(D'_{i_j})$ and $e'_{i_j} = \operatorname{coll}(D''_{i_j})$ of $(\mathcal{T}|F_w, \alpha|F_w)$. By the definition of $r(\varphi)$, after possibly switching e_{ij} with e'_{i_j} for some $1 \le j \le k$, there is $m \ge 1$ and a sequence $1 \le l_1 < l_2 < \cdots < l_m \le k$ such that $r(\varphi)(e_{i_{l_j}}) = e_{i_{l_j+1}}$ for every $1 \le j \le m$. This gives an edge of $\mathcal{T}^\varphi$ which is composed entirely of mixed edges of $(\mathcal{T}|F_w, \alpha|F_w)$. □

Proposition 3.16 *The mutant triangulation $\mathcal{T}^\varphi$ admits a taut structure if and only if every vertical annulus or Möbius band in M^φ lies in a prismatic region of M^φ.*

Proof The fact that when every vertical annulus or Möbius band in M^φ lies in a prismatic region of M^φ then $\mathcal{T}^\varphi$ admits a taut structure follows from Lemmas 3.12 and 3.15.

We prove the other direction by contraposition. Suppose that there is a vertical annulus or a Möbius band V in M^φ which does not lie in a prismatic region of M^φ. Let T be a boundary torus of M such that $T \cap V \neq \varnothing$. Since V does not consist entirely of edge product disks which have prisms on both sides, T does not consist entirely of prismatic D_w-rectangles. It follows from the proof of Theorem 3.10 (Case 1) that $M^{r(\varphi)}$, the manifold underlying $\mathcal{T}^\varphi$, admits a spherical boundary component. Therefore, by Lemma 2.3, $M^{r(\varphi)}$ does not have a taut triangulation. In particular, $\mathcal{T}^\varphi$ does not admit a taut structure. □

It follows that $\mathcal{T}^\varphi$ admits a taut structure if and only if orientations on the edges of the dual spine $\mathcal{D}^\varphi$ inherited from $(\mathcal{T}|F_w, \alpha|F_w)$ determine a taut structure on $\mathcal{T}^\varphi$. In this case we denote the taut structure on $\mathcal{T}^\varphi$ by α^φ. We also say that $(\mathcal{T}, \alpha)$ and $(\mathcal{T}^\varphi, \alpha^\varphi)$ are *taut mutants*.

The assumption that φ misaligns edge product disks is stronger than the assumption that every vertical annulus or Möbius band in M^φ lies in a prismatic region of M^φ. However, since it is a necessary condition for $\mathcal{T}^\varphi$ to be an ideal triangulation of M^φ (Theorem 3.10), it is reasonable to assume this stronger condition for the rest of the paper. Below we also prove that when φ aligns edge product disks then M^φ does not admit a veering triangulation. This further justifies restricting our considerations only to automorphisms which misalign edge product disks.

Proposition 3.17 *If $\varphi \in \mathrm{Aut}^+(\mathcal{Q}_{\mathcal{V},w})$ aligns edge product disks then M^φ does not admit a veering triangulation.*

Proof Since only hyperbolic manifolds can admit veering triangulations [23, Theorem 1.5] (stated here as Theorem 2.11), it suffices to show that M^φ is not hyperbolic. Recall that when φ aligns edge product disks M^φ must admit a vertical annulus or a vertical Möbius band. By passing to a finite cover, we can assume that there is a vertical annulus A in M^φ. We will show that A is essential, that is, incompressible, boundary-incompressible and not boundary parallel. First we will prove that M^φ is irreducible and boundary-irreducible.

Claim 3.17.1 *M^φ is irreducible and boundary-irreducible.*

Proof of Claim 3.17.1 Lackenby proved that every 3-manifold with a taut triangulation is irreducible and boundary-irreducible [27, Proposition 10]. Therefore it suffices to show that M^φ has a taut triangulation.

If every vertical annulus and Möbius band lies in a prismatic region of M^φ then, by Proposition 3.16, $\mathcal{T}^\varphi$ admits a taut structure, and we are done. To construct a taut triangulation on M^φ when there are vertical annuli or Möbius bands outside of the prismatic region of M^φ we first modify the triangulation $(\mathcal{T}, \alpha)$

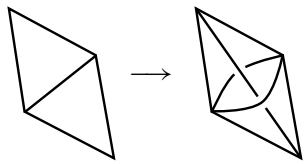

Figure 16: The 0-2 Pachner move. If f and g are on opposite sides of e we can cut $(\mathcal{T},\alpha)$ along $f\cup g$ and glue in a "taut pillow", producing a new taut triangulation of M.

of M using 0-2 *Pachner moves*. Such a move can be performed on any pair of adjacent triangles f and g which are on opposite sides of an edge e of $(\mathcal{T},\alpha)$. First, we cut $(\mathcal{T},\alpha)$ along $f\cup g$. The resulting cut triangulation has four boundary faces: f^+, g^+, f^- and g^-. Using two additional taut tetrahedra t and t' we construct a "taut pillow" by identifying the square consisting of the top faces of t with the square consisting of the bottom faces of t' so that the top diagonal of t is identified with the bottom diagonal of t'; see Figure 16, right. Now there is a natural way to identify $f^+\cup g^+$ with the bottom faces of t and the top faces of t' with $f^-\cup g^-$ to get a new taut triangulation of M. The key feature of the 0-2 moves is that by applying them finitely many times above pairs of triangles adjacent to edges with weight greater than one, we can construct a taut triangulation $(\mathcal{T}_*,\alpha_*)$ of M with the following properties:

(a) $(\mathcal{T}_*,\alpha_*)$ carries a surface S_{w_*} whose induced triangulation $\mathcal{Q}_*$ is combinatorially isomorphic to $\mathcal{Q}_{\mathcal{V},w}$.

(b) The weight system w_* on $(\mathcal{T}_*,\alpha_*)$ is such that no edge of $(\mathcal{T}_*,\alpha_*)$ has weight greater than one.

(c) Each edge product disk $D\in D_w$ gives a pair of edges of $(\mathcal{T}_*,\alpha_*)$ which are homotopic to each other (while keeping their endpoints on the boundary tori); one of these edges corresponds to $\partial^- D$, and the other to $\partial^+ D$; see Figure 16.

From (a) it follows that there is $\varphi_*\in \mathrm{Aut}^+(\mathcal{Q})$ such that $M^\varphi = M^{\varphi_*}$. Part (b) implies that $M|S^\epsilon_{w_*}$ does not admit any edge product disks and thus φ_* misaligns edge product disks. Therefore, by Proposition 3.16 and Theorem 3.10, we can use φ_* to construct a taut triangulation $(\mathcal{T}_*^{\varphi_*},\alpha_*^{\varphi_*})$ of $M^\varphi = M^{\varphi_*}$. □

By construction, the core curve c of the vertical annulus A of M^φ is homotopic to an essential simple closed curve on some boundary torus T of M^φ. Claim 3.17.1 implies that T is incompressible, and thus A is incompressible.

Since A is composed entirely of edge product disks in $M|S^\epsilon_w$, an essential arc γ in A is homotopic to the image of the bottom boundary $\partial^- D$ of some edge product disk $D\in D_w$ under the quotient map $M|S^\epsilon_w\to M^\varphi$. By property (c) of the triangulation $(\mathcal{T}_*,\alpha_*)$ constructed in the proof of Claim 3.17.1, there is an edge of $(\mathcal{T}_*^{\varphi_*},\alpha_*^{\varphi_*})$ which is homotopic to γ. This implies that A cannot be boundary parallel, because in a taut triangulation an edge is never homotopic into a vertex neighborhood while keeping its ends in the vertex neighborhood [24, Theorem 6.1]. If there was a boundary-compression disk for A, A would compress into a properly embedded disk D. By boundary-irreducibility of M^φ (Claim 3.17.1), D must be boundary parallel. Hence A must be boundary parallel, which contradicts our previous observation that it is not. Thus A is boundary-incompressible.

We showed that, up to passing to a finite cover, M^φ admits an essential annulus. So it either contains an essential torus or is a small Seifert fibered manifold [33, Lemma 11.2.10]. In either case, M^φ is not hyperbolic, and thus cannot admit a veering triangulation. □

From now on we assume that φ misaligns edge product disks. The taut triangulation $(\mathcal{T}^\varphi, \alpha^\varphi)$ is veering if and only if its dual spine $\mathcal{D}^\varphi$ has a smoothing into a branched surface which locally looks like in Figure 4; see Definition 2.5. One way of ensuring that is to construct the required branched surface structure on $\mathcal{D}^\varphi$ using the branched surface structure $\mathcal{B}|F_w$ on $\mathcal{D}|F_w$. Extending the (partial) veering structure $\mathcal{B}|F_w$ to a veering structure on $\mathcal{D}^\varphi$ is possible only if for every $f^+ \in F_w^+$ the regluing map $r(\varphi)$ maps the large edge of f^+ to the large edge of $r^\varphi(f^+)$. For this reason we define the group $\mathrm{Aut}^+(\mathcal{Q}_{\mathcal{V},w} \mid \tau_{\mathcal{V},w})$ of orientation-preserving combinatorial automorphisms of $\mathcal{Q}_{\mathcal{V},w}$ which preserve $\tau_{\mathcal{V},w}$.

Lemma 3.18 *Let $\varphi \in \mathrm{Aut}^+(\mathcal{Q}_{\mathcal{V},w} \mid \tau_{\mathcal{V},w})$. If e is the large edge of $f^+ \in F_w^+$ then $r^\varphi_{f^+}(e)$ is the large edge of $r^\varphi(f^+) \in F_w^-$.*

Proof Suppose that $g^\varphi(f) = (g_1, \dots, g_k)$. Then $g_1 = \varphi(L(f))$, $g_{i+1} = \varphi(\mathfrak{a}(g_i))$ for $i = 1, \dots, k-1$, and $r^\varphi(f^+)$ is the triangle $f'^- \in F_w^-$ such that $U(f') = g_k$. Furthermore, $r(\varphi)$ maps e to

$$((\sigma^U_{f'})^{-1} \circ (\varphi_i \circ \delta_i)_{i=1}^{k-1} \circ \varphi_{\check{f}} \circ \sigma^L_f)(e).$$

We refer the reader to Sections 3.2 and 3.5 to recall the notation.

The large edge of $L(f)$ is given by $\sigma^L_f(e)$. Since $\varphi \in \mathrm{Aut}^+(\mathcal{Q}_{\mathcal{V},w} \mid \tau_{\mathcal{V},w})$, we get that $(\varphi_{\check{f}} \circ \sigma^L_f)(e)$ is the large edge of g_1. By the definition of δ_i, $(\delta_1 \circ \varphi_{\check{f}} \circ \sigma^L_f)(e)$ is the large edge of $\mathfrak{a}(g_1)$. Again, the assumption that $\varphi \in \mathrm{Aut}^+(\mathcal{Q}_{\mathcal{V},w} \mid \tau_{\mathcal{V},w})$ implies that $(\varphi_1 \circ \delta_1 \circ \varphi_{\check{f}} \circ \sigma^L_f)(e)$ is the large edge of g_2. Continuing this way, $((\varphi_i \circ \delta_i)_{i=1}^{k-1} \circ \varphi_{\check{f}} \circ \sigma^L_f)(e)$ is the large edge of g_k, and thus $((\sigma^U_{f'})^{-1} \circ (\varphi_i \circ \delta_i)_{i=1}^{k-1} \circ \varphi_{\check{f}} \circ \sigma^L_f)(e)$ is the large edge of $r^\varphi(f^+) = f'^-$. □

The above lemma gives a sufficient condition for when the dual spine of $\mathcal{T}^\varphi$ admits a smoothing into a branched surface. Combining it with Proposition 3.16 gives sufficient conditions for the existence of a veering structure on $\mathcal{T}^\varphi$.

Theorem 3.19 *Let S_w be a surface properly carried by a veering triangulation $\mathcal{V} = (\mathcal{T}, \alpha, \mathcal{B})$ of M. Suppose that $\varphi \in \mathrm{Aut}^+(\mathcal{Q}_{\mathcal{V},w})$ misaligns edge product disks. If additionally $\varphi \in \mathrm{Aut}^+(\mathcal{Q}_{\mathcal{V},w} \mid \tau_{\mathcal{V},w})$ then $(\mathcal{T}^\varphi, \alpha^\varphi)$ admits a veering structure.*

Proof By Proposition 3.16, the assumption that φ misaligns edge product disks implies the existence of a taut structure α^φ on $\mathcal{T}^\varphi$. If $\varphi \in \mathrm{Aut}^+(\mathcal{Q}_{\mathcal{V},w} \mid \tau_{\mathcal{V},w})$ then, by Lemma 3.18, for every $f^+ \in F_w^+$ the regluing map $r(\varphi)$ maps the large edge of f^+ to the large edge of $r^\varphi(f^+)$. Thus the branched surface $\mathcal{B}|F_w$ can be extended to a branched surface $\mathcal{B}^\varphi$ which combinatorially is just the dual spine $\mathcal{D}^\varphi$ of $(\mathcal{T}^\varphi, \alpha^\varphi)$. For every tetrahedron t of $\mathcal{T}^\varphi$ the branched surface $\mathcal{B}^\varphi_t = \mathcal{B}^\varphi \cap t$ looks as in Figure 4, because there is a tetrahedron t' of $\mathcal{V}$ with $\mathcal{B}_{t'} = \mathcal{B} \cap t' = B^\varphi_t$ and $(\mathcal{T}, \alpha, \mathcal{B})$ is veering. Thus $\mathcal{B}^\varphi$ satisfies Definition 2.5 and $\mathcal{V}^\varphi = (\mathcal{T}^\varphi, \alpha^\varphi, \mathcal{B}^\varphi)$ is veering. □

We say that $\mathcal{V}^\varphi = (\mathcal{T}^\varphi, \alpha^\varphi, \mathcal{B}^\varphi)$ is obtained from $\mathcal{V} = (\mathcal{T}, \alpha, \mathcal{B})$ by a *veering mutation*, or that $\mathcal{V}^\varphi$ and $\mathcal{V}$ are *veering mutants*. For instance, the first two veering triangulations in the veering census, the veering triangulation `cPcbbbdxm_10` of the figure eight knot sister (manifold m003 in the SnapPy census [8]) and the veering triangulation `cPcbbbiht_12` of the figure eight knot (m004), are veering mutants.

Remark 3.20 By Lemma 3.18, a combinatorial automorphism $\varphi \in \mathrm{Aut}^+(\mathcal{Q}_{\mathcal{V},w} \mid \tau_{\mathcal{V},w})$ is uniquely determined by the associated bijection $\varphi\colon F_{\mathcal{V},w} \to F_{\mathcal{V},w}$. For this reason, when discussing examples of veering mutants in Section 4 we will not label the vertices of tetrahedra nor talk about bijections between vertices of identified triangles.

Theorem 3.19 gives a sufficient condition for veeringness of a taut mutant, but this condition is not necessary. It is possible that $(\mathcal{T}^\varphi, \alpha^\varphi)$ admits a veering structure even though $\varphi \notin \mathrm{Aut}^+(\mathcal{Q}_{\mathcal{V},w} \mid \tau_{\mathcal{V},w})$. We discuss this possibility briefly, and give an example of this phenomenon, in the next subsection.

3.8 Generalizations

We say that $(\mathcal{T}|F_w, \alpha|F_w)$ admits a veering structure if it is possible to smooth its dual spine $\mathcal{D}|F_w$ into a branched surface which locally around every vertex looks like one of the options in Figure 4. Suppose that $(\mathcal{T}|F_w, \alpha|F_w)$ admits a veering structure $\mathcal{B}^*|F_w$. Let t be a tetrahedron of $(\mathcal{T}|F_w, \alpha|F_w)$. Let $\mathcal{B}^*_t = \mathcal{B}^*|F_w \cap t$. By $-\mathcal{B}^*_t$ we denote the other possible veering structure on t; see Figure 4 to see the two options. Lemma 2.12 implies that if t has a top face f which is a bottom face of some tetrahedron of $(\mathcal{T}|F_w, \alpha|F_w)$ then we cannot change the veering structure on t from $\mathcal{B}^*_t$ to $-\mathcal{B}^*_t$ without destroying veeringness. On the other hand, if both top faces of t are in F_w^+ then we can freely change $\mathcal{B}^*_t$ to $-\mathcal{B}^*_t$ and the resulting branched surface still defines a veering structure on $(\mathcal{T}|F_w, \alpha|F_w)$.

Let $\tau^{*\,+}_{\mathcal{V},w}$ and $\tau^{*\,-}_{\mathcal{V},w}$ be the train tracks in $\mathcal{Q}^+_{\mathcal{V},w}$ and $\mathcal{Q}^-_{\mathcal{V},w}$, respectively, induced by $\mathcal{B}^*|F_w$. Using the same arguments as in the proof of Theorem 3.19 we can show that if $\varphi \in \mathrm{Aut}^+(\mathcal{Q}_{\mathcal{V},w})$ misaligns edge product disks and sends $\tau^{*\,+}_{\mathcal{V},w}$ to $\tau^{*\,-}_{\mathcal{V},w}$ then the veering structure $\mathcal{B}^*|F_w$ on $(\mathcal{T}|F_w, \alpha|F_w)$ glues up into a veering structure on $(\mathcal{T}^\varphi, \alpha^\varphi)$. The advantage of considering this more general setup is that now we can derive both sufficient and necessary conditions for veeringness of a taut mutant.

Theorem 3.21 *Let S_w be a surface properly carried by a veering triangulation $\mathcal{V} = (\mathcal{T}, \alpha, \mathcal{B})$ of M. Suppose that $\varphi \in \mathrm{Aut}^+(\mathcal{Q}_{\mathcal{V},w})$ misaligns edge product disks. The taut triangulation $(\mathcal{T}^\varphi, \alpha^\varphi)$ admits a veering structure if and only if there is a veering structure $\mathcal{B}^*|F_w$ on $(\mathcal{T}|F_w, \alpha|F_w)$ such that the isomorphism $\varphi\colon \mathcal{Q}^+_{\mathcal{V},w} \to \mathcal{Q}^-_{\mathcal{V},w}$ sends $\tau^{*\,+}_{\mathcal{V},w}$ to $\tau^{*\,-}_{\mathcal{V},w}$.*

Proof The backward direction can be proved exactly as Theorem 3.19. If $(\mathcal{T}^\varphi, \alpha^\varphi)$ has a veering structure $\mathcal{B}^*$ then $(\mathcal{T}|F_w, \alpha|F_w)$ must have a veering structure $\mathcal{B}^*|F_w$ such that $r(\varphi)$ sends the train track on F_w^+ induced by $\mathcal{B}^*|F_w$ to the train track induced by $\mathcal{B}^*|F_w$ on F_w^-. Since φ misaligns edge product disks, for every $g \in \mathcal{Q}_{\mathcal{V},w}$ we have a trichotomy: $g \in L(F_w)$, g appears in $g^\varphi(f)$ for some $f \in F_w$, or $\mathfrak{a}(g)$ appears in $g^\varphi(f)$ for some $f \in F_w$. Equivalently, when constructing $r(\varphi)$ from φ we have passed through every triangular prism of M_w. Therefore Lemma 3.6 implies that φ sends $\tau^{*\,+}_{\mathcal{V},w}$ to $\tau^{*\,-}_{\mathcal{V},w}$. □

The more general setup of Theorem 3.21 is not just theoretical. There are veering triangulations $(\mathcal{T}, \alpha, \mathcal{B})$ and $(\mathcal{T}^\varphi, \alpha^\varphi, \mathcal{B}')$ which are taut mutants but not veering mutants. One such pair is given by the veering triangulation `gLMzQbcdefffhhhqxdu_122100` of the manifold s463 and the veering triangulation `gLMzQbcdefffhhhqxti_122100` of the manifold s639.

Another generalization we might consider is a *veering mutation with insertion*. Let $(\mathcal{T}|F_w, \alpha|F_w, \mathcal{B}|F_w)$ be a veering cut triangulation. If there are two triangles $f_1^+, f_2^+ \in F_w^+$ which are adjacent along an edge which is large in both f_1^+ and f_2^+, we might stack another veering tetrahedron on top of $f_1^+ \cup f_2^+$. We then obtain another cut triangulation with a veering structure which has more tetrahedra than $\mathcal{T}|F_w$. We can also add a new veering tetrahedron on top of two faces $f_1^+, f_2^+ \in F_w^+$ whose large edges are mixed.

Suppose that $(\mathcal{T}^*|F_{w_*}, \alpha^*|F_{w_*}, \mathcal{B}^*|F_{w_*})$ is obtained from $(\mathcal{T}|F_w, \alpha|F_w, \mathcal{B}|F_w)$ by adding finitely many veering tetrahedra on top of F_w^+. If there is a map $r\colon F_{w_*}^+ \to F_{w_*}^-$ such that identifying $F_{w_*}^+$ with $F_{w_*}^-$ yields a veering triangulation $\mathcal{V}^r = (\mathcal{T}^r, \alpha^r, \mathcal{B}^r)$ then we say that $\mathcal{V}^r$ is obtained from $\mathcal{V}$ by a *veering mutation with insertion*. For instance, the veering triangulation `dLQbccchhfo_122` of the manifold m009 is obtained from the veering triangulation `cPcbbbiht_12` of the manifold m004 (the figure eight knot complement) by a veering mutation with insertion.

4 Homeomorphic veering mutants

A manifold M and its mutant M^φ can be homeomorphic. This can happen for instance for many graph manifolds mutated along one of their decomposing tori. If veering mutants $\mathcal{V}$ and $\mathcal{V}^\varphi$ live on the same manifold, they might be combinatorially isomorphic or combinatorially distinct. For instance, the veering triangulation `eLMkbcddddedde_2100` of the 6_2^2 link complement carries a four-times punctured sphere such that mutating the triangulation along it via an involution yields `eLMkbcddddedde_2100` back. We discuss a few examples of combinatorially distinct veering mutants of the same manifold in Sections 4.1, 4.2 and 4.4.

Recall from Theorem 2.26 that veering triangulations combinatorially represent faces of the Thurston norm ball. A pair of veering mutants on a 3-manifold M may represent either the same face or different faces of the Thurston norm ball in $H_2(M, \partial M; \mathbb{R})$. The main obstacle to finding examples of measurable veering mutants which represent the same face of the Thurston norm ball is that when $b_1(M) > 1$ there are infinitely many distinct bases for $H_2(M, \partial M; \mathbb{Z})$. While it is relatively easy to find the cones $\mathcal{C}(\mathcal{V})$ and $\mathcal{C}(\mathcal{V}^\varphi)$ of homology classes of surfaces carried by $\mathcal{V}$ and $\mathcal{V}^\varphi$, respectively (this is explained in [44, Section 11.2]), it is not always straightforward to figure out whether they are the same up to a change of basis.

The above problem does not appear in the $b_1(M) = 1$ case. Then, up to $\eta \mapsto -\eta$, there is only one (0-dimensional) face of the Thurston norm ball in $H_2(M, \partial M; \mathbb{R})$. If M admits a pair of veering mutants $\mathcal{V}$ and $\mathcal{V}^\varphi$ then neither $\mathcal{C}(\mathcal{V})$ nor $\mathcal{C}(\mathcal{V}^\varphi)$ is empty. Hence $\mathcal{V}$ and $\mathcal{V}^\varphi$ must combinatorially represent the same face of the Thurston norm ball; see Remark 4.1. When $b_1(M) > 1$ it is sometimes possible to verify

if $\mathcal{C}(\mathcal{V}) = \mathcal{C}(\mathcal{V}^\varrho)$ using the combinatorics of the Thurston norm ball. We do this in Sections 4.2 (where the faces are the same) and 4.4 (where the faces are different).

Remark 4.1 Recall that veering triangulations come in pairs $\mathcal{V}$ and $-\mathcal{V}$ having the same taut signature and representing opposite faces of the Thurston norm ball; see Remarks 2.10 and 2.28. In what follows we will refer to veering triangulations using their taut signatures, without specifying coorientations on the faces. Thus when we say that two veering triangulations $\mathcal{V}$ and $\mathcal{V}'$ represent the same face of the Thurston norm ball, or write $\mathcal{C}(\mathcal{V}) = \mathcal{C}(\mathcal{V}')$, we really mean $\mathcal{C}(\mathcal{V}) \cup \mathcal{C}(-\mathcal{V}) = \mathcal{C}(\mathcal{V}') \cup \mathcal{C}(-\mathcal{V}')$.

In this section we will establish the following facts connecting veering mutations and faces of the Thurston norm ball:

Fact 4.2 (Veering mutations and faces of the Thurston norm ball) (1) *There are nonfibered faces of the Thurston norm ball that can be represented by two combinatorially nonisomorphic veering mutants.*

(2) *A veering mutation along a surface representing a class lying at the boundary of the cone on a fibered face may yield a veering triangulation representing a nonfibered face of the Thurston norm ball of the mutant manifold.*

Proof In Section 4.1 we discuss four veering mutants $\mathcal{V}$, $\mathcal{V}^\varrho$, $\mathcal{V}^\sigma$ and $\mathcal{V}^{\varrho\sigma}$ such that $\mathcal{V}$ and $\mathcal{V}^{\varrho\sigma}$ represent the same nonfibered face of the Thurston norm ball in a certain manifold M with $b_1(M) = 1$, and $\mathcal{V}^\varrho$ and $\mathcal{V}^\sigma$ represent adjacent fibered faces of $M^\varrho \cong M^\sigma$ with $b_1(M^\varrho) = 2$. Triangulations $\mathcal{V}$ and $\mathcal{V}^{\varrho\sigma}$ prove (1) in the $b_1(M) = 1$ case, while triangulations $\mathcal{V}^\varrho$ and $\mathcal{V}^{\sigma\varrho}$ prove (2); see also Proposition 4.4. Veering mutants proving (1) in the case $b_1(M) > 1$ are discussed in Section 4.2. □

4.1 Two veering mutants representing the same face of the Thurston norm ball when $b_1(M) = 1$

Let M be the manifold t12488 from the SnapPy census. This manifold is not fibered and $H_1(M;\mathbb{Z}) = \mathbb{Z} \oplus \mathbb{Z}/8$. It also admits a pair of distinct measurable veering triangulations which, since $b_1(M) = 1$, must represent the same face of the Thurston norm ball; see Remark 4.1. We will show that they differ by a veering mutation.

Let $\mathcal{V}$ be a veering triangulation of M with the taut signature

`iLLLPQccdgefhhghqrqqssvof_02221000`.

We present the tetrahedra of $\mathcal{V}$ in Figure 17.

By solving the system of branch equations associated to $\mathcal{V}$ one can verify that $\mathcal{V}$ carries four surfaces that can be expressed as the following (relative) 2-cycles (which we identify with the induced triangulations):

$$\mathcal{Q}_0 = f_2 + f_5 + f_7 + f_{11}, \quad \mathcal{Q}_1 = f_1 + f_5 + f_8 + f_{11},$$
$$\mathcal{Q}_2 = f_2 + f_7 + f_{10} + f_{12}, \quad \mathcal{Q}_3 = f_1 + f_8 + f_{10} + f_{12}.$$

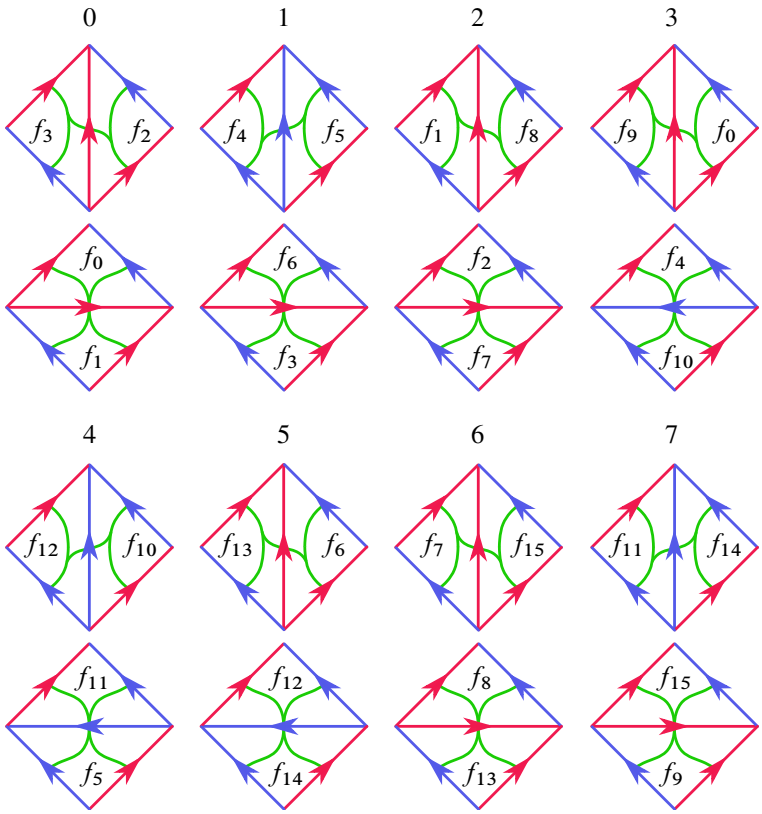

Figure 17: Veering triangulation `iLLLPQccdgefhhghqrqqssvof_02221000` of the manifold t12488.

All these surfaces are twice punctured tori. Triangulations $\mathcal{Q}_0$ and $\mathcal{Q}_3$ are presented in Figure 18. Since the first Betti number of M is equal to one, these punctured tori are homologous. In fact, it is easy to see that they are all homotopic. $\mathcal{Q}_0$ consists of two bottom faces of tetrahedron 2 and two bottom faces of tetrahedron 4. By performing the diagonal exchange corresponding to tetrahedron 2, one obtains triangulation $\mathcal{Q}_1$. By performing the diagonal exchange corresponding to tetrahedron 4, one obtains triangulation $\mathcal{Q}_2$. Triangulation $\mathcal{Q}_3$ can be obtained from $\mathcal{Q}_0$ by performing diagonal exchanges through both tetrahedra 2 and 4.

Let τ_i be the train track dual to $\mathcal{Q}_i$ induced by the stable train track of $\mathcal{V}$. That is, $\tau_i = \tau_{\mathcal{V},w_i}$ where w_i is the weight system on $\mathcal{V}$ determining $\mathcal{Q}_i$. As visible in Figure 18, the complementary regions of τ_i are punctured bigons, and thus, by Corollary 2.14, $\mathcal{Q}_i$ is properly carried. Let $\mathrm{Aut}^+(\mathcal{Q}_i \mid \tau_i)$ be the group of orientation-preserving combinatorial automorphisms of $\mathcal{Q}_i$ which preserve τ_i. Then

$$\mathrm{Aut}^+(\mathcal{Q}_0 \mid \tau_0) = \mathbb{Z}/2 \oplus \mathbb{Z}/2, \quad \mathrm{Aut}^+(\mathcal{Q}_1 \mid \tau_1) = \mathbb{Z}/2,$$
$$\mathrm{Aut}^+(\mathcal{Q}_2 \mid \tau_2) = \mathbb{Z}/2, \qquad \mathrm{Aut}^+(\mathcal{Q}_3 \mid \tau_3) = \mathbb{Z}/2.$$

The group $\mathrm{Aut}^+(\mathcal{Q}_0 \mid \tau_0)$ is generated by a rotation by π about the center of the red edge between faces f_7 and f_{11} and a "shift by one square" map; see Figure 18, left. We denote these combinatorial

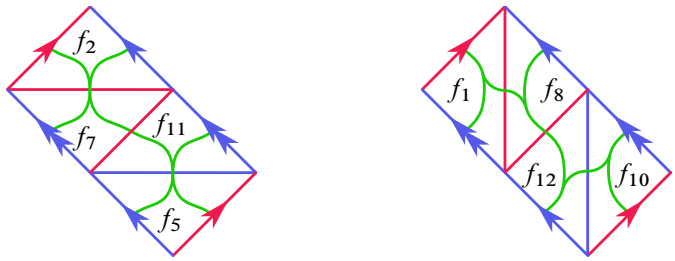

Figure 18: Left: the triangulation $\mathcal{Q}_0 = f_2 + f_5 + f_7 + f_{11}$ and its dual stable track τ_0. The group $\mathrm{Aut}^+(\mathcal{Q}_0 \mid \tau_0)$ is generated by a rotation ϱ by π about the center of the red edge between faces f_7 and f_{11} and a "shift by one square" map σ. Right: the triangulation $\mathcal{Q}_3 = f_1 + f_8 + f_{10} + f_{12}$ and its dual stable track τ_3. The group $\mathrm{Aut}^+(\mathcal{Q}_3 \mid \tau_3)$ is generated by $\rho\sigma$ only.

isomorphisms of $\mathcal{Q}_0$ by ϱ and σ, respectively. For $i = 1, 2, 3$ the group $\mathrm{Aut}^+(\mathcal{Q}_i \mid \tau_i)$ is generated by $\varrho\sigma$; see Figure 18, right, for the $i = 3$ case. The fact that $\mathrm{Aut}^+(\mathcal{Q}_0 \mid \tau_0)$ is the largest is not surprising; the surface underlying $\mathcal{Q}_0$ is the lowermost carried representative of the generator of $H_2(M, \partial M; \mathbb{Z})$, and thus the stable train track τ_0 has the most large branches (is minimally split).

Since $\mathcal{Q}_0$ does not traverse any edge of $\mathcal{V}$ more than once, we automatically get that ϱ, σ and $\varrho\sigma$ do not align edge product disks. Thus by Theorem 3.19 we get three veering mutants $\mathcal{V}^\varrho$, $\mathcal{V}^\sigma$ and $\mathcal{V}^{\varrho\sigma}$ of $\mathcal{V}$. Information about the regluing maps $r(\varrho)$, $r(\sigma)$ and $r(\varrho\sigma)$ is presented in Table 1. Recall from Remark 3.20 that since we are looking only at elements of $\mathrm{Aut}^+(\mathcal{Q}_0 \mid \tau_0)$, the regluing maps are uniquely determined by their associated bijections $\{f_2^+, f_5^+, f_7^+, f_{11}^+\} \to \{f_2^-, f_5^-, f_7^-, f_{11}^-\}$. In Figure 19 we present taut signatures of the four mutants, as well some additional information about their underlying manifolds.

Proposition 4.3 *A nonfibered face* F *of the Thurston norm ball of the* **t12488** *manifold can be combinatorially represented by two combinatorially distinct veering mutants.*

Proof Triangulations $\mathcal{V}$ and $\mathcal{V}^{\varrho\sigma}$ are two combinatorially distinct measurable veering mutants. Since there is a sequence of Pachner moves from $\mathcal{V}$ to $\mathcal{V}^{\varrho\sigma}$, their underlying manifolds are homeomorphic. (One can use Regina [7] to verify that the shortest such path has length four and consists of two 2-3 moves and two 3-2 moves.) Both these triangulations carry a twice punctured torus, which in particular means that the cones $\mathcal{C}(\mathcal{V})$ and $\mathcal{C}(\mathcal{V}^{\varrho\sigma})$ are nonempty. Since the first Betti number of M is equal to 1, up to $\eta \mapsto -\eta$ there is only one face F of the Thurston norm ball in $H^1(M; \mathbb{R})$. After possibly switching coorientations on faces of one of the triangulations we get that $\mathcal{C}(\mathcal{V}) = \mathcal{C}(\mathcal{V}^{\varrho\sigma}) = \mathbb{R}_+ \cdot (\mathrm{F})$; see Remark 4.1. □

f^+	f_2^+	f_5^+	f_7^+	f_{11}^+
$r^\varrho(f^+)$	f_5^-	f_2^-	f_{11}^-	f_7^-
$r^\sigma(f^+)$	f_{11}^-	f_7^-	f_5^-	f_2^-
$r^{\varrho\sigma}(f^+)$	f_7^-	f_{11}^-	f_2^-	f_5^-

Table 1: The regluing maps determined by ϱ, σ and $\varrho\sigma$.

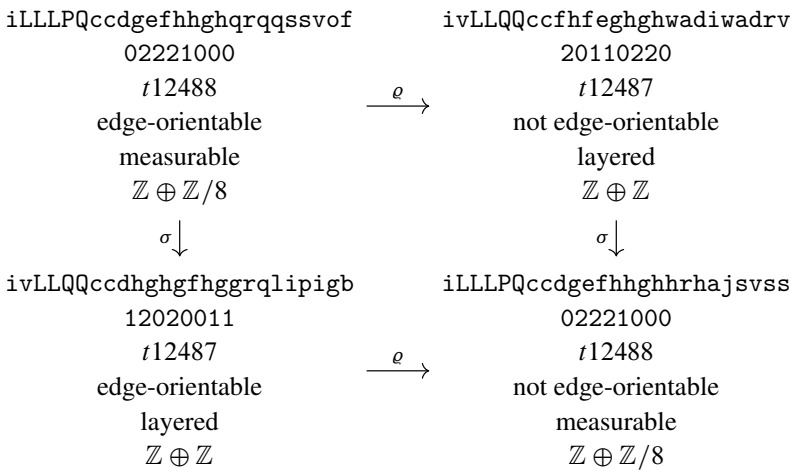

Figure 19: Four veering mutants. Each dataset consists of the isomorphism signature of the triangulation (first row), the taut angle structure (second row), the name of the underlying manifold in the SnapPy's census (third row), information about edge-orientability (fourth row), the type of the triangulation (fifth row) and the first homology group with integer coefficients of the underlying manifold (sixth row).

Another conclusion that we can draw from Figure 19 is that a mutant of a measurable veering triangulation does not have to be measurable. Observe however that if a layered veering triangulation $\mathcal{V}$ admits a measurable veering mutant $\mathcal{V}^\varphi$ then the homology class of the mutating surface must lie in the boundary of the fibered cone represented by $\mathcal{V}$.

Proposition 4.4 *Let $\mathcal{V}$ be a finite layered veering triangulation of a 3-manifold M. Suppose that $\mathcal{V} \to \mathcal{V}^\varphi$ is a veering mutation such that $\mathcal{V}^\varphi$ is measurable. Then the homology class of the mutating surface lies in the boundary of the cone on the fibered face represented by $\mathcal{V}$.*

Proof Since $\mathcal{V}$ is layered, the face $\mathtt{F}$ of the Thurston norm ball represented by $\mathcal{V}$ is fibered; see [32, Theorem 5.15], stated here as Theorem 2.26. Denote by S_w the surface carried by $\mathcal{V}$ that can be used to mutate $\mathcal{V}$ into $\mathcal{V}^\varphi$, and by S_w^ϵ the embedded surface obtained from S_w by slightly pulling apart overlapping regions of S_w. The surface S_w^ϵ is a Thurston norm minimizing representative of its homology class [27, Theorem 3]. If that homology class lies in the interior of $\mathbb{R}_+ \cdot (\mathtt{F})$ then $M|S_w^\epsilon$ is a product sutured manifold [50, Theorem 3]. Therefore the mutant manifold M^φ is fibered over the circle with the mutating surface being the fiber. The assumption that $\mathcal{V} \to \mathcal{V}^\varphi$ is a veering mutation implies that φ misaligns edge product disks, and therefore, by Theorems 3.10 and 3.19, $\mathcal{V}^\varphi$ is a veering triangulation of M^φ. Therefore $\mathcal{V}^\varphi$ carries a fiber of a fibration of M^φ over the circle. But a veering triangulation that carries fibers of fibrations over the circle is layered [32, Theorem 5.15]. This is a contradiction with the assumption that $\mathcal{V}^\varphi$ is measurable. □

The other two mutants, $\mathcal{V}^\varrho$ and $\mathcal{V}^\sigma$, both live on the same 3-manifold t12487, which is the L11n222 link complement. Since we cannot have two combinatorially distinct veering triangulations representing the

same fibered face of the Thurston norm ball [38, Proposition 2.7], we deduce that $\mathcal{V}^\varrho$ and $\mathcal{V}^\sigma$ represent different faces of the Thurston norm ball. In particular, it is possible that two different fibered faces of the Thurston norm ball of the same manifold are related by a veering mutation.

Let F^ϱ and F^σ be the fibered faces represented by $\mathcal{V}^\varrho$ and $\mathcal{V}^\sigma$, respectively. The Thurston norm ball of the L11n222 link complement is a quadrilateral with two pairs of fibered faces. Therefore the mutating twice punctured torus S represents the primitive integral class lying either on the ray $\mathbb{R}_+ \cdot \mathrm{F}^\varrho \cap \mathbb{R}_+ \cdot \mathrm{F}^\sigma$ or on the ray $\mathbb{R}_+ \cdot \mathrm{F}^\varrho \cap (-\mathbb{R}_+ \cdot \mathrm{F}^\sigma)$. Since the stable train tracks τ^ϱ and τ^σ on S induced from $\mathcal{V}^\varrho$ and $\mathcal{V}^\sigma$, respectively, are equal, under the same mutation (eg by ϱ) two different veering triangulations on t12487 mutate into two different veering triangulations on t12488. It is the fact that the first Betti number of t12488 is equal to one that makes these two distinct veering triangulations represent the same top-dimensional face of the Thurston norm ball. In other words, in this example the phenomenon of a top-dimensional nonfibered face of the Thurston norm ball represented by multiple distinct veering triangulations arises from mutating a fibered 3-manifold with a higher first Betti number along a surface representing a class lying at the intersection of multiple fibered faces.

Remark 4.5 In the veering census there are 110 manifolds with the first Betti number equal to one which admit two measurable veering triangulations. Among those, (at least) 87 differ by a veering mutation along a connected surface. The mutating surface is either a four times punctures sphere (8 cases), a twice punctured torus (75 cases) or a four times punctured torus (4 cases).

4.2 Two veering mutants representing the same face of the Thurston norm ball when $b_1(M) = 2$

As explained at the beginning of this section, finding examples of two different measurable veering triangulations representing the same face of the Thurston norm ball is harder when $b_1(M) > 1$ because then $H_2(M, \partial M; \mathbb{R})$ admits infinitely many distinct bases. A possible approach to overcome this problem is to focus on manifolds for which any two nonfibered nonopposite faces of the Thurston norm ball have different combinatorics, or which have only one pair of opposite nonfibered faces. For instance, we searched for a cusped hyperbolic 3-manifold M such that

- $b_1(M) = 2$,
- the Thurston norm ball in $H_2(M, \partial M; \mathbb{R})$ is a quadrilateral,
- M is fibered,
- M admits at least two measurable veering triangulations $\mathcal{V}$ and $\mathcal{V}'$ with different taut signatures and such that the cones $\mathcal{C}(\mathcal{V})$ and $\mathcal{C}(\mathcal{V}')$ are 2-dimensional.

When the first three conditions are satisfied, the Thurston norm ball of M admits only one pair of top-dimensional nonfibered faces. Therefore if additionally M admits at least two measurable veering triangulations whose cones of homology classes of carried surfaces are 2-dimensional, they either represent the same nonfibered face or opposite nonfibered faces; see Remark 4.1. If they represent opposite faces

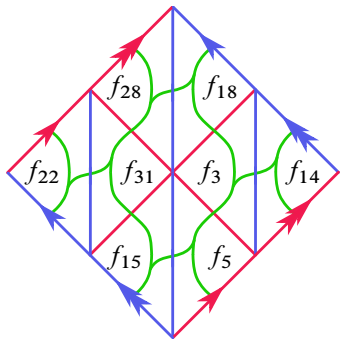

Figure 20: Ideal triangulation $\mathcal{Q}_{\mathcal{V}_1,w}$ and the stable train track $\tau_{\mathcal{V}_1,w}$ of a four times punctured torus carried by $\mathcal{V}_1$.

then switching coorientations on faces of one of the triangulations makes them represent the same face. In the veering census [20] there is a 3-manifold M which satisfies all these conditions. It admits (at least) three veering triangulations $\mathcal{V}_1$, $\mathcal{V}_2$ and $\mathcal{V}_3$ with the taut signatures

```
qLLLzvQMQLMkbeeekljjlmljonpppphhhhaaahhahhaahha_0111022221111001,
qLLLzvQMQLMkbeeekljjlmljonpppphhhhaaahhahhaahha_1200111112020112,
qLLLzvQMQLMkbeeekljjlmljonpppphhhhaaahhahhaahha_2111200001111221,
```

respectively. Observe that $\mathcal{V}_1$, $\mathcal{V}_2$ and $\mathcal{V}_3$ are combinatorially isomorphic as triangulations, but they have different taut structures. Triangulations $\mathcal{V}_1$ and $\mathcal{V}_3$ are measurable, and $\mathcal{V}_2$ is layered. Using `tnorm` [54] we can verify that M indeed has only two pairs of faces of the Thurston norm ball. One pair has to be fibered because M admits a layered veering triangulation. Thus, after possibly replacing $\mathcal{V}_1$ by $-\mathcal{V}_1$, we must have that $\mathcal{C}(\mathcal{V}_1) = \mathcal{C}(\mathcal{V}_3)$.

Triangulations $\mathcal{V}_1$ and $\mathcal{V}_3$ not only represent the same nonfibered face of the Thurston norm ball, but they are also each other's mutants. Triangulation $\mathcal{V}_1$ carries a four times punctured torus which, using the same labels as in the veering census, can be represented by the 2-cycle

$$S_w = f_3 + f_5 + f_{14} + f_{15} + f_{18} + f_{22} + f_{28} + f_{31}.$$

To save some space, we do not include the picture of the tetrahedra of $\mathcal{V}_1$ (this is a triangulation with 16 tetrahedra). We do, however, present the induced triangulation $\mathcal{Q}_{\mathcal{V}_1,w}$ and the induced train track $\tau_{\mathcal{V}_1,w}$ in Figure 20. Since all complementary regions of $\tau_{\mathcal{V}_1,w}$ are punctured bigons, S_w is properly carried by $\mathcal{V}_1$; see Corollary 2.14. We have

$$\mathrm{Aut}^+(\mathcal{Q}_{\mathcal{V}_1,w} \mid \tau_{\mathcal{V}_1,w}) = \mathbb{Z}/2 \oplus \mathbb{Z}/2 \oplus \mathbb{Z}/2.$$

The group $\mathrm{Aut}^+(\mathcal{Q}_{\mathcal{V}_1,w} \mid \tau_{\mathcal{V}_1,w})$ is generated by the rotation by π around the center of Figure 20, which we denote by ϱ, the shift by one "layer" in the northeast direction σ_+, and the shift by one "layer" in the northwest direction σ_-. The surface S_w does not traverse any edge of $\mathcal{V}_1$ more than once, and thus there are no edge product disks in $M|S_w^\epsilon$. Consequently, we can construct eight veering mutants of $\mathcal{V}_1$. They

Figure 21: Six veering mutants of $\mathcal{V}_1$. Each dataset consists of the isomorphism signature of the triangulation (split into the first and second row), the taut angle structure (third row), information about edge-orientability (fourth row), the type of the triangulation (fifth row) and the first homology group with integer coefficients of the underlying manifold (sixth row).

do not have pairwise-distinct taut signatures. In particular, $\mathcal{V}_3$ has the same taut signature as both $\mathcal{V}_1^{\varrho}$ and $\mathcal{V}_1^{\varrho\sigma-}$. Data on the remaining mutants of $\mathcal{V}_1$ is available in Figure 21. Observe that in each column we have veering triangulations with the same isomorphism signature but different taut structure. Thus in each column we have two veering triangulations of the same manifold. The manifold in the right column is the complement of the L14n62847 link.

It is worth mentioning that in this example the mutating surface represents a homology class that lies in the interior of the cone $\mathcal{C}(\mathcal{V}_1) = \mathcal{C}(\mathcal{V}_3)$, and thus in the interior of the cone over a face of the Thurston norm ball, but over a vertex of the Alexander norm ball. See [35] for the relationship between the Thurston and Alexander norms on $H_2(M, \partial M; \mathbb{R})$. The Alexander polynomial of M is equal to

$$\Delta_M = a^2b^2 + 2a^2b + 4ab + 4a + 2b + 6 + 2b^{-1} + 4a^{-1} + 4a^{-1}b^{-1} + 2a^{-2}b^{-1} + a^{-2}b^{-2}.$$

Using this we present the Alexander norm ball of M in Figure 22. We also marked the cones $\mathcal{C}(\mathcal{V}_1)$, $\mathcal{C}(\mathcal{V}_2)$ and $\mathcal{C}(\mathcal{V}_3)$ of homology classes carried by $\mathcal{V}_1$, $\mathcal{V}_2$ and $\mathcal{V}_3$, respectively. We can see that $\mathcal{C}(\mathcal{V}_1) = \mathcal{C}(\mathcal{V}_3)$, and that this cone is a cone on two adjacent faces of the Alexander norm ball, but one face of the Thurston norm ball. The homology class of the mutating surface lies over a vertex of the Alexander norm ball.

4.3 Nonmutants representing the same nonfibered face

Even though the focus of this paper is on veering mutants, it is important to note that there are faces of the Thurston norm ball which are combinatorially represented by two combinatorially nonisomorphic veering triangulations which do not differ by a mutation.

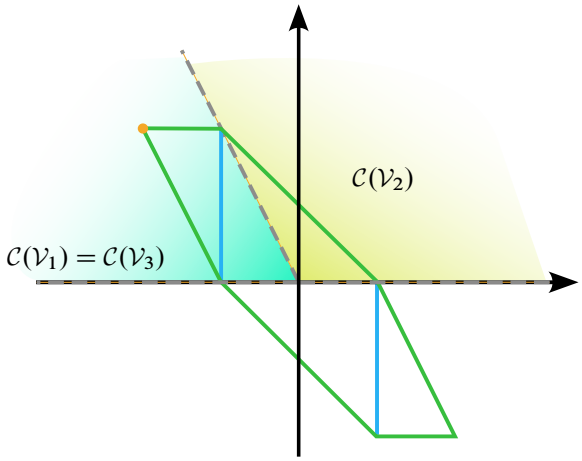

Figure 22: The unit norm ball of the Alexander norm on $H_2(M, \partial M; \mathbb{R})$ has vertices at $\left(\pm\frac{1}{2}, \mp\frac{1}{2}\right)$, $\left(\pm\frac{1}{4}, \mp\frac{1}{2}\right)$ and $\left(\pm\frac{1}{4}, 0\right)$. Its boundary is marked green. The unit norm ball of the Thurston norm has vertices at $\left(\pm\frac{1}{4}, \mp\frac{1}{2}\right)$ and $\left(\pm\frac{1}{4}, 0\right)$. The part of its boundary which does not overlap with the boundary of the Alexander norm ball is marked blue. The cones of homology classes carried by $\mathcal{V}_1$ and $\mathcal{V}_3$ are equal to the cone on two adjacent faces of the Alexander norm ball. The surface mutating $\mathcal{V}_1$ to $\mathcal{V}_3$ represents the class $(-1, 1)$ lying over the vertex $\left(-\frac{1}{2}, \frac{1}{2}\right)$ of the Alexander norm ball (marked orange).

Fact 4.6 *There are nonfibered faces of the Thurston norm ball that can be combinatorially represented by two distinct veering triangulations which do not differ by a mutation or a mutation with insertion.*

Proof Let $\mathcal{V}_1$ and $\mathcal{V}_2$ be veering triangulations with the taut signatures

`lLLvLMQQccdjgkihhijkkqrwsdcfkfjdq_02221000012`,

`pvLLALLAPQQcdhehlkjmonmoonnwrawwaewaamgwwvn_122221111122002`,

respectively. These are two measurable veering triangulations on a 3-manifold M with $H_1(M; \mathbb{Z}) = \mathbb{Z} \oplus \mathbb{Z}/4$. Thus they must represent the same face of the Thurston norm ball. Since $\mathcal{V}_1$ and $\mathcal{V}_2$ have different numbers of tetrahedra (the strings describing their taut angle structures have different length), they cannot be mutants.

To show that $\mathcal{V}_2$ is not obtained from $\mathcal{V}_1$ by a single mutation with insertion, consider the set $F_{\max}$ of faces of $\mathcal{V}_1$ which have a nonzero weight for some weight system on $\mathcal{V}_1$. If $\mathcal{V}_2$ was obtained from $\mathcal{V}_1$ by a single mutation with insertion then the dual graph Γ_2 of $\mathcal{V}_2$ would have a subgraph isomorphic to the graph $\Gamma_1^{\max} = \Gamma_1 - F_{\max}$ obtained from the dual graph Γ_1 of $\mathcal{V}_1$ by deleting all its edges dual to the faces from $F_{\max}$. The graph $\Gamma_1^{\max}$ has three simple cycles: one of length three, and two of length four. The unique simple cycle of length three shares an edge with one of the cycles of length four. The graph Γ_2 has four simple cycles of length three and six simple cycles of length four, but none of the cycles of length three shares an edge with any cycle of length four. Thus $\mathcal{V}_2$ cannot be obtained from $\mathcal{V}_1$ by a single mutation with insertion. □

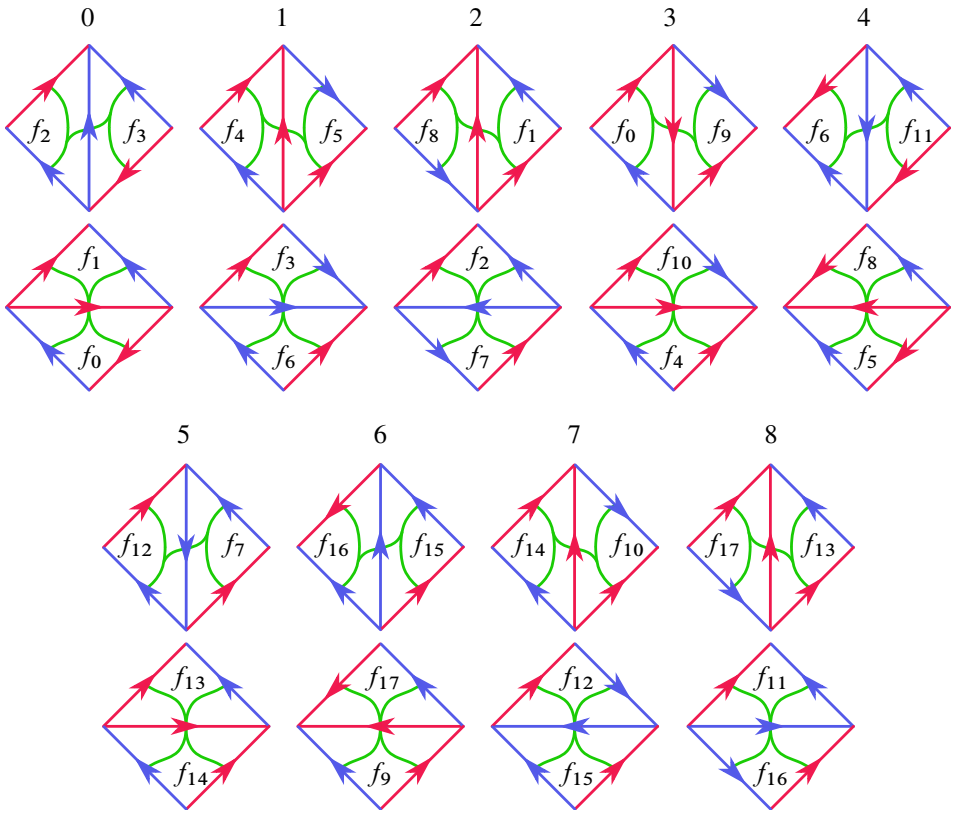

Figure 23: Veering triangulation `jLLAvQQcedehihiihiinasmkutn_011220000`.

4.4 Mutating along a higher-genus surface

In Sections 4.1 and 4.2 we discussed pairs of homeomorphic veering mutants for which the mutating surface was of genus one. In Remark 4.5 we also mentioned homeomorphic mutants with mutating surface of genus zero. In this subsection we discuss a pair of veering triangulations of the same manifold which differ by a mutation along a surface of genus two. This example differs from the previous ones not only by the genus of the mutating surface, but also by the fact that this surface is a fiber of a fibration over the circle. Moreover, the sutured manifold $M\,|S_w^\epsilon$ has edge product disks.

Let $\mathcal{V}$ and $\mathcal{V}'$ be veering triangulations with taut signatures

`jLLAvQQcedehihiihiinasmkutn_011220000`, `jvLLAQQdfghhfgiiijttmtltrcr_201102102`,

respectively. These are two veering triangulations of the 10_{12}^3 link complement. We present tetrahedra of $\mathcal{V}$ in Figure 23.

Let $S_w = 2f_0 + f_2 + f_6 + 2f_7 + 2f_9 + 2f_{11} + f_{12} + f_{16}$. This is a genus-two surface with four punctures; see Figure 24. The stable train track $\tau_{\mathcal{V},w}$ has two complementary regions with five cusps and

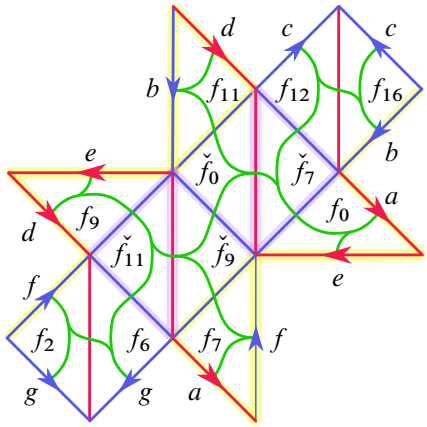

Figure 24: Ideal triangulation $\mathcal{Q}_{\mathcal{V},w}$ and the stable train track $\tau_{\mathcal{V},w}$ of a four times punctured genus-two surface S_w properly carried by $\mathcal{V}$. An edge e of $\mathcal{Q}_{\mathcal{V},w}$ is shaded yellow (respectively, purple) if the edge e^+ of $\mathcal{Q}^+_{\mathcal{V},w}$ (respectively, edge e^- of $\mathcal{Q}^-_{\mathcal{V},w}$) is the top (respectively, the bottom) base of an edge product disk in $M|S^\epsilon_w$. To distinguish between the two copies of $f_i \in F_w$ in $\mathcal{Q}_{\mathcal{V},w}$ when $w_{f_i} > 1$, we denote the lowermost copy of f_i by $\check{f}_i$. The letters a, b, c, d, e, f and g indicate side identifications. The only nontrivial element of $\mathrm{Aut}^+(\mathcal{Q}_{\mathcal{V},w} \mid \tau_{\mathcal{V},w})$ is the rotation by π around the center of the edge between $\check{f}_9$ and $\check{f}_0$. It misaligns edge product disks, because no edge shaded yellow is mapped to an edge shaded purple.

two complementary regions with one cusp. Thus, by Corollary 2.14, S_w is properly carried. Let ϱ be the generator of $\mathrm{Aut}^+(\mathcal{Q}_{\mathcal{V},w} \mid \tau_{\mathcal{V},w}) = \mathbb{Z}/2$. Information on the bijection $r^\varrho\colon F^+_w \to F^-_w$ determined by ϱ is included in Table 2. In this example $M|S^\epsilon_w$ admits edge product disks — in Figure 24 their top bases are shaded yellow and their bottom bases are shaded purple. We can directly check that no edge which is the top base of some edge product disk in $M|S^\epsilon_w$ is mapped by ϱ to an edge which is the bottom base of some edge product disk in $M|S^\epsilon_w$. This means that ϱ misaligns edge product disks. Therefore, by Theorems 3.10 and 3.19, $\mathcal{V}^\varrho$ is a veering triangulation of M^ϱ. Using Regina [7] we can verify that $\mathcal{V}^\varrho$ is combinatorially isomorphic to $\mathcal{V}'$, and thus M^ϱ is homeomorphic to M.

With some choice of basis for $H_2(M, \partial M; \mathbb{Z})$ the cone $\mathcal{C}(\mathcal{V})$ is spanned by $(0,0,1)$, $(0,1,-1)$ and $(1,0,0)$, and the homology class of S_w is then given by $(1,2,-1)$. In particular, S^ϵ_w is a fiber of a fibration of M over the circle. The taut polynomial of $\mathcal{V}$ and its specialization at $[S^\epsilon_w]$ are equal to

$$\Theta(a,b,c) = a^2b^3c^2 - a^2b^2c^2 - ab^3c^2 - a^2b^2c + ab^2c + abc - bc - a - b + 1,$$
$$\Theta^{(1,2,-1)}(z) = \Theta(z^1, z^2, z^{-1}) = z^6 - 2z^5 - 2z + 1,$$

f^+	f_0^+	f_2^+	f_6^+	f_7^+	f_9^+	f_{11}^+	f_{12}^+	f_{16}^+
$r^\sigma(f^+)$	f_0^-	f_{16}^-	f_{12}^-	f_7^-	f_9^-	f_{11}^-	f_6^-	f_2^-

Table 2: The regluing map determined by σ.

respectively. It follows from [32, Theorem 7.1; 34, Theorem 4.2] that the stretch factor λ of the monodromy f of the fibration with fiber S^{ϵ}_{w} is equal to the largest real root of $\Theta^{(1,2,-1)}(z)$, that is

$$\lambda = \tfrac{1}{4}(1+\sqrt{17}+\sqrt{2(1+\sqrt{17})}) \approx 2.081.$$

The mutating surface in $\mathcal{V}^{\varrho}$ is a fiber of a fibration of M over the circle with monodromy ϱf and thus the same stretch factor. The fibered faces $\mathtt{F}$ and $\mathtt{F}^{\varrho}$ represented by $\mathcal{V}$ and $\mathcal{V}^{\varrho}$, respectively, must be different because there is at most one veering triangulation associated to a fibered face $\mathtt{F}$ of the Thurston norm ball (zero if the associated circular flow has singular orbits); see [38, Proposition 2.7]. In this case we can actually deduce a stronger statement, that there is no automorphism Φ of $H_2(M,\partial M;\mathbb{R})$ that sends $\mathtt{F}$ to $\mathtt{F}^{\varrho}$. This follows from the fact that $\mathtt{F}$ is a triangle, while $\mathtt{F}^{\varrho}$ is a pentagon. Thus ϱf and f are not conjugate in the mapping class group of a genus-two surface with four punctures.

Fact 4.7 *Let M be the complement of the 10^3_{12} link.*

- *M fibers in two different ways with fiber being a genus-two surface with four punctures and such that the monodromy of one fibration is obtained from the monodromy of the other fibration by postcomposing it with an involution ϱ.*
- *The two fibrations lie over different faces of the Thurston norm ball, and no automorphism of $H_2(M,\partial M;\mathbb{R})$ sends one face to the other. Thus the monodromies are not conjugate in the mapping class group of a genus-two surface with four punctures.*

5 Flows representing the same face of the Thurston norm ball

We will show that the flows built from some of the combinatorially nonisomorphic veering triangulations discussed in Section 4 are topologically inequivalent using the following lemma:

Lemma 5.1 *Let Ψ_1 and Ψ_2 be two pseudo-Anosov flows on a closed 3-manifold N. If the stable lamination of Ψ_1 is transversely orientable and the stable lamination of Ψ_2 is not, then Ψ_1 and Ψ_2 are not topologically equivalent. An analogous statement holds for blown-up flows Ψ_1° and Ψ_2°.*

Proof If Ψ_1 and Ψ_2 are topologically equivalent there is a homeomorphism $h\colon M\to M$ taking oriented orbits of Ψ_1 to oriented orbits of Ψ_2 (see Definition 2.18). This homeomorphism must take leaves of the stable lamination of Ψ_1 to the leaves of the stable lamination of Ψ_2. But the stable lamination of Ψ_2 admits Möbius band leaves, while the stable lamination of Ψ_1 has only planar and annular leaves. Therefore Ψ_1 and Ψ_2 cannot be topologically equivalent. □

Thus if a face $\mathtt{F}$ of the Thurston norm ball is combinatorially represented by two veering triangulations one of which is edge-orientable and the other is not, Lemma 5.1 together with Corollary 2.21 imply that the flows built out of these veering triangulations have to be topologically inequivalent.

Theorem 5.2 *There are nonfibered faces of the Thurston norm ball that can be dynamically represented by two topologically inequivalent flows.*

Proof For the cusped case apply Lemma 5.1 and Corollary 2.21 to the blown-up flows built from the veering mutants $\mathcal{V}$ and $\mathcal{V}^{\varrho\sigma}$ discussed in Section 4.1 (for the $b_1 = 1$ case) or from the veering mutants $\mathcal{V}_1, \mathcal{V}_3 = \mathcal{V}_1^{\varrho}$ discussed in Section 4.2 (for the $b_1 = 2$ case) using Theorem 2.20. The maximality condition from Definition 2.24 is satisfied in both cases because the faces are top dimensional.

Both these pairs of veering mutants differ by a mutation along a punctured torus. Thus Dehn filling their underlying 3-manifolds along the slopes determined by the boundaries of these tori yields toroidal 3-manifolds. Consequently, these veering triangulations cannot be used to construct two distinct pseudo-Anosov flows on a closed hyperbolic 3-manifold which represent the same face of the Thurston norm ball. However, to do so we can use veering triangulations $\mathcal{V}_1$ and $\mathcal{V}_2$ that we discussed in the proof of Fact 4.6:

(a) $\mathcal{V}_1$ and $\mathcal{V}_2$ are two measurable veering triangulations of the same manifold M with $H_1(M;\mathbb{Z}) = \mathbb{Z} \oplus \mathbb{Z}/4$.

(b) $\mathcal{V}_1$ is edge-orientable, while $\mathcal{V}_2$ is not.

(c) For $i = 1, 2$ every connected surface S carried by $\mathcal{V}_i$ has genus three and four punctures, and all complementary regions of its stable train track have four cusps.

It follows from (a) that $\mathcal{V}_1$ and $\mathcal{V}_2$ represent the same face of the Thurston norm ball in $H_2(M, \partial M;\mathbb{R})$. Part (c) and Remark 2.27 imply that both $\mathcal{V}_1$ and $\mathcal{V}_2$ carry a surface S of genus three with four punctures such that each boundary component of S intersects the ladderpole curves of $\mathcal{V}_i$ four times. Thus, by Theorem 2.30, the 3-manifold N obtained from M by Dehn filling it along the slope determined by ∂S is hyperbolic.

For $i = 1, 2$ let Ψ_i be the pseudo-Anosov flow on N built from $\mathcal{V}_i$ via the Agol–Tsang construction. Since triangulations $\mathcal{V}_1$ and $\mathcal{V}_2$ represent the same face of the Thurston norm ball in $H_2(M, \partial M;\mathbb{R})$ and both carry S, Theorem 2.30 implies that $\mathcal{C}(\Psi_1) = \mathcal{C}(\Psi_2) \neq \varnothing$. By (a) and the fact that N contains an incompressible surface, $b_1(N) = 1$. Thus the maximality condition from Definition 2.24 must be satisfied. Therefore Ψ_1 and Ψ_2 dynamically represent the same face of the Thurston norm ball in $H_2(N;\mathbb{R})$. The fact that they are not topologically equivalent follows from (b), Lemma 5.1 and Corollary 2.21. □

Remark 5.3 In Section 4.1 we constructed a pair of veering mutants $\mathcal{V}$ and $\mathcal{V}^{\varrho\sigma}$ on the manifold t12488. Let N denote the manifold obtained from t12488 by Dehn filling it along the boundary of the mutating surface. Using Regina [7] it is possible to verify that N is a graph manifold obtained from the orientable circle bundle N_0 over a 2-holed $\mathbb{R}P^2$ by identifying its two toroidal boundary components. Thus N is a so-called *BL-manifold*, as defined by Barbot in [2].

Langevin and Bonatti constructed an Anosov flow on one BL-manifold in [5]; a description of this flow written in English can be found in [25]. Barbot generalized the construction to most other BL-manifolds

[2, Theorem A] and called the resulting Anosov flows *BL-flows*. If a BL-manifold is not a circle bundle then the constructed flow is not $\mathbb{R}$-covered, because it is not circular but is transverse to a torus.

In [2, Theorem B(2)] Barbot claims that all non-$\mathbb{R}$-covered Anosov flows on a fixed BL-manifold which is not a circle bundle are topologically equivalent. This is in contradiction with our results. It follows from Theorem 2.20 and Lemma 5.1 that N admits a pair of topologically inequivalent BL-flows — one constructed from $\mathcal{V}$ and the other constructed from $\mathcal{V}^{\varrho\sigma}$. We denote them by Ψ and $\Psi^{\varrho\sigma}$, respectively. The flows Ψ and $\Psi^{\varrho\sigma}$ are constructed from the same semiflow Φ_0 on N_0, but — unsurprisingly, given that $\mathcal{V}$ and $\mathcal{V}^{\varrho\sigma}$ are mutants — by gluing the two boundary tori in different ways. More specifically, if for $i = 1, 2$ we choose a basis (o_i, f_i) on the boundary torus T_i of N_0 so that f_i is a fiber of a Seifert fibration while o_i corresponds to the boundary of the 2-holed $\mathbb{R}P^2$ contained in T_i, then one gluing $T_1 \to T_2$ can be represented by a matrix

$$A = \begin{bmatrix} 1 & 1 \\ 1 & 0 \end{bmatrix},$$

and the other by $-A$. These two gluings result in the same manifold N because N_0 admits an involution which fixes (o_1, f_1) and sends (o_2, f_2) to $(-o_2, -f_2)$. This involution can be obtained as the composition of the reflection across the stable leaf through the periodic orbit of Φ_0 missing T_i and the reflection which fixes every fiber of the Seifert fibration, but reverses their orientation.

In Remark 4.5 we mentioned 79 pairs of veering mutants on manifolds with first Betti number equal to one for which the mutating surface is a punctured torus. In most cases Regina recognizes their appropriate Dehn fillings as BL-manifolds.

6 Polynomial invariants of veering triangulations

In [34] McMullen introduced a polynomial invariant of fibered faces of the Thurston norm ball called the *Teichmüller polynomial*. Recall that associated to a fibered face $\mathtt{F}$ there is a unique circular flow Ψ; see [13, Theorem 7], stated here as Theorem 2.23. The Teichmüller polynomial of $\mathtt{F}$ is an invariant of the module of transversals to the preimage of the stable lamination of Ψ in the maximal free abelian cover of the manifold [34, Section 3]. Its main feature is that it can be used to compute the stretch factors of monodromies of all fibrations lying over $\mathtt{F}$ [34, Theorem 4.2].

McMullen asked whether it is possible to define a similar invariant for nonfibered faces. If a nonfibered face is dynamically represented by a pseudo-Anosov flow Ψ, one could try to replicate the definition of the Teichmüller polynomial using the stable lamination of Ψ. Landry, Minsky and Taylor used veering triangulations to devise such a polynomial invariant [32]. In fact, they defined two polynomial invariants of veering triangulations: the *taut polynomial* and the *veering polynomial*. Furthermore, they showed that if a face $\mathtt{F}$ of the Thurston norm ball represented by a veering triangulation $\mathcal{V}$ is fibered, then the taut polynomial of $\mathcal{V}$ is equal to the Teichmüller polynomial of $\mathtt{F}$ [32, Theorem 7.1]. Therefore the taut

	`iLLLPQccdgefhhghqrqqssvof_02221000`
Θ	$4(a+1)$
$\mathbb{V}$	$(a-1)^3\Theta$
	`iLLLPQccdgefhhghhrhajsvss_02221000`
Θ	$4(a-1)$
$\mathbb{V}$	$(a-1)^2(a+1)\Theta$
	`qLLLzvQMQLMkbeeekljjlmljonpppphhhhaaahhahhaahha_0111022221111001`
Θ	$a^2b^2-2a^2b+4ab-4a-2b+6-2b^{-1}-4a^{-1}+4a^{-1}b^{-1}-2a^{-2}b^{-1}+a^{-2}b^{-2}$
$\mathbb{V}$	0
	`qLLLzvQMQLMkbeeekljjlmljonpppphhhhaaahhahhaahha_2111200001111221`
Θ	$a^2b^2+2a^2b+4ab+4a+2b+6+2b^{-1}+4a^{-1}+4a^{-1}b^{-1}+2a^{-2}b^{-1}+a^{-2}b^{-2}$
$\mathbb{V}$	0
	`lLLvLMQQccdjgkihhijkkqrwsdcfkfjdq_02221000012`
Θ	$(a+1)(a^2+1)(a^2-a+1)^2$
$\mathbb{V}$	$(a+1)(a-1)^2(a^2+1)(a^4+a^3+a^2+a+1)(a^6+a^5+a^4+a^3+a^2+a+1)\Theta$
	`pvLLALLAPQQcdhehlkjmonmoonnwrawwaewaamgwwvn_122221111122002`
Θ	$(a-1)(a^2+1)(a^2+a+1)^2$
$\mathbb{V}$	0

Table 3: The taut and veering polynomials of pairs of veering triangulations representing the same face of the Thurston norm ball discussed in Section 4. Θ denotes the taut polynomial and $\mathbb{V}$ denotes the veering polynomial. The variables correspond to the basis elements of $H = H_1(M;\mathbb{Z})/\text{torsion}$. The invariants are well defined up to a change of basis of H and multiplication by $\pm h$ for $h \in H$.

polynomial (and its specializations under Dehn fillings) can be seen as a generalization of the Teichmüller polynomial to (some) nonfibered faces.

However, in Section 4 we showed that a veering triangulation representing a nonfibered face of the Thurston norm ball is not necessarily unique. This means that the taut and veering polynomials of a veering triangulation might actually not be invariants of the face represented by the triangulation.

An algorithm to compute the taut and veering polynomials of a veering triangulation is explained in [46]. A much faster algorithm for the computation of the taut polynomial follows from the fact that it is equal to the Alexander polynomial of the underlying manifold twisted by a certain representation $\omega\colon \pi_1(M) \to \mathbb{Z}/2$ [45, Proposition 5.7] and can therefore be computed using *Fox calculus*. Both algorithms have been implemented by the author, Saul Schleimer and Henry Segerman; see Veering on GitHub [47]. Using this software, we computed the taut and veering polynomials of the pairs of veering triangulations representing the same face of the Thurston norm ball discussed in Section 4. We include this data in Table 3.

Fact 6.1 *A nonfibered face of the Thurston norm ball can be combinatorially represented by two distinct veering triangulations with different taut polynomials, and different veering polynomials.*

Proof See Table 3. □

The only pair of veering triangulations from Table 3 which have different both taut and veering polynomials are not veering mutants; see Fact 4.6. Hence the question still remains whether two homeomorphic veering mutants representing the same face of the Thurston norm ball can have different both taut and veering polynomials. The answer to this question is positive. One such pair consists of veering triangulations is

`mvLLMvQQQegffhijkllkklreuegggvvrggr_120200111111`,

`mvLLMvQQQegffhjikllkklreuegrrvvrwwr_120200111111`.

They differ by a veering mutation along a four times punctured torus. Their taut polynomials are $8(a+1)$ and $8(a-1)$, respectively, and their veering polynomials are $8(a-1)(a+1)^3$ and $8(a-1)^3(a+1)$, respectively.

7 Further questions

7.1 Operations on flows underlying veering mutations

Throughout the paper we worked combinatorially with veering triangulations and used existing literature [1; 31; 32] to deduce statements about pseudo-Anosov flows on closed manifolds or their blow-ups on manifolds with toroidal boundary. We have intentionally avoided discussing how the flows underlying veering mutants are related. A naive expectation would be that the flows differ by a *mutation of* (*blown-up*) *pseudo-Anosov flows*. In the closed case this would be a mutation along a surface transverse to a pseudo-Anosov flow whose intersections with the stable and unstable foliations of the flow are invariant under some nontrivial symmetry. Mutating these foliations via this symmetry gives a pair of 2-dimensional singular foliations intersecting along "recombined flow lines". It remains to find sufficient conditions for a flow along recombined flow lines (a *mutant flow*) to admit a parametrization which makes it pseudo-Anosov. When $\partial M \neq \varnothing$ one could expect a similar operation performed on the stable and unstable laminations of a blown-up pseudo-Anosov flow.

However, examples presented in Section 4.1 suggest that the problem may be more complicated. Namely, let $\mathcal{V}$ be a veering triangulation with taut signature `iLLLPQccdgefhhghqrqqssvof_02221000`. We showed that $\mathcal{V}$ admits four veering mutants: $\mathcal{V}$, $\mathcal{V}^{\varrho}$, $\mathcal{V}^{\sigma}$ and $\mathcal{V}^{\varrho\sigma}$. Denote by M the manifold underlying $\mathcal{V}$. By [1, Theorem 5.1], there is a transitive Anosov flow Ψ on the manifold obtained from M by Dehn filling it along the boundary of the mutating surface, and the blown-up flow Ψ° on M. It can be deduced from Figure 18, right, that the intersection $\mathcal{L}_{\Psi^\circ,S}$ of the mutating twice punctured torus S with the stable lamination of Ψ° has two closed leaves and the remaining leaves spiral into them; we approximate this lamination in Figure 25. It is clear from Figure 25 that $\mathcal{L}_{\Psi^\circ,S}$ is invariant only under the identity and $\varrho\sigma$. This means that even though we can mutate the veering branched surface carrying the stable lamination of Ψ° in four different ways, the lamination itself can only be mutated in two different ways.

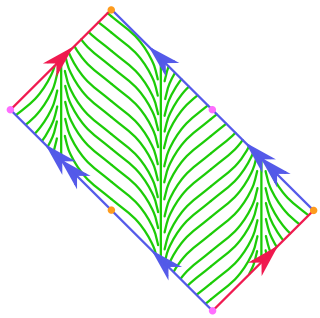

Figure 25: The intersection of the stable lamination of the blown-up Anosov flow determined by the veering triangulation `iLLLPQccdgefhhghqrqqssvof_02221000` and a twice punctured torus carried by this triangulation.

Working with veering triangulations as opposed to working directly with flows has both advantages and disadvantages. On one hand, it allowed us to find explicit examples of topologically inequivalent flows on the same manifold which differ by a veering mutation and represent the same face of the Thurston norm ball (Theorem 5.2). On the other hand, the fact that veering triangulations exist only on hyperbolic 3-manifolds means that if a mutation along a surface transverse to some (blown-up) pseudo-Anosov flow yields a (blown-up) pseudo-Anosov flow on a nonhyperbolic manifold, there will not be a corresponding mutation on the level of triangulations. This can happen when we mutate along $\varphi \in \mathrm{Aut}^+(\mathcal{Q}_{\mathcal{V},w} \mid \tau_{\mathcal{V},w})$ which aligns edge product disks; see Proposition 3.17. Another obstruction for a veering mutation that would not be an obstruction for a mutation of flows is the "no perfect fits" condition. It is possible that a flow which is without perfect fits relative to a finite collection Λ of closed orbits mutates into a flow which does have perfect fits relative to the recombined collection of orbits Λ^φ. In this case again we do not have a corresponding veering mutation. For these reasons, it is still of interest to properly define and study mutations of pseudo-Anosov flows (and possibly other operations underlying veering mutations) without referring to veering triangulations. This would fit into a more general framework of constructing new flows out of old, similarly to the Goodman–Fried surgery [15; 21], and Handel–Thurston shearing along tori [22].

7.2 The orbit spaces of mutant flows and recognizing mutative flows

Associated to a pseudo-Anosov flow Ψ there is a bifoliated plane called the *orbit space* of Ψ; see [11, Proposition 4.1]. Suppose that flows Ψ and Ψ^φ differ by a mutation along a transverse surface S in the sense introduced in Section 7.1. If S is a fiber of a fibration over the circle there is a homeomorphism from the orbit space of Ψ to the orbit space of Ψ^φ which sends foliations of one to the foliations of the other; this follows from the fact these orbit spaces are the universal covers of S and S^φ equipped with the invariant foliations lifted from S and S^φ, respectively. It is not immediately clear how the orbit spaces differ when S is not a virtual fiber. More generally, it would be advantageous to have an invariant which is equal for flows which are *mutative*, that is, differ by a finite number of mutations, and distinguishes flows which are not mutative.

7.3 A general result on the relationship between two flows representing the same face of the Thurston norm ball

We showed that two blown-up Anosov flows representing the same face of the Thurston norm ball can differ by a veering mutation (Sections 4.1 and 4.2). However, we also noted that there are examples of veering triangulations that represent the same face of the Thurston norm ball and do not differ by a veering mutation or even a veering mutation with insertion (Fact 4.6). We have not explained how these veering triangulations, or their underlying flows, are related. Ideally, we would like to have a theorem that describes all possible ways in which two distinct flows can represent the same face of the Thurston norm ball.

7.4 Homology classes versus free homotopy classes of closed orbits of flows

In recent work Barthelmé, Frankel and Mann found an invariant which distinguishes distinct transitive pseudo-Anosov flows, provided that their orbit spaces satisfy a technical condition called *no tree of scalloped regions*; see [3, Definition 3.21]. More precisely, they showed that two such flows Ψ_1 and Ψ_2 on N are isotopically equivalent if and only if the sets $\mathcal{P}(\Psi_1)$ and $\mathcal{P}(\Psi_2)$ of unoriented free homotopy classes of their closed orbits are equal, and topologically equivalent if these sets differ by an automorphism of $\pi_1(N)$; see [3, Theorem 1.1].

In the proof of Theorem 5.2 we discussed veering triangulations which, after appropriate Dehn filling, yield topologically inequivalent transitive pseudo-Anosov flows Ψ_1 and Ψ_2 on a closed hyperbolic 3-manifold N representing the same face of the Thurston norm ball in $H_2(N,\mathbb{R})$. By [3, Proposition 1.2], the orbit spaces of Ψ_1 and Ψ_2 do not have trees of scalloped regions. Thus it follows from [3, Theorem 1.1] that $\mathcal{P}(\Psi_1) \neq \Phi\mathcal{P}(\Psi_2)$ for any $\Phi \in \mathrm{Aut}(\pi_1(N))$. On the other hand, we know that the homology classes of closed orbits of Ψ_1 and Ψ_2 span the same rational cone in $H_1(N;\mathbb{R})$. This motivates the question of how exactly the sets $\mathcal{P}(\Psi_1)$ and $\mathcal{P}(\Psi_2)$ differ, not just for these particular flows from the proof of Theorem 5.2, but for any two flows which represent the same face of the Thurston norm ball.

7.5 Many distinct flows representing the same face of the Thurston norm ball in the $b_1(M) = 1$ case

Suppose that S is a Thurston norm minimizing surface representing a primitive integral class lying at the intersection of two fibered cones $\mathbb{R}_+ \cdot \mathtt{F}_1$ and $\mathbb{R}_+ \cdot \mathtt{F}_2$. Let Ψ_1 and Ψ_2 be the circular flows associated to $\mathtt{F}_1$ and $\mathtt{F}_2$ as in Theorem 2.23. If the intersections of S with the stable and unstable foliations of Ψ_1 and Ψ_2 are isotopic, we may be able to perform a mutation along S which yields two distinct noncircular flows Ψ_1^φ and Ψ_2^φ representing the same top-dimensional nonfibered face in the mutant manifold. A combinatorial version of this phenomenon occurs for manifolds t12487 and t12488; see Section 4.1. This leads to a question: given $k > 2$ is there a 3-manifold M with $b_1(M) > 2$ such that

- M admits k fibered faces, intersecting at a point α, dynamically represented by topologically inequivalent circular flows $\Psi_1, \Psi_2, \ldots, \Psi_k$,

taut signature	volume
gLLPQccdfeffhggaagb_201022	5.33348956689812
gLLPQccdfeffhwraarw_201022	5.33348956689812
gLLPQbefefefhhxhqhh_211120	5.07470803204827
gLLPQbefefefhhhhhha_011102	5.07470803204827

Table 4: Veering mutants of gLLPQccdfeffhggaagb_201022.

- the primitive integral class on $\mathbb{R}_+ \cdot \alpha$ can be represented by a Thurston norm minimizing surface S such that mutating M along S gives a nonfibered 3-manifold M^φ with $b_1(M^\varphi) = 1$ and $[S^\varphi] \in \mathcal{C}(\Psi_i^\varphi)$ for $i = 1, 2, \dots, k$?

More generally, can a face of the Thurston norm ball be dynamically represented by more than two topologically inequivalent flows? Can it be represented by infinitely many flows?

7.6 Veering mutants and hyperbolic geometry

Recall that if $\mathcal{V}$ and $\mathcal{V}^\varphi$ are veering mutants then they are both hyperbolic [23, Theorem 1.5]. However, they do not always have the same hyperbolic volume. In Table 4 we list the taut signatures and volumes of certain veering mutants of the veering triangulation gLLPQccdfeffhggaagb_201022 of the 6_3^2 link complement. The mutating surface is a twice punctured torus with the induced triangulation $\mathcal{Q}_{\mathcal{V},w}$ and the stable train track $\tau_{\mathcal{V},w}$ satisfying $\mathrm{Aut}^+(\mathcal{Q}_{\mathcal{V},w} \mid \tau_{\mathcal{V},w}) \cong \mathbb{Z}/2 \oplus \mathbb{Z}/2$.

Ruberman studied mutations of hyperbolic 3-manifolds and found sufficient conditions for a mutant of a hyperbolic 3-manifold to be a hyperbolic 3-manifold of the same volume. One of his results concerns only mutating via very special types of involutions of certain surfaces [48, Theorem 1.3]; another concerns only mutating along surfaces which are not virtual fibers [48, Theorem 4.4]. Conditions of neither of these theorems are satisfied when mutating the first triangulation from the table to either the third or the fourth one; the mutating involutions are not of the type required by [48, Theorem 1.3], and the mutating surface is a fiber of a fibration over the circle. Nonetheless, there are plenty of veering mutants with the same hyperbolic volume. In particular, all nonhomeomorphic veering mutants discussed in Section 4 have the same volume. It would be interesting to know if it is possible to figure out purely combinatorially when a veering mutation along a carried surface results in a hyperbolic 3-manifold of the same volume. The relationship between a veering structure and a hyperbolic structure is still not well understood, and perhaps analyzing it in this fairly narrow setup of mutations would give some new insight on the matter.

References

[1] **I Agol**, **C C Tsang**, *Dynamics of veering triangulations: infinitesimal components of their flow graphs and applications*, Algebr. Geom. Topol. 24 (2024) 3401–3453 MR Zbl

[2] **T Barbot**, *Generalizations of the Bonatti–Langevin example of Anosov flow and their classification up to topological equivalence*, Comm. Anal. Geom. 6 (1998) 749–798 MR Zbl

[3] **T Barthelmé**, **S Frankel**, **K Mann**, *Orbit equivalences of pseudo-Anosov flows*, Invent. Math. (online publication March 2025)

[4] **C Bonatti**, **I Iakovoglou**, *Anosov flows on 3-manifolds: the surgeries and the foliations*, Ergodic Theory Dynam. Systems 43 (2023) 1129–1188 MR Zbl

[5] **C Bonatti**, **R Langevin**, *Un exemple de flot d'Anosov transitif transverse à un tore et non conjugué à une suspension*, Ergodic Theory Dynam. Systems 14 (1994) 633–643 MR Zbl

[6] **B A Burton**, *The Pachner graph and the simplification of 3-sphere triangulations*, from "Computational geometry", ACM, New York (2011) 153–162 MR Zbl

[7] **B A Burton**, **R Budney**, **W Pettersson**, et al., *Regina*: *software for low-dimensional topology* (1999) Available at `https://regina-normal.github.io`

[8] **M Culler**, **N M Dunfield**, **M Goerner**, **J R Weeks**, *SnapPy*, *a computer program for studying the geometry and topology of 3-manifolds* Available at `http://snappy.computop.org`

[9] **N M Dunfield**, *Alexander and Thurston norms of fibered 3-manifolds*, Pacific J. Math. 200 (2001) 43–58 MR Zbl

[10] **N M Dunfield**, **S Garoufalidis**, **A Shumakovitch**, **M Thistlethwaite**, *Behavior of knot invariants under genus 2 mutation*, New York J. Math. 16 (2010) 99–123 MR Zbl

[11] **S Fenley**, **L Mosher**, *Quasigeodesic flows in hyperbolic 3-manifolds*, Topology 40 (2001) 503–537 MR Zbl

[12] **S Frankel**, **S Schleimer**, **H Segerman**, *From veering triangulations to link spaces and back again*, preprint (2019) arXiv 1911.00006

[13] **D Fried**, *Fibrations over S^1 with pseudo-Anosov monodromy*, from "Travaux de Thurston sur les surfaces" (A Fathi, F Laudenbach, V Poénaru, editors), Astérisque 66-67, Soc. Math. France, Paris (1979) 251–266 Zbl

[14] **D Fried**, *The geometry of cross sections to flows*, Topology 21 (1982) 353–371 MR Zbl

[15] **D Fried**, *Transitive Anosov flows and pseudo-Anosov maps*, Topology 22 (1983) 299–303 MR Zbl

[16] **S Friedl**, **W Lück**, *The L^2-torsion function and the Thurston norm of 3-manifolds*, Comment. Math. Helv. 94 (2019) 21–52 MR Zbl

[17] **D Futer**, **F Guéritaud**, *Explicit angle structures for veering triangulations*, Algebr. Geom. Topol. 13 (2013) 205–235 MR Zbl

[18] **D Gabai**, *Foliations and the topology of 3-manifolds*, J. Differential Geom. 18 (1983) 445–503 MR Zbl

[19] **D Gabai**, *Foliations and genera of links*, Topology 23 (1984) 381–394 MR Zbl

[20] **A Giannopolous**, **S Schleimer**, **H Segerman**, *A census of veering triangulations*, electronic reference (2019) Available at `https://math.okstate.edu/people/segerman/veering.html`

[21] **S Goodman**, *Dehn surgery on Anosov flows*, from "Geometric dynamics", Lecture Notes in Math. 1007, Springer (1983) 300–307 MR Zbl

[22] **M Handel**, **W P Thurston**, *Anosov flows on new three manifolds*, Invent. Math. 59 (1980) 95–103 MR Zbl

[23] **C D Hodgson**, **J H Rubinstein**, **H Segerman**, **S Tillmann**, *Veering triangulations admit strict angle structures*, Geom. Topol. 15 (2011) 2073–2089 MR Zbl

[24] **C D Hodgson**, **J H Rubinstein**, **H Segerman**, **S Tillmann**, *Triangulations of 3-manifolds with essential edges*, Ann. Fac. Sci. Toulouse Math. 24 (2015) 1103–1145 MR Zbl

[25] **S Kamatani**, **H Kodama**, **T Noda**, *A Birkhoff section for the Bonatti–Langevin example of Anosov flow*, from "Foliations 2005", World Sci., Hackensack, NJ (2006) 229–243 MR Zbl

[26] **P Kirk**, **C Livingston**, *Concordance and mutation*, Geom. Topol. 5 (2001) 831–883 MR Zbl

[27] **M Lackenby**, *Taut ideal triangulations of 3-manifolds*, Geom. Topol. 4 (2000) 369–395 MR Zbl

[28] **M Landry**, *Taut branched surfaces from veering triangulations*, Algebr. Geom. Topol. 18 (2018) 1089–1114 MR Zbl

[29] **M P Landry**, *Veering triangulations and the Thurston norm: homology to isotopy*, Adv. Math. 396 (2022) art. id. 108102 MR Zbl

[30] **M Landry**, *Stable loops and almost transverse surfaces*, Groups Geom. Dyn. 17 (2023) 35–75 MR Zbl

[31] **M P Landry**, **Y N Minsky**, **S J Taylor**, *Flows, growth rates, and the veering polynomial*, Ergodic Theory Dynam. Systems 43 (2023) 3026–3107 MR Zbl

[32] **M P Landry**, **Y N Minsky**, **S J Taylor**, *A polynomial invariant for veering triangulations*, J. Eur. Math. Soc. 26 (2024) 731–788 MR Zbl

[33] **B Martelli**, *An introduction to geometric topology*, self published, Pisa, Italy (2016)

[34] **C T McMullen**, *Polynomial invariants for fibered 3-manifolds and Teichmüller geodesics for foliations*, Ann. Sci. École Norm. Sup. 33 (2000) 519–560 MR Zbl

[35] **C T McMullen**, *The Alexander polynomial of a 3-manifold and the Thurston norm on cohomology*, Ann. Sci. École Norm. Sup. 35 (2002) 153–171 MR Zbl

[36] **C T McMullen**, **C H Taubes**, *4-manifolds with inequivalent symplectic forms and 3-manifolds with inequivalent fibrations*, Math. Res. Lett. 6 (1999) 681–696 MR Zbl

[37] **C Millichap**, *Mutations and short geodesics in hyperbolic 3-manifolds*, Comm. Anal. Geom. 25 (2017) 625–683 MR Zbl

[38] **Y N Minsky**, **S J Taylor**, *Fibered faces, veering triangulations, and the arc complex*, Geom. Funct. Anal. 27 (2017) 1450–1496 MR Zbl

[39] **H R Morton**, **P Traczyk**, *The Jones polynomial of satellite links around mutants*, from "Braids", Contemp. Math. 78, Amer. Math. Soc., Providence, RI (1988) 587–592 MR Zbl

[40] **L Mosher**, *Surfaces and branched surfaces transverse to pseudo-Anosov flows on 3-manifolds*, J. Differential Geom. 34 (1991) 1–36 MR Zbl

[41] **L Mosher**, *Dynamical systems and the homology norm of a 3-manifold, II*, Invent. Math. 107 (1992) 243–281 MR Zbl

[42] **L Mosher**, *Laminations and flows transverse to finite depth foliations*, preprint (1996) Zbl

[43] **P Ozsváth**, **Z Szabó**, *Link Floer homology and the Thurston norm*, J. Amer. Math. Soc. 21 (2008) 671–709 MR Zbl

[44] **A Parlak**, *Veering triangulations and polynomial invariants of three-manifolds*, PhD thesis, University of Warwick (2021) Available at `http://wrap.warwick.ac.uk/162096`

[45] **A Parlak**, *The taut polynomial and the Alexander polynomial*, J. Topol. 16 (2023) 720–756 MR Zbl

[46] **A Parlak**, *Computation of the taut, the veering and the Teichmüller polynomials*, Exp. Math. 33 (2024) 1–26 MR Zbl

[47] **A Parlak**, **S Schleimer**, **H Segerman**, *Veering code for studying taut and veering ideal triangulations* Available at https://github.com/henryseg/Veering

[48] **D Ruberman**, *Mutation and volumes of knots in S^3*, Invent. Math. 90 (1987) 189–215 MR Zbl

[49] **M Shannon**, *Hyperbolic models for transitive topological Anosov flows in dimension three*, preprint (2021) arXiv 2108.12000

[50] **W P Thurston**, *A norm for the homology of 3-manifolds*, Mem. Amer. Math. Soc. 339, Amer. Math. Soc., Providence, RI (1986) 99–130 MR Zbl

[51] **C C Tsang**, *Veering branched surfaces, surgeries, and geodesic flows*, New York J. Math. 29 (2023) 1425–1495 MR Zbl

[52] **C C Tsang**, *Veering triangulations and pseudo-Anosov flows*, PhD thesis, University of California, Berkeley (2023) Available at https://escholarship.org/uc/item/26h9h6dp

[53] **C C Tsang**, *Constructing Birkhoff sections for pseudo-Anosov flows with controlled complexity*, Ergodic Theory Dynam. Systems 44 (2024) 2308–2360 MR Zbl

[54] **W Worden**, *Tnorm*, Sage package, version 1.0.2 (2021) Available at https://pypi.org/project/tnorm

Department of Mathematics, University of California, Davis
Davis, CA, United States

anna.parlak@gmail.com

Proposed: Ian Agol
Seconded: Leonid Polterovich, David Fisher

Received: 4 May 2023
Revised: 21 February 2024

GEOMETRY & TOPOLOGY

msp.org/gt

See inside back cover or msp.org/gt for submission instructions.

The subscription price for 2025 is US $865/year for the electronic version, and $1210/year (+$75, if shipping outside the US) for print and electronic. Subscriptions, requests for back issues and changes of subscriber address should be sent to MSP. Geometry & Topology is indexed by Mathematical Reviews, Zentralblatt MATH, Current Mathematical Publications and the Science Citation Index.

Geometry & Topology (ISSN 1465-3060 printed, 1364-0380 electronic) is published 9 times per year and continuously online, by Mathematical Sciences Publishers, c/o Department of Mathematics, University of California, 798 Evans Hall #3840, Berkeley, CA 94720-3840. Periodical rate postage paid at Oakland, CA 94615-9651, and additional mailing offices. POSTMASTER: send address changes to Mathematical Sciences Publishers, c/o Department of Mathematics, University of California, 798 Evans Hall #3840, Berkeley, CA 94720-3840.

GT peer review and production are managed by EditFLOW® from MSP.

PUBLISHED BY

mathematical sciences publishers

nonprofit scientific publishing

http://msp.org/

GEOMETRY & TOPOLOGY

Volume 29 Issue 4 (pages 1693–2250) 2025